

**Organotypic functional cultures of  
human liver cells for long-term  
maintenance and assessment of drug-  
induced metabolome effects**

**Dissertation**

**zur Erlangung des Grades  
des Doktors der Naturwissenschaften  
der Naturwissenschaftlich-Technischen Fakultät III  
Chemie, Pharmazie, Bio-und Werkstoffwissenschaften  
der Universität des Saarlandes**

**von**

**Daniel Müller**

**Saarbrücken  
2011**

Tag des Kolloquiums: 20.04.2012

Dekan: Prof. Dr. Wilhelm F. Maier

Berichterstatter: Prof. Dr. Elmar Heinzle

Prof. Dr. Manfred J. Schmitt

Vorsitz: Prof. Dr. Uli Müller

Akad. Mitarbeiter: Dr. Johannes Meiser

**„Grau is‘ alle Theorie, entscheidend is‘ aufm Platz“**

**Alfred „Adi“ Preissler**

**1921 - 2003**

## DANKSAGUNG

Ich bin froh und dankbar, dass ich meine Doktorarbeit in der Arbeitsgruppe von Prof. Dr. Elmar Heinzle durchführen durfte. Ich danke ihm für das Vertrauen, für viele Ideen und Diskussionen sowie für die Möglichkeit, weiterhin in diesem großartigen Forschungsgebiet tätig zu sein.

Herrn Prof. Dr. Manfred Schmitt danke ich vielmals für die Bereitschaft zur Begutachtung dieser Arbeit.

Sehr großer Dank gebührt Dr. Fozia Noor für die Ratschläge, Diskussionen, Vertrauen und für Motivation und Unterstützung, was enorm zum Gelingen dieser Arbeit beigetragen hat.

Ich danke unseren Projektpartnern: Dr. Ursula Müller-Vieira, Dr. Klaus Biemel und Manuela Mayer von der Pharmacelsus GmbH für die LC-MS Analysen; Prof. Andreas Nüssler, Dr. Daniel Knobloch und Dr. Gregor Damm für die Versorgung mit primären humanen Hepatozyten sowie Dr. Katrin Zeilinger für die Bereitstellung der 3D Bioreaktor-Technologie.

Vielen Dank an Dr. Klaus Hollemeyer, Dr. Susanne Kohring, Robert Schmidt und Veronika Witte für ihre Unterstützung und Hilfe in allen Belangen des täglichen (Labor-) Lebens.

Großer Dank gebührt Michel Fritz für seine unbezahlbare Hilfe in allen HPLC- und GC-Angelegenheiten.

Bei Georg Tascher möchte ich mich für die intensive Zusammenarbeit während des gesamten Projektes bedanken. Bei Saskia Müller und Anika Kötemann bedanke ich mich für die im Rahmen dieser Dissertation durchgeführten Diplom- bzw. Bachelorarbeiten. Angela Sudhoff und Esther Hoffmann danke ich für ihre hervorragenden Laborarbeiten.

Den ehemaligen und aktuellen Mitgliedern des „Zoiga“ Labors (Dr. Simone Beckers, Esther Hoffmann, Saskia Müller, Jens Niklas, Malina Orsini, Christian Priesnitz, Alexander Strigun, Angela Sudhoff, Georg Tascher, Judith Wahrheit) möchte ich ebenso wie allen anderen Mitgliedern der gesamten Arbeitsgruppe für die hervorragende Arbeitsatmosphäre danken. Ich wünsche allen viel Glück und Erfolg in Zukunft.

Ich möchte mich bei meinen langjährigen Freunden für Ablenkung und Unterstützung in den letzten und auch in den nächsten Jahren bedanken! Grüße von Herzen gehen nach Anrath, Duisburg, Ensdorf, Felsberg, Hülzweiler, Lisdorf, Saarlouis und Wadgassen!

Ohne die Hilfe meiner Familie wäre diese Arbeit nie zustande gekommen. Vielen Dank Alfred, Nina und ganz besonders meiner Mutter für ihre Unterstützung.

Ich danke Steffi für alles! Ohne Dich hätte ich das nicht geschafft!

---

**TABLE OF CONTENT**

<b>DANKSAGUNG</b> .....	<b>1</b>
<b>TABLE OF CONTENT</b> .....	<b>2</b>
<b>ABSTRACT</b> .....	<b>4</b>
<b>ZUSAMMENFASSUNG</b> .....	<b>5</b>
<b>CHAPTER 1: GENERAL INTRODUCTION</b> .....	<b>6</b>
1.1 The liver.....	7
1.2 <i>In vitro</i> human liver cell culture .....	9
1.3 Cell culture in three dimensions .....	10
1.4 Pharmaceutical drug development.....	12
1.5 The omics era.....	14
1.6 GCTOF-MS .....	15
1.7 Analysis of chromatographic datasets .....	18
1.8 Aims of the BMBF-project “3D <i>in vitro</i> model for hepatic drug toxicity” .....	20
1.9 Outline of this thesis .....	22
<b>CHAPTER 2: IN-DEPTH PHYSIOLOGICAL CHARACTERIZATION OF PRIMARY HUMAN HEPATOCYTES IN A 3D HOLLOW FIBER BIOREACTOR</b> .....	<b>24</b>
2.1 Introduction.....	26
2.2 Materials and Methods.....	29
2.3 Results.....	36
2.4 Discussion.....	44
2.5 Conclusion.....	48
<b>CHAPTER 3: REAL-TIME <i>IN SITU</i> VIABILITY ASSESSMENT IN 3D BIOREACTOR WITH HUMAN LIVER CELLS USING RESAZURINE ASSAY DURING DRUG EXPOSURE</b> .....	<b>49</b>
3.1 Introduction.....	51
3.2 Materials and Methods.....	53
3.3 Results.....	57
3.4 Discussion.....	62
<b>CHAPTER 4: ORGANOTYPIC CULTURES OF HEPG2 GENERATED BY HANGING DROP METHOD AS <i>IN VITRO</i> MODEL FOR TOXICITY STUDIES</b> .....	<b>65</b>
4.1 Introduction.....	67
4.2 Material and methods.....	70
4.3 Results.....	74

**TABLE OF CONTENT**

---

4.4	Discussion.....	83
4.5	Conclusion.....	87
<b>CHAPTER 5: GCTOF-MS BASED METABOLOMICS REVEALS METABOLIC EFFECTS OF THERAPEUTIC DRUG CONCENTRATIONS ON HUMAN LIVER CELLS .....</b>		<b>88</b>
5.1	Introduction.....	90
5.2	Materials and Methods.....	92
5.3	Results.....	97
5.4	Discussion.....	112
<b>CHAPTER 6: BIOTRANSFORMATION OF DICLOFENAC AND METABOLIC EFFECTS UPON REPEATED DOSE EXPOSURE TO PRIMARY HUMAN HEPATOCYTES .....</b>		<b>115</b>
6.1	Introduction.....	117
6.2	Materials and Methods.....	119
6.3	Results.....	125
6.4	Discussion.....	133
<b>CHAPTER 7: SUMMARY, CONCLUSION AND OUTLOOK.....</b>		<b>137</b>
7.1	Summary.....	138
7.2	Conclusion and Outlook .....	140
<b>REFERENCES .....</b>		<b>144</b>
<b>CURRICULUM VITAE.....</b>		<b>162</b>

## ABSTRACT

The goals of this thesis were (i) to establish and improve organotypic liver cell culture techniques for long-term pharmacological studies and (ii) to develop and apply a metabolomics based approach for the assessment of drug-induced effects.

As first model, a 3D bioreactor system was characterized in terms of cell physiology and functionality. Primary human hepatocytes could be kept viable and functional for more than 2 weeks in this system. Optimization of the system allowed determination of oxygen uptake rates and viability. As second 3D system, a hanging drop method was successfully applied for the generation of organotypic cultures as high-throughput *in vitro* model for toxicity studies.

For the investigation of drug-induced metabolic effects, a metabolomics approach based on GCTOF-MS combined with multivariate statistics was developed. In 2D cultures of primary human hepatocytes, both short-term (up to 4 days) and long-term (3 weeks) drug-induced effects were detected at clinically relevant concentrations, showing the sensitivity of the established method.

Both 3D cultivation methods used in this thesis represent a step forward to organotypic cultures as *in vitro* alternatives to animals and are particularly suitable for the investigation of chronic toxicity. The established metabolomics approach is a sensitive tool to assess drug-induced changes even at subtoxic concentrations and can be applied to other cell types and cultivation systems in the future.

### ZUSAMMENFASSUNG

Die Ziele dieser Arbeit waren (i) die Etablierung und Verbesserung von organotypischen Leberzellkulturtechniken für pharmakologische Studien und (ii) die Entwicklung und Anwendung einer Metabolomics-Methode zur Detektion von Wirkstoff-induzierten Effekten.

Als erstes Modell wurde ein 3D Bioreaktor in Hinblick auf Zellphysiologie und –funktionalität untersucht. Primäre Hepatozyten konnten über mehr als 2 Wochen vital und funktionell in diesem System kultiviert werden. Eine Systemoptimierung erlaubte die Bestimmung von Sauerstoffaufnahme- und Viabilitätsraten. Als zweites 3D System wurde die Methode des hängenden Tropfens erfolgreich zur Herstellung von organotypischen Kulturen für Toxizitätsstudien eingesetzt.

Zur Untersuchung von Wirkstoff-induzierten metabolischen Effekten wurde in dieser Arbeit eine Metabolomics-Methode entwickelt, basierend auf einer Kombination von GCTOF-MS und multivariater Statistik. In 2D Kulturen von primären Hepatozyten wurden sowohl Kurzzeit- (bis zu 4 Tagen) als auch Langzeit- (3 Wochen) Effekte bei klinisch relevanten Konzentrationen nachgewiesen, was die Sensitivität der Methode zeigt.

Beide 3D Systeme, die in dieser Arbeit eingesetzt wurden, sind als organotypische *in vitro* Alternativen zu Tierversuchen zur Untersuchung von chronischer Toxizität geeignet. Die etablierte Metabolomics-Methode ist eine sensitive Technik um Wirkstoff-induzierte, subtoxische Effekte zu detektieren und kann in Zukunft auf andere Zelltypen und -systeme angewendet werden.

# CHAPTER 1: GENERAL INTRODUCTION

## 1.1 The liver

The liver is the central organ of drug and xenobiotic metabolism. All substances released from the gastrointestinal tract into the blood are entering the liver via the portal vein. The liver is divided into four liver lobes (two major and two minor), whereas each lobe is subdivided into lobules. Within these lobules, parenchymal cells (the hepatocytes) are the main cell type (70-80% of total liver cell number) and are organized in unicellular liver plates. The liver plates are located around the central vein as depicted in figure 1-1.

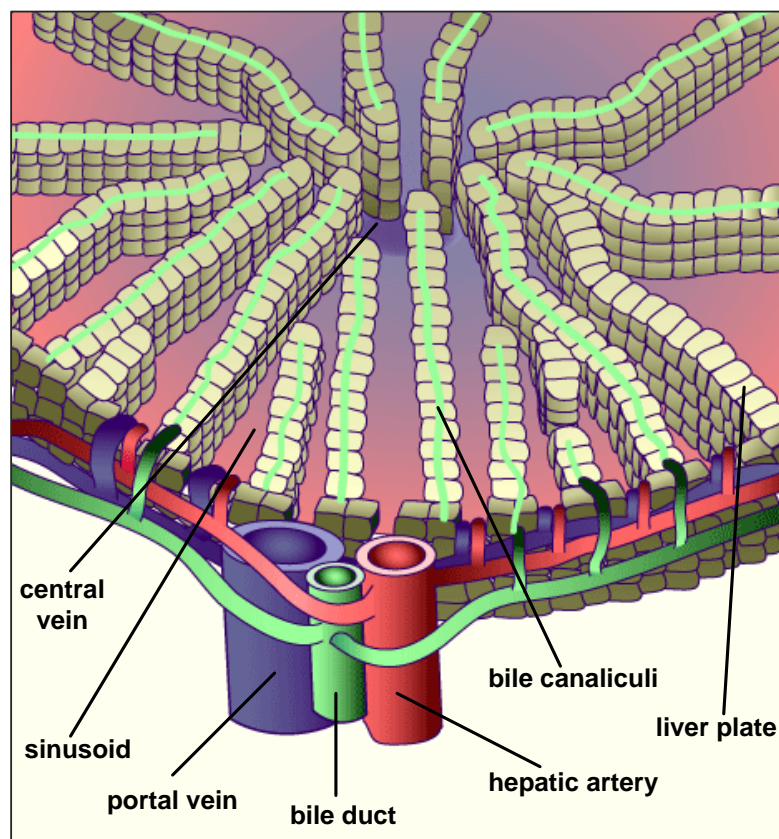


**Figure 1-1: Architecture of the liver lobule** (source: [www.unifr.ch/anatomy](http://www.unifr.ch/anatomy))

The sinusoids, vascular channels responsible for blood flow, are located between the liver plates. Bile-canaliculi between the hepatocytes collect the bile and flow into the bile duct. In the liver, hepatocytes are polar which means that two different domains can be distinguished. The apical domain (to the bile canaliculi) is morphological characterized by microvilli and is enclosed by tight junctions (Depreter *et al.*, 2002). The basolateral domain is directed to the sinusoids and has therefore contact to the blood flow (Bartles *et al.*, 1985; Maurice *et al.*, 1994). The polarity is not only morphological, but also protein distribution on the plasma membrane is strongly polarized. In the apical membrane, important transport proteins are located, such as the bile salt export pump (BSEP), multidrug resistance protein 1 (MDR-1) and multidrug

resistance-associated protein 2 (MRP-2), which are responsible for the transport of bile salts, non bile-acid organic anions, bilirubin and phosphatidylcholines (Kipp and Arias, 2000; Meier and Stieger, 2002).

The hepatocytes are the site of biotransformation in the liver. Non-polar and lipophilic substances are converted to polar and hydrophilic metabolites which are then excreted via the renal pathway. The biotransformation consists of three pathways as schematically depicted in figure 1-2.

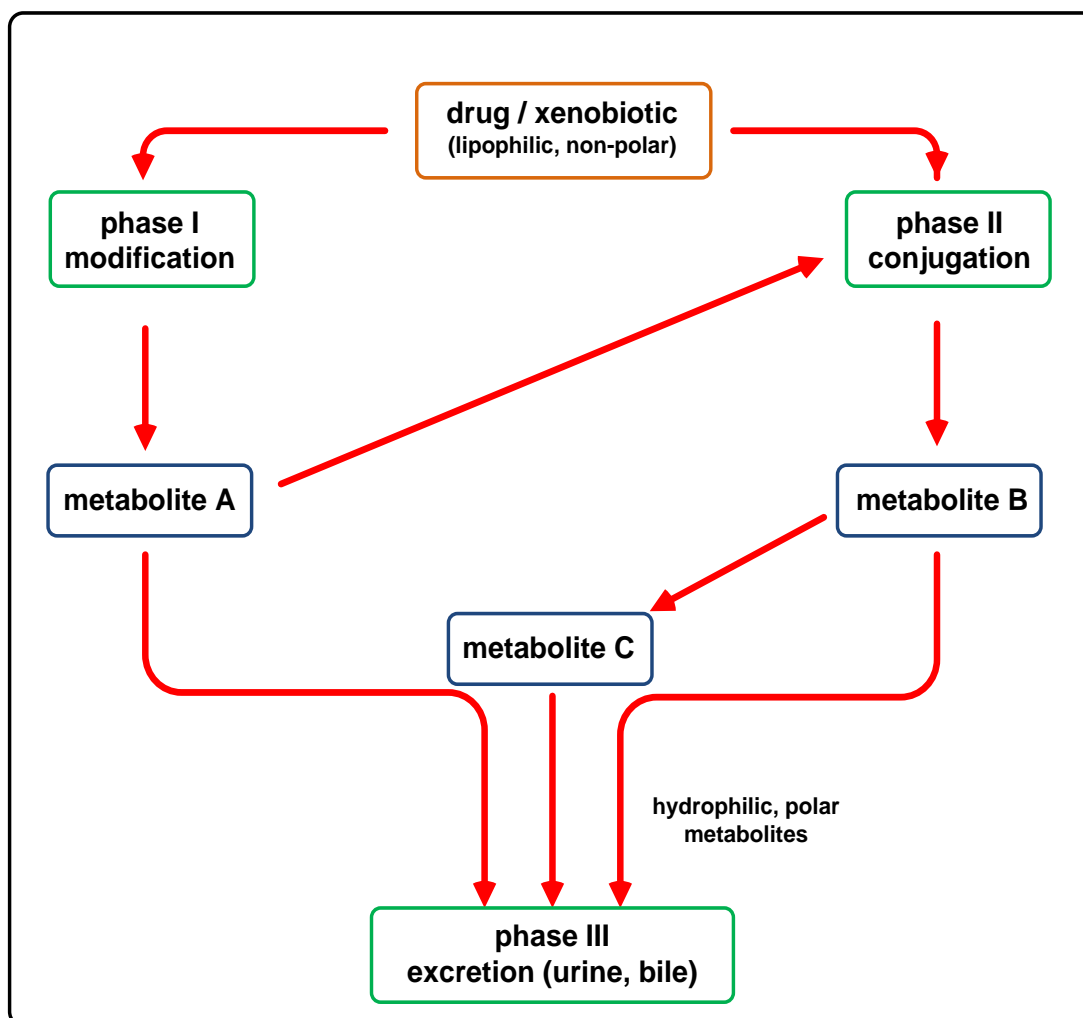


**Figure 1-2: Biotransformation pathways and metabolite formation in human hepatocytes.**

In the phase I, reactive and polar groups are introduced into the xenobiotics mainly by enzymes of the cytochrome P450 family. In further phase II reactions, the activated metabolites are conjugated with groups such as glutathione, glucuronic acid, sulfate or glycine. However, a direct phase II conjugation without previous phase I reaction is also possible. The subsequent

phase III metabolism includes the excretion of the conjugates from the cells via membrane transporters of the MRP family (Homolya *et al.*, 2003).

## **1.2 *In vitro* human liver cell culture**

*In vitro* liver cell culture models include the cultivation of primary hepatocytes as well as hepatic tumor cell lines. Primary human hepatocytes can be isolated during tumor resections. However, based on visual and physical check-up by experts, only tumor-free tissue should be used as done in this work.

Primary human hepatocytes have short-term phase I and II activities comparable to *in vivo* situation, but are only limited available, the quality is donor dependent and they lose their functionality *in vitro* quite rapidly. Moreover, the polarity is rapidly lost in monolayer cultures. Morphologically, the primary human hepatocytes are mostly hexagonal and often have two nuclei (figure 1-3 a).

HepG2 is a human hepatoma cell line derived from tissue of a 15 year old Caucasian American male (Aden *et al.*, 1979). This cell line is of unlimited availability and easy to handle. However, CYP450 activity is very low or even absent (Wilkening *et al.*, 2003). Moreover, the HepG2 cells show an abnormal karyotype (chromosome number 55) and are epithelial in morphology (figure 1-3 b). Besides these disadvantages, HepG2 cells were reported being a suitable *in vitro* model for studying hepatocyte polarity (Hoekstra *et al.*, 1999).

The HepaRG cell line (figure 1-3 c) was more recently established from a hepatocarcinoma of a female patient and reported to be the first *in vitro* model for hepatitis B infection (Gripon *et al.*, 2002). These cells were shown to remain liver-specific functions including CYP450 activity, phase II metabolism as well as expression of MRP transporter proteins (Guillouzo *et al.*, 2007; Marion *et al.*, 2010; Lubberstedt *et al.*, 2011). The cell line has further unique characteristics. It consists of two cell types in a 50:50 ratio. The first cell type forms clusters of granular epithelial cells resembling hepatocytes. The second cell type is more flattened, has a clear cytoplasm and resembles biliary cells (Guillouzo *et al.*, 2007). Moreover, the cells show a normal human karyotype and are well-suited for genotoxicity studies (Josse *et al.*, 2008).

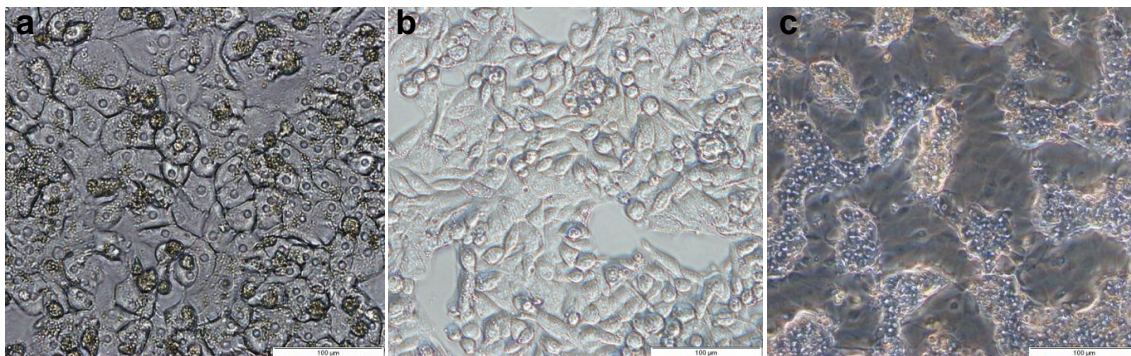


**Figure 1-3: Morphology of a) primary human hepatocytes, b) HepG2 cell, c) HepaRG cells. Scale bars represent 100  $\mu\text{m}$ .**

### 1.3 Cell culture in three dimensions

Tissues are arranged in three dimensions. This architecture leads to intensive cell-cell contacts as well as contacts to the extracellular matrix. The interactions between cells and tissue environment induce and maintain cellular differentiation, functionality and viability (Godoy *et al.*, 2009; Celebi *et al.*, 2011; van der Smissen *et al.*, 2011). Conventional cell culture systems are arranged in two dimensions which do not provide any physiological stimulus to the cells such as concentration gradients, blood flow, pressure or mechanical shear stress. Cell culture in three dimensions clearly improves the physiological relevance of cell based assays and the comparability between *in vitro* cultures and living organisms (Pampaloni *et al.*, 2007).

For liver cells, this is of special interest. Primary hepatocytes actively dedifferentiate in 2D cultures within several days (Godoy *et al.*, 2009) and thereby lose the drug-metabolizing capacities which are essential for toxicity testing. Therefore, tissue engineering of liver cells in a three-dimensional cell culture system with concomitant maintenance of liver functionality will improve *in vitro* test methods in the preclinical phase of pharmaceutical drug development.

Nowadays, a range of 3D liver cell culture systems are available.

Whole perfused organs are the closest model to *in vivo* situation but are hardly available. They retain the complex 3D architecture including cell-cell and cell-matrix interactions, but they need strong technical expertise and the cell viability is limited to a few hours.

Liver slices also retain at least parts of the complex 3D architecture and maintain viability and liver specific functions for a few days. However, studies for more than one week are not possible using this model.

Different types of 3D bioreactors have been developed for liver cell cultivation, including small and large scale systems for primary cells of different species. Dynamic systems such as the

rotating radial flow type bioreactor (RRFB) were developed inducing 3D aggregation and enhancement of liver-specific functionality (Miyazawa *et al.*, 2007). Moreover, these rotating systems show high mass transfer capacities ensuring sufficient nutrient and oxygen supply (Anton *et al.*, 2008).

Perfused 3D hollow-fiber bioreactors enable convection-based mass transfer and maintain cell viability and liver-specific functions for several weeks. Such bioreactor systems were originally developed as bioartificial livers for extracorporeal liver support (Gerlach *et al.*, 2008). Down-scaled to laboratory sizes, they provide a physiological *in vivo* like environment, whereas the hollow-fibers serve as capillary network for nutrient and oxygen supply as well as surface for cell adhesion (De Bartolo *et al.*, 2009). A 3D hollow-fiber bioreactor system, developed at the Charité Berlin, was used in this thesis for the cultivation of liver cells and was characterized and improved as shown in Chapters 2 and 3.

The combination of high-throughput 2D microtiter plates and *in vivo* like environment of 3D bioreactors led to the development of perfused multiwell plates for 3D liver cell cultivation. Domansky and colleagues described a 24-well plate based perfusion system which is suitable for oxygen monitoring and which promotes 3D tissue formation of rat hepatocytes on scaffolds. This approach is even down-scalable e.g. to 96 well plate format and applicable to other cell types e.g. heart or kidney cells (Domansky *et al.*, 2010). Further down-scaling leads to the body-on-a-chip approach, which applies microfluidic-based devices or also called micro cell culture analogs ( $\mu$ CCA), simulating the interactions of tissues under physiological-like conditions (Esch *et al.*, 2011). By cell encapsulation using hydrogels, the cells can be cultivated three-dimensional. Prototypic studies revealed the feasibility of these systems to assess drug efficacy and toxicity (Sung and Shuler, 2009; Sung *et al.*, 2010; Sung and Shuler, 2010). The  $\mu$ CCAs can be equipped with different optical probes such as oxygen sensors or fluorescence sensors for real-time monitoring of CYP450 activity (Sin *et al.*, 2004; Sung *et al.*, 2009), indicating the immense potential to improve *in vitro* studies during pharmaceutical drug development.

3D cultivation of liver cells is also possible using gel-based cultures with synthetic materials such as self-assembling peptides (Liebmann *et al.*, 2007) or natural materials like alginate (Glicklis *et al.*, 2000), collagen (Tuschl *et al.*, 2009) or matrigel (Haouzi *et al.*, 2005). Moreover, a range of synthetic polymers are used as scaffolds in 3D cell culture providing physical and structural support for tissue engineering applications (Kim *et al.*, 1998).

Organotypic cultures (OTC) of liver cells e.g. multicellular spheroids are produced scaffold-free in multiwell plates (Kelm *et al.*, 2003) or also in bioreactors (Miranda *et al.*, 2009). Due to the

low required cell number, high-throughput applications are easily performable. The OTC show liver-like structures and activities comparable to *in vivo* and are suitable for repeated dose testing during pharmaceutical drug development (Tostoes *et al.*, 2011a). In this thesis, a high-throughput, scaffold-free technology based on the hanging drop method was used to produce, characterize and test OTC of human liver cells (Chapter 4).

## 1.4 Pharmaceutical drug development

Drug development in the pharmaceutical industry includes the process of drug screening and discovery, the following preclinical and clinical studies, the marketing of the drug and postmarketing studies. As depicted in figure 1-4, the process starts with about 10.000 candidates of which 250 access the phase of *in vitro* and *in vivo* testing. After this preclinical phase, about five compounds comply the requirements for the clinical phase with testing on humans. In the USA, this decision is made during the Food and Drug Administration's (FDA) program of Investigational New Drug (IND). After the clinical trials, the manufacturer applies for New Drug Application (NDA) which is then proved and potentially approved by the FDA. In the post-marketing phase, the safety of the drug is further monitored and more accurate evaluations are possible by including information of a larger number of patients.

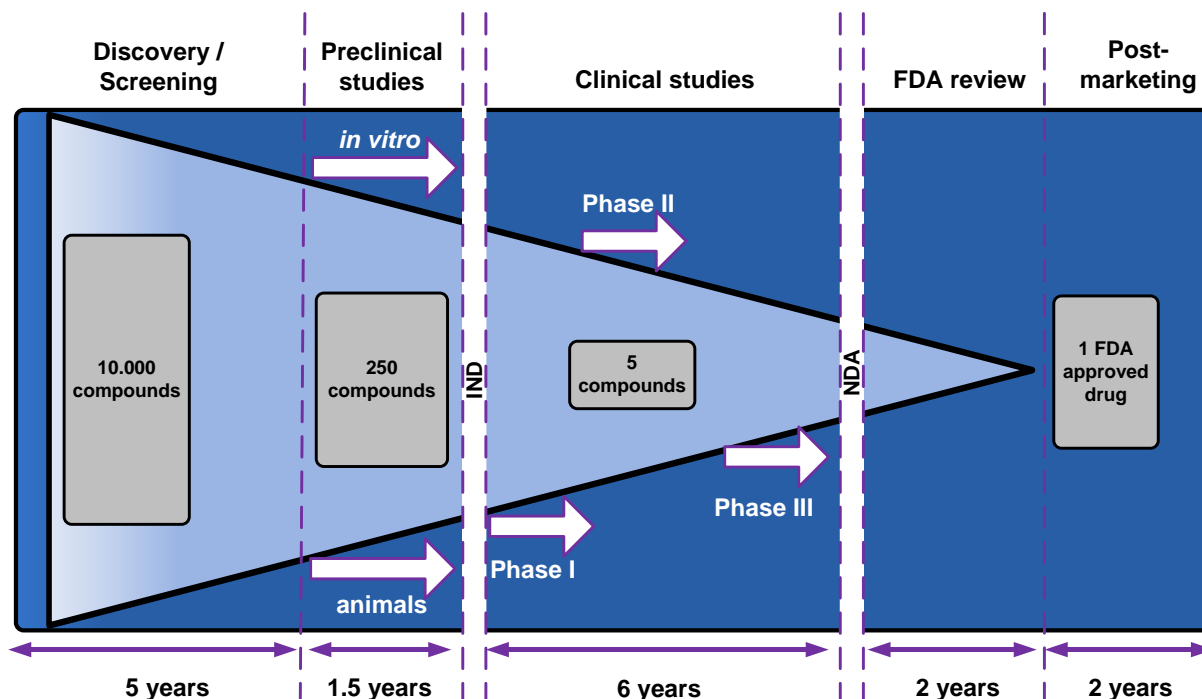


Figure 1-4: Pharmaceutical drug development process in the USA. IND=investigational new drug; NDA=new drug application. Picture modified from <http://cdn.pharmacologycorner.com/wp-content>.

Toxicity is one of the main reasons for the attrition of candidates in drug development and for the withdrawal of drugs from the market. Although every compound is toxic at high doses, there is an urgent need to detect toxicity and adverse drug reactions of a drug candidate at moderate, physiologically relevant concentrations in the very early phases of drug development.

A systematic classification defines five classes of drug toxicity (Liebler and Guengerich, 2005):

**1.) On-target or mechanism based toxicity** occurs due to interactions of the drug with its actual pharmacological target. This means that the binding of the drug to its target does not only cause the pharmacological effect but also produce toxicity. Adverse effects of statins belong to this class (Johnson *et al.*, 2004).

**2.) Hypersensitive responses** are mainly because of an activation of the immune response by protein binding of the drug, e.g. allergic reactions to penicillin (Torres and Blanca, 2010).

**3.) Off-target toxicity** is defined as toxicity provoked by the binding of a drug to an alternate target. The most common cited example for this is the cardiac potassium channel (hERG) inhibiting effect of terfenadine, leading to fatal cardiac arrhythmias (Batey and Coker, 2002).

**4.) Bioactivation** often leads to reactive metabolites which can cause toxicity. As a major example, acetaminophen is metabolized to the reactive product *N*-acetyl-*p*-benzoquinone imine (NAPQI), which covalently binds to cellular macromolecules (Jaeschke, 2005; Laine *et al.*, 2009).

**5.) Idiosyncratic toxicity** is very difficult to predict since it is quite uncommon and individual, meaning that the toxic response is exerted in a few patients but in most of them not. The mechanism behind is not well-understood and the occasions are rather rare, however, for widely used drugs such as diclofenac (Aithal, 2004), it is a severe problem.

The main sites affected by drug toxicity are the cardiovascular tract and the liver (Guengerich, 2011). Therefore, it is of common interest to study drug-induced effects on these tissues with the aim to detect hepatotoxic and cardiotoxic events as early as possible during pharmaceutical development. Therefore, suitable *in vitro* test methods as well as predictive test methods have to be developed (Mandenius *et al.*, 2011a; Mandenius *et al.*, 2011b).

State-of-the art analytical technologies such as modern mass spectrometry (MS) and nuclear magnetic resonance (NMR) applied in different –omics technologies and particularly systems biological approaches, combining different –omics fields and bioinformatics methods, are promising for the detection of biomarkers for the prediction of certain diseases (Herder *et al.*, 2011) and for the early detection of drug toxicity (Blomme *et al.*, 2009; Harrill *et al.*, 2009; Beger *et al.*, 2010; Rodriguez *et al.*, 2010; West *et al.*, 2010; Van Summeren *et al.*, 2011).

## 1.5 The omics era

The neologism -omics refers to a wide field in modern biology. A schematic representation of the -omics hierarchy is shown in figure 1-5, which leave out some more recently defined -omics e.g. phenomics, miRNAomics or interactomics.

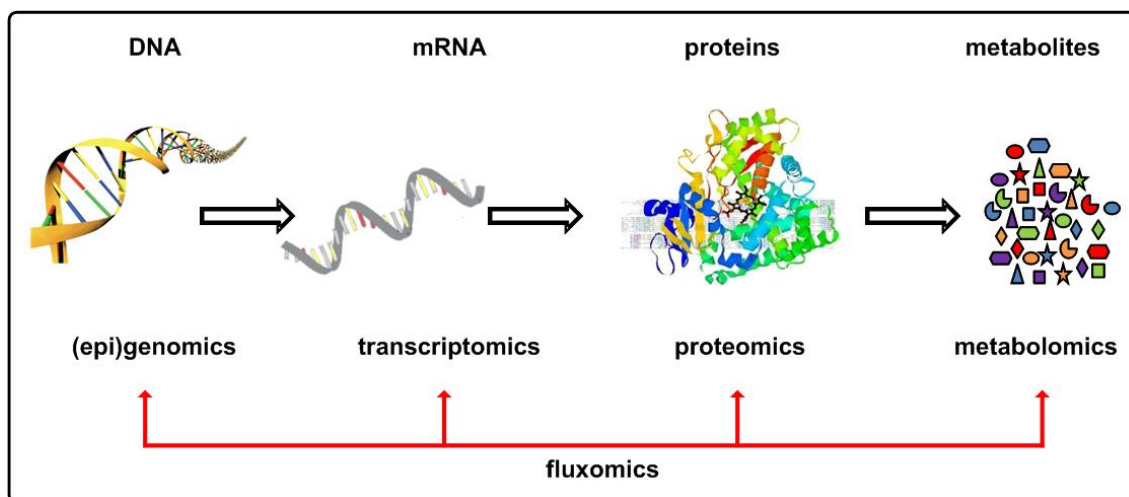


**Figure 1-5: Scheme of the -omics hierarchy: (epi)genomics, transcriptomics, proteomics, metabolomics, fluxomics.**

Genomics, the study of an organisms genes as well as non-coding DNA sequences (the genome), was strongly advanced in recent years due to modern DNA sequencing technologies and international initiatives such as the Human Genome project (Venter *et al.*, 2001). As a newer, but immense promising technology, epigenomics provides information about the effects of chromatin structure on gene function (Gomase and Tagore, 2008), whereas DNA methylation and histone modifications are the major mechanisms.

Transcriptomics, the study of the expression profile in a given cell population at certain conditions, give deep insights into cellular processes e.g. cell differentiation or signalling (Brien and Bracken, 2009; Theunissen *et al.*, 2011).

Proteomics is the qualitative and quantitative study of cellular proteins including their modifications at large scale. In contrast to the genome, the cellular proteome is dynamic and dependent on cell type, differentiation state, cellular environment, extracellular signals and other factors. There is a strong connection between transcriptomics and proteomics, however often no or only weak correlations are found between mRNA and protein amounts e.g. because of different dynamic profiles (Nie *et al.*, 2006; Nie *et al.*, 2007) or regulatory post-transcriptional events.

Metabolomics is defined as the systematic study of the metabolites in a cell, fluid, tissue, organ or organism. In contrast to other -omics technologies, the study of the metabolome is a real snapshot of the cellular physiology of a cell at a specific time point under specific conditions. Therefore, it is interesting to study the metabolic response of an organism, tissue or cell to pathophysiological stimuli such as the exposure to a drug (Nicholson *et al.*, 1999). Metabolomics was successfully applied to biomarker discovery in drug toxicity (Manna *et al.*, 2010; Kleinstreuer *et al.*, 2011; Manna *et al.*, 2011; Stewart and Bolt, 2011; Yang *et al.*, 2011) and can improve preclinical and clinical phases in drug development (Robertson *et al.*, 2011).

Fluxomics or metabolic flux analysis (MFA) provides a quantitative description of the intracellular reaction rates in a certain metabolic network including regulation on (epi)genome, transcriptome, proteome and metabolome level (Niklas and Heinzle, 2011). The fluxes, defined as the turnover rate of metabolites through a metabolic pathway, can be quantified using metabolite balancing or <sup>13</sup>C MFA, whereby a <sup>13</sup>C isotope-labeled substrate is used and fractional labeling of certain metabolites is measured using gas chromatography–mass spectrometry (GC-MS) or NMR (Bonarius *et al.*, 2001). Besides applications like metabolic engineering, metabolic flux analysis can be applied for the detection of drug-induced effects *in vitro* (Strigun *et al.*, 2011a) but also for the improvement of the production of pharmaceuticals by human cell lines (Niklas *et al.*, 2011a; Niklas *et al.*, 2011b; Niklas *et al.*, 2011d).

## **1.6 GCTOF-MS**

GC-MS is an analytical method that combines the features of gas chromatography and mass spectrometry. Thereby, a wide range of small compounds with different chemical properties can be identified within a test sample.

GCTOF-MS combines conventional GC with time-of-flight (TOF) mass spectrometry. In a TOF-MS, a compound is fragmented to ions (in GCTOF-MS typically positive) by electron impact (EI), which are then accelerated through an electric field (figure 1-6).

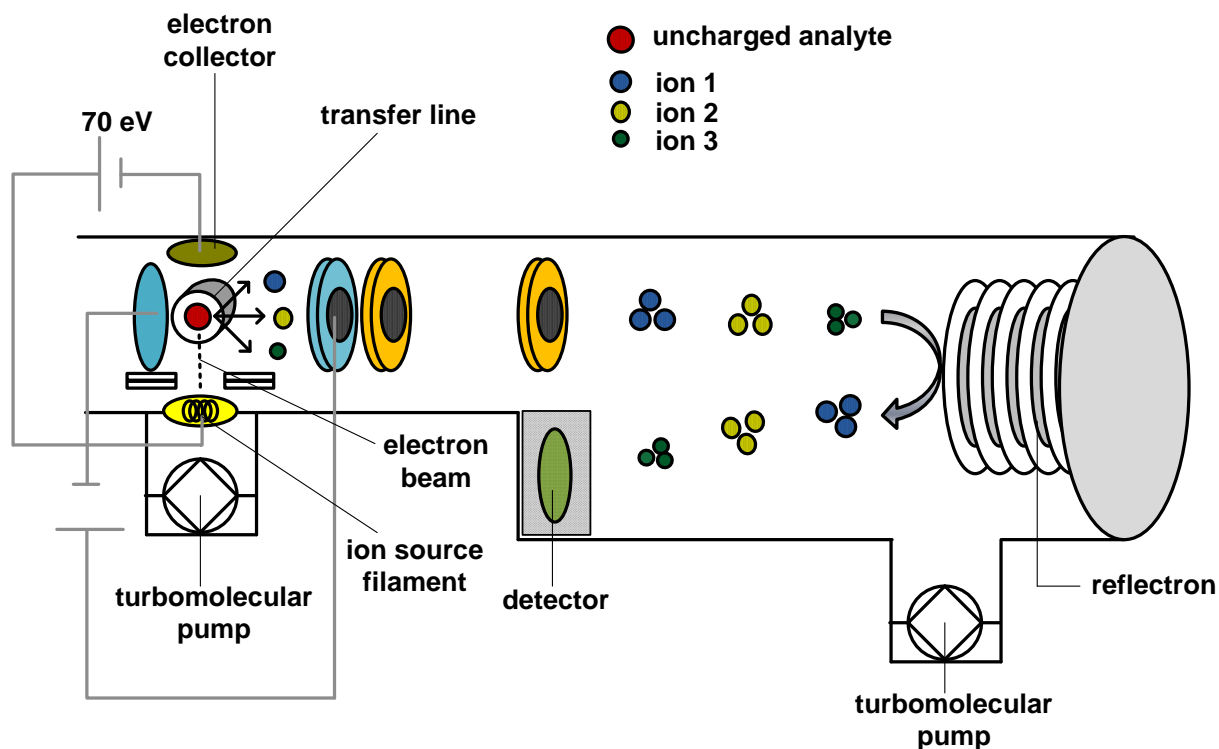


Figure 1-6: Schematic assembly of the time-of-flight tube as component of a GC-TOFMS.

The potential energy for an ion in an electric field is defined as:

$$E_{pot} = z \times U \quad [\text{Eq. 1-1}]$$

Whereas  $z$  is the charge of the ion and  $U$  is the electric voltage. Since the ions are accelerated into the drift region of the TOF tube, the potential energy is converted to kinetic energy, which is defined as:

$$E_{kin} = \frac{1}{2}mv^2 \quad [\text{Eq. 1-2}]$$

Whereas  $m$  is the ion mass and  $v$  the velocity,

$$E_{kin} = E_{pot} \quad [\text{Eq. 1-3}]$$

$$\equiv \frac{1}{2}mv^2 = zU \quad [\text{Eq. 1-4}]$$

Since  $v$  is defined as:

$$v = \frac{d}{t} \quad [\text{Eq. 1-5}]$$

Eq. 1-4 can be converted to:

$$\frac{1}{2}m\left(\frac{d}{t}\right)^2 = z \times U \quad [\text{Eq. 1-6}]$$

Eq. 1-6 can be solved for  $t^2$ :

$$t^2 = \frac{d^2}{2U} \times \frac{m}{z} \quad [\text{Eq. 1-7}]$$

Eq 1-7 can be solved for  $t$ :

$$t = \frac{d}{\sqrt{2U}} \times \sqrt{\frac{m}{z}} \quad [\text{Eq. 1-8}]$$

This shows that the ion flight time in the TOF-tube depends on the mass to charge ( $m/z$ ) ratio. Smaller ions (low  $m/z$ ) reach higher velocities in the field-free drift region than larger fragments (figure 1-6). The time needed to reach the detector is measured for every ion and the mass spectrum is calculated.

Generally, the compounds measured by GC-MS analysis have to be both volatile and thermally stable, because the mobile phase is gaseous and high temperatures  $>300^\circ\text{C}$  are reached. However, most compounds in a biological sample are polar and non-volatile, so that they have to be chemically modified. This derivatization procedure is a key step in GC-MS analysis. *N*-methyl-*N*-trimethylsilyltrifluoroacetamid (MSTFA) is a widely used derivatisation reagent suitable for the silylation of primary amides and amines as well as of hydroxy- and carboxyl-groups. Additionally, carbonyl- and keto- groups are usually methoximated using methylhydroxylamine prior to silylation. This causes the opening of ring sugars and results in two stereoisomers (the *syn*- and *anti*- isomers) which are separated during GC-MS analysis. For quantitative analysis, the derivatization step is one critical point since it is often done manually which could bring in imprecision. Moreover, for larger sample sets, the low stability of the derivatized compounds impairs the analysis. Therefore, automatized sample derivatization is

useful and improves the quality of the analysis. In this study, the automatized two-step chemical derivatization for the GCTOF-MS analysis was established. Thereby, exact volumes as well as constant incubation times for each sample are guaranteed.

## **1.7 Analysis of chromatographic datasets**

Metabolomics analyses by modern state-of-the-art techniques such as NMR or chromatography coupled to mass spectrometry generate huge amounts of datasets. Data acquisition, processing and analysis are highly important. Data processing or pretreatment includes data scaling. Hereby, each variable is divided by the scaling factor. This scaling factor could be the standard deviation of each variable (auto-scaling) or the square root of the standard deviation (pareto-scaling). The overall aim of scaling is to adjust for fold differences between the single metabolites (van den Berg *et al.*, 2006). Peak normalization is also important in metabolomics since differences in sample preparation steps or experimental conditions lead to alterations in peak areas, retention times or derivatization efficiencies. The optimal internal standards would be isotopes (e.g.  $^{13}\text{C}$  labeled) of each analyzed metabolites, because of their identical chemical properties. However, this would drastically rise costs and increase experimental work. Moreover, the analyzed metabolites are often unknown such as in untargeted metabolomics. In this thesis,  $\alpha$ -aminobutyric acid was used as internal standard, as far as known not existing in such biological samples. This amino acid has similar chemical properties as the proteinogenic amino acids analyzed in this study. Moreover, it could be shown that the relative standard deviations (RSD) are reduced after normalization to peak area of the predominant  $\alpha$ -aminobutyric peak (see chapter 4).

Principal component analysis (PCA) is applied in metabolomics to reduce the dimensions in the dataset and to describe the variance in the dataset using a set of underlying orthogonal variables (the principal components). The number of principal components is less than or equal to the number of original variables. The first principal component describes the highest variance. The other components then have the highest variances possible under the constraint that they are uncorrelated with the respective preceding ones. This method is suitable to visualize differences in complete metabolomics datasets, to identify the variables which contribute mostly to the variance and also to detect experimental outliers.

In this thesis, a work flow for metabolomics studies was developed and is depicted figure 1-7. Thereby, the aim was to identify drug-induced effects on different human liver cell models upon single or repeated exposure.

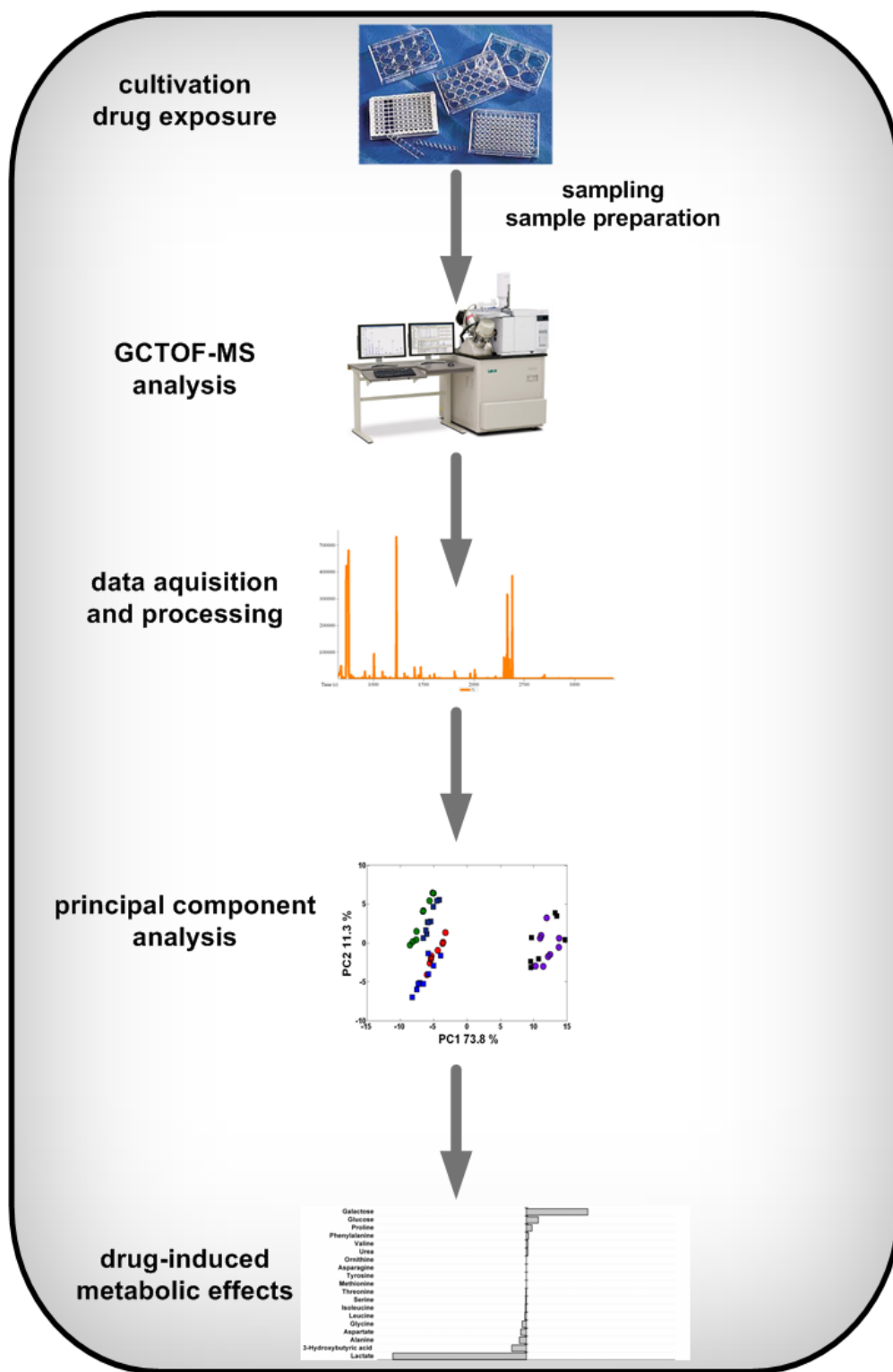


Figure 1-7: Schematic workflow of the developed metabolomics approach.

## 1.8 Aims of the BMBF-project “3D *in vitro* model for hepatic drug toxicity”

The work presented in this thesis was carried within the project “3D *in vitro* model for hepatic drug toxicity”, which was funded by the Bundesministerium für Bildung und Forschung (BMBF) and lasts from February 2008 to December 2011. The project consortium deals with the problem that *in vitro* data for hepatic drug toxicity are only transferable to humans if the *in vitro* environment reflects human liver function. Therefore, the development and in-depth characterization of 3D *in vitro* cell culture models is the main project topic. Moreover, methods for the assessment of drug-induced effects should be established using defined reference substances. Both could lead to a reduction of animal testing in preclinical drug development.

In detail, the project defined 5 major goals:

1. Establishment of methods for the isolation and cultivation of human liver cells
2. Development of a 3D bioreactor perfusion technology for the assessment of drug-induced hepatotoxicity
3. Establishment of read-out parameters for the evaluation of drug-induced hepatotoxicity
4. Investigation of drug-induced hepatotoxicity in 3D- and 2D-cultures using reference substances
5. Evaluation and inter-lab-application of the developed methods

The project consortium consists of five academic and industrial partners (figure 1-8):

1. PHARMACELSUS GMBH, SAARBRUECKEN (PROJECT COORDINATOR)
2. BIOCHEMICAL ENGINEERING INSTITUTE, SAARLAND UNIVERSITY
3. BIOREACTOR GROUP, CHARITÉ UNIVERSITÄTSMEDIZIN BERLIN
4. DEPARTMENT OF TRAUMATOLOGY, TU MUNICH
5. ELEXOPHARM GMBH, SAARBRUECKEN

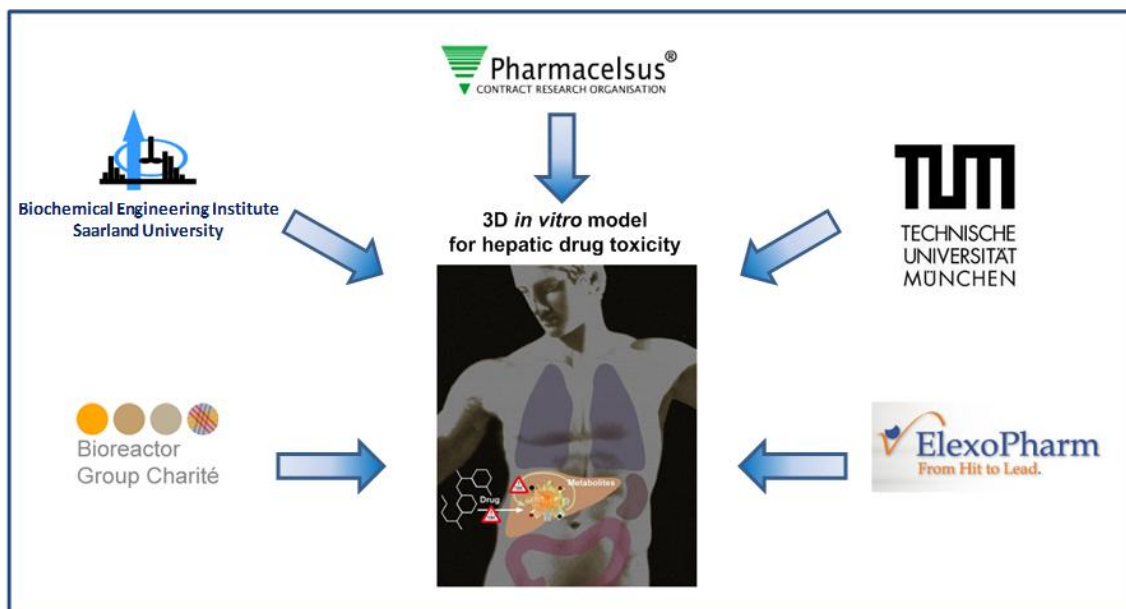


Figure 1-8: Consortium of the BMBF project: “3D *in vitro* model for hepatic drug toxicity”.

## 1.9 Outline of this thesis

Long-term maintenance of organotypic functional cultures of human liver cells is highly needed for the assessment of chronic toxicity and adverse drug reactions. 3D hollow-fiber bioreactors were shown to improve long-term maintenance of primary human hepatocytes (Zeilinger *et al.*, 2004) and to induce the formation of *in vivo* like structures (Gerlach *et al.*, 2003b; Schmelzer *et al.*, 2009). However, an in depth characterization of general and liver specific parameters would lead to a more detailed view on the cellular behavior as well as on long-term viability and functionality.

In **Chapter 2**, primary human hepatocytes of three different donors were cultivated in 3D bioreactors and investigated in terms of liver specific functions (urea and albumin production) during two weeks of cultivation. One single bioreactor was characterized in terms of cell viability (AST, LDH), substrate consumption (glucose, galactose, sorbitol), lactate production, amino acid metabolism and drug metabolizing capacities (CYP450 activity). Moreover, the 3D bioreactor system was modified to allow direct determination of the oxygen uptake rates as indicator of cell viability. Different from 2D cultures, the accurate assessment of cellular viability in the 3D bioreactor is limited due to its black box character. Indirect viability measurements such as substrate consumption are helpful, but metabolic changes during cultivation restrict accurate determination of viable cells. The modifications done in this work permit oxygen uptake rate determination. Nevertheless, a further direct viability assay in the 3D bioreactor would be of high value particularly concerning pharmacological studies.

In **Chapter 3**, the resazurine viability assay, which is well established in 2D cultures, was applied to HepG2 and primary human hepatocytes maintained in the 3D bioreactor system. The assay was proved to be non-invasive, fast and was applied to assess viability upon drug exposure.

In pharmaceutical drug development, high throughput experiments are strongly required e.g. for the assessment of dose response relationships. Using *in vitro* systems, parallel studies are routinely designed in microtiter-plate format, ranging from 6-well to 1536-wells per plate. Three-dimensional cell cultures can be produced in multiwell plates using specific scaffolds, but also by the scaffold-free hanging drop method.

In **Chapter 4**, we applied this method to the human liver cell line HepG2 using the 96 well plate based Gravity<sup>Plus</sup> system (InSphero, Zurich, Switzerland). By this, 3D organotypic cultures of adjustable sizes can be produced which were analyzed including general cellular parameter and long term cultivation at very low serum concentrations. Due to the high reproducibility and the

low amount of required cells, the system could be applied to pharmacological studies. The dose response relationship of the anti-cancer drug tamoxifen was assessed in the organotypic cultures and compared to 2D monolayer and collagen-sandwich cultures. CYP450 induction was investigated as well as toxicity of the anti-cancer drug tamoxifen. The activity of the membrane transporter MRP-2 was analyzed to study mechanisms of chemotherapy resistance. The possibility of high-throughput application and of spheroid size adjustment makes the system attractive for a wide range of research fields.

Every chemical compound is toxic at high doses, but many drugs show adverse effects at low physiological relevant concentrations or only after repeated exposure.

In **Chapter 5** we established a metabolomics-based approach to detect drug-induced effects on primary human hepatocytes as well as on HepG2 cells at physiologically relevant, subtoxic concentrations. The reference drugs diclofenac and troglitazone were tested in single and repeated dose exposure experiments. The effects on the cellular exometabolome were assessed by a combination of GCTOF-MS and PCA. We found that this method is well-suited for the sensitive assessment of drug induced metabolic changes and concluded that it can also be applied to any other alternative testing system.

The assessment of long-term, chronic drug toxicity is still a major hurdle in preclinical drug development using *in vitro* test systems since primary hepatocytes have limited viability and functionality of about one week after isolation. However, chronic toxicity does not occur until long-term repeated dose applications of a drug at low concentrations.

In **Chapter 6**, we assessed chronic diclofenac effects upon repeated dose exposure to primary human hepatocytes which were maintained in long-term serum free cultivation medium. Physiology, viability and drug metabolizing capacities of the cells were analyzed and acute (24 h) and chronic (3 weeks) toxicity of diclofenac in the serum-free medium was measured and compared. Biotransformation of diclofenac as well as chronic drug-induced effects on the exometabolome was investigated. Repeated dose testing using functional *in vitro* systems combined with the developed metabolomics approach can improve drug safety evaluation as alternative to *in vivo* animal based methods.

At the end of this thesis (**Chapter 7**), the main results, achievements and developed methods are summarized and critically discussed in general, whereas the specific results are discussed at the end of each chapter. The outlook provides information about potential future studies and projects and how to further use the results and strategies of this thesis.

# CHAPTER 2: IN-DEPTH PHYSIOLOGICAL CHARACTERIZATION OF PRIMARY HUMAN HEPATOCYTES IN A 3D HOLLOW FIBER BIOREACTOR

This chapter has been published as:

**Mueller D**, Tascher G, Müller-Vieira U, Knobloch D, Nuessler AK, Zeilinger K, Heinzle E, Noor F (2011):

**In-depth physiological characterization of primary human hepatocytes in a 3D-hollow fiber bioreactor**

*Journal of Tissue Engineering and Regenerative Medicine*, DOI: 10.1002/term.418

## **Abstract**

As major research focus is shifting to 3D cultivation techniques, hollow-fiber bioreactors, allowing the formation of tissue-like structures, show immense potential as they permit controlled *in vitro* cultivation while supporting *in vivo* environment. In this study, we carried out a systematic and detailed physiological characterization of human liver cells in a 3D-hollow fiber bioreactor system continuously run for longer than two weeks. Primary human hepatocytes were maintained viable and functional over the whole period of cultivation. Both general cellular functions such as oxygen uptake, amino acid metabolism, substrate consumption and liver-specific functions like drug-metabolizing capacities as well as production of liver-specific metabolites were found to be stable for over two weeks. As expected, donor to donor variability was observed in liver specific functions such as urea and albumin production. Moreover, we show the maintenance of primary human hepatocytes in serum-free conditions in this setup. The stable basal Cytochrome P450 activity three weeks after isolation of the cells demonstrates the potential of such a system for pharmacological applications. Liver cells in the presented 3D bioreactor system could be eventually used not only for long-term metabolic and toxicity studies but also for chronic repeated dose toxicity assessment.

## **2.1 Introduction**

Liver is a complex organ which performs many vital functions including metabolism and detoxification. Hepatocytes are highly polarized cells and their functions depend on extracellular contacts within the tissue. Primary hepatocytes in conventional monolayer culture lose their differentiated state and functions (Kono *et al.*, 1997; Tuschl *et al.*, 2009) rendering them unsuitable for long-term *in vitro* use. Cellular cultivation systems that ensure adequate functioning of hepatocytes will have a tremendous potential for the study of not only pathophysiology of liver but also for toxicological studies especially those involving pharmacological toxicity screening. Such cellular systems must allow 3D maintenance of liver cells so that the rearrangement of cells leading to the formation of microtissues is possible thereby providing a functional *in vitro* test system. Various approaches have been lately reported. The 3D bioreactors, originally developed for extracorporeal liver support as bioartificial liver (BAL) are a step forward towards *in vivo* simulation of tissues and even organs. A hollow fiber cartridge bioreactor with primary rat hepatocytes to evaluate the detoxification properties was reported for clinical purposes (Rodriguez *et al.*, 2008). Others such as the HepatAssist model used cryopreserved primary porcine hepatocytes as cell system (Demetriou *et al.*, 1995). The human hepatoma derived cell line C3A was used in the Extracorporeal Liver Assist Device (ELAD) (Ellis *et al.*, 1996). A further BAL approach, the AMC-BAL (Academic Medical), developed in Amsterdam, Netherlands was applied clinically using primary porcine hepatocytes (Flendrig *et al.*, 1999; van de Kerkhove *et al.*, 2002; van de Kerkhove *et al.*, 2003). Another system, the MELS-BAL (Modular Extracorporeal Liver Support), was developed at Charité Virchow clinic, Berlin, Germany (Sauer *et al.*, 2002). Primary human liver cells from donor organs were charged into the bioreactor and the system used as BAL to a patient after primary graft non-function (PNF) following liver transplantation (aSauer *et al.*, 2003b). A similar system was applied in clinical phase I using primary porcine liver cells. The cell compartment had a volume of about 600 ml and was charged with  $1.8\text{--}4.4 \times 10^{10}$  porcine liver cells (Sauer *et al.*, 2003a). Histological studies on similar bioreactor systems have been reported. The cell morphology and ultrastructure showed that liver cells aggregate to three dimensional, tissue-like structures forming bile-duct like channels within the bioreactor (Gerlach *et al.*, 2003a; Schmelzer *et al.*, 2009).

Obviously, for detailed analytical characterization of human liver cells cultivated in a three dimensional manner, this bioreactor system is limited due to its large volume, requirement for high cell numbers, capacity and closed design. In addition, most of these reported studies were

carried out using animal material. It is now well known that toxicity is species specific (Xu *et al.*, 2004; Uehara *et al.*, 2008; Lauer *et al.*, 2009) due to differences in metabolism and bioactivation. Therefore, for any *in vitro* application, a human relevant cell system is extremely important. Nevertheless, in case of hepatic cells, donor to donor variability as well as limited availability of the primary human hepatocytes (PHH) in sufficient numbers hamper comparative experimental work and replicate measurements at least in commercial bioreactor systems. This bottleneck has led to many studies focusing on alternative primary cells such as the stem cell derived hepatocyte like cells (Snykers *et al.*, 2006; Shiraki *et al.*, 2008), hepatic progenitor cells (Schmelzer *et al.*, 2009; Stachelscheid *et al.*, 2009) as well as differentiation of embryonic stem cells in 3D bioreactors (Gerlach *et al.*, 2010b). Yet no ideal solution for this problem exists currently. Stringent control of primary cells quality and set up parameters in such a bioreactor will give a stable system which is suitable for long-term maintenance of hepatic culture and its characterization. The choice of characterizing parameters, such as initial viability of cells, medium composition, extracellular environment and oxygen, is very important. Liver specific functions are highly dependent on optimum oxygen concentration for metabolic output (Kidambi *et al.*, 2009). Oxygen uptake rate measurement in well-mixed mammalian cell bioreactors was previously reported using liquid or gas phase balances (Eyer *et al.*, 1995; Oeggerli *et al.*, 1995) and was applied for culture medium optimization purposes (Deshpande *et al.*, 2004). Moreover, the *on line* monitoring of oxygen was also shown to be a promising tool in terms of toxicity testing in hepatocyte cultures (Niklas *et al.*, 2009; Noor *et al.*, 2009; Beckers *et al.*, 2010). In a perfused multiwell plate designed for 3D cultivation on scaffolds, oxygen consumption as well as oxygen transport was modeled and consumption rates were measured using optical probes, showing the possibility of long-term maintenance of liver cells on the basis of viability and immunostaining for albumin (Domansky *et al.*, 2010).

Despite these diverse but important studies, there is yet a need for a detailed physiological characterization of liver cells in 3D-hollow fiber bioreactors for its subsequent *in vitro* application. For analytical purposes, we used a miniaturized 3D-hollow fiber bioreactor (purchased from Stem Cell Systems, Germany) with a cell compartment volume of 2 ml.

In order to characterize and improve the bioreactor model, we systematically investigated a whole range of parameters such as the hepatic metabolic functionality as well as other metabolic parameters. To show long-term stability and functionality of the system, we show liver-specific parameters i.e. the production of urea and albumin in three bioreactor runs with PHH of different donors. Because of high donor to donor variability, we present one stable 3D bioreactor with cells from a single donor in detail. Consumption of different substrates, amino

acid metabolism and liver-specific urea and albumin production in the 3D bioreactor were monitored. Aspartate aminotransferase and lactate dehydrogenase activities as parameters for cell viability were measured. Drug metabolizing capacity was determined by CYP activity assay. Moreover, the miniaturized 3D bioreactor system was modified to allow *on line* respiration measurements as an additional indicator of viability *in situ*. Thus the viability and metabolic state of the PHH was monitored kinetically. We carried out a detailed comprehensive physiological study for the evaluation and optimization of this promising 3D cell culture technique using the “gold standard” i.e. the primary human hepatocytes in an attempt to extend its use for other applications such as human relevant screening of drug candidates during preclinical drug development especially for long-term toxicity.

## **2.2 Materials and Methods**

### **2.2.1 Materials**

Williams medium E with Glutamax, HEPES, sodium pyruvate and MEM were purchased from Gibco (Paisley, Scotland, UK). Fortecortin was purchased from Merck (Darmstadt, Germany) and human Insulin from Sanofi Aventis (Frankfurt am Main, Germany). Percoll and fetal calf serum (FCS) was purchased from PAA (Pasching, Austria). Bovine serum Albumin (BSA) was from Sigma-Aldrich (St. Louis, USA). Rat tail collagen was prepared according to a published protocol (Rajan *et al.*, 2006). Hepatocyte transport solution was purchased from Hepacult (Regensburg, Germany). Heparmed, a Williams medium E based, 3D cell culture medium, was from Biochrom AG, Berlin, Germany. This medium was supplemented with insulin (20 IU/l), transferrin (5 mg/l) and glucagon (3 µg/l), all from Biochrom AG, Berlin, Germany. For Cytochrome P450 activity assays, midazolam was purchased from Cerrilant (Wesel, Germany). Bupropion, phenacetin, diclofenac and all other chemicals and solvents of reagent grade were purchased from Sigma-Aldrich, Steinheim, Germany, unless otherwise specified.

### **2.2.2 3D bioreactor system**

The 3D bioreactor (Stem Cell Systems GmbH Berlin, Germany) consists of three interwoven hollow fiber capillary bundles which form four different compartments integrated into a polyurethane housing. Two bundles are made of hydrophilic polyethersulfone membranes with a pore size of 0.5 µm (Membrana, Wuppertal, Germany) and serve for medium supply. These capillary bundles are perfused as depicted in figure 2-1b providing decentral convective mass exchange leading to small solute gradients in the cell compartment. The third bundle consists of hydrophobic multilaminate hollow fiber membranes (MHF, Mitsubishi, Tokyo, Japan) for gas supply. However, in this study, these fibers were filled with sterile water and the oxygen supply was ensured using a different system that allowed for controlled oxygen concentration in the medium. This was necessary for the measurement of oxygen uptake rates. In detail, a small, gas permeable silicone tubing (inner diameter 1.47 mm, wall thickness 0.5 mm; Helix Medical, Carpinteria, USA) was integrated into the system and placed into a gassing unit in front of the 3D bioreactor. Incoming medium was saturated with oxygen by diffusion of air through the silicone tubing. Moreover, 5% CO<sub>2</sub> was also adjusted using this gassing system. The tubing system was equipped with two oxygen sensors (PreSens, Regensburg, Germany), one in front of the bioreactor and one behind (figure 2-1a).

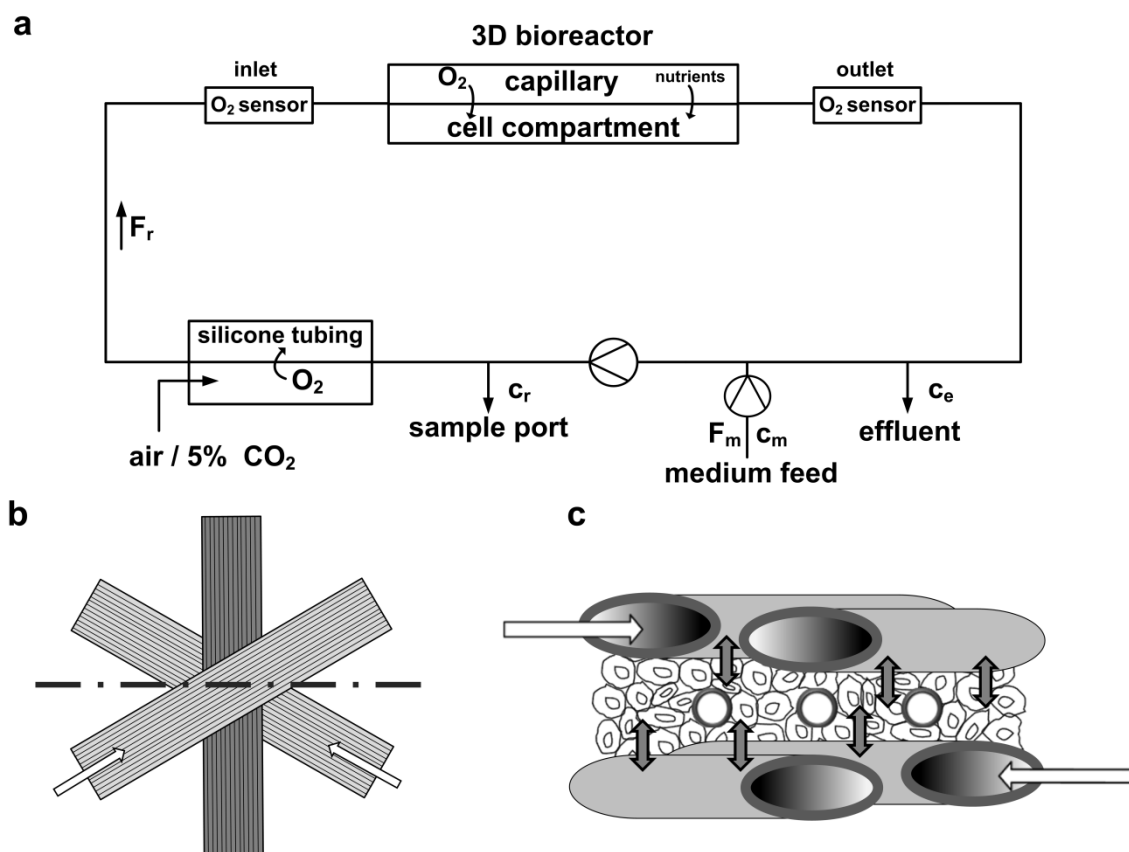


Figure 2-1: a) Schematic representation of 3D bioreactor system. Two pumps for recirculation and feed are integrated in the perfusion system. Sampling is possible via sample port and effluent medium. Medium gassing unit was added in the recirculation system allowing oxygenation of medium using gas-permeable silicone tubing. Oxygen sensors in front and behind the 3D bioreactor as indicated were used for the estimation of oxygen uptake rates. The bioreactor is divided into a capillary system for medium supply and removal and an extra-capillary system serving as cell compartment.  $c_r$  = recirculation concentration;  $F_r$  = recirculation flow rate;  $c_{O_2}$  = oxygen concentration;  $c_e$  = effluent concentration;  $F_m$  = fresh medium flow;  $c_m$  = fresh medium concentration b) Hollow-fibers arrangement within the 3D bioreactor, light grey: medium capillaries, dark grey: gas capillaries (not used in our study and filled with sterile water). The dashed line indicates cross-section for figure 2c c) Cross section of cell compartment and capillary layers of the 3D bioreactor showing nutrients and oxygen exchange locally. Cells are lodged between the capillaries.

The bioreactor polyurethane housing is equipped with separate access ports for each individual capillary bundle. One additional port provides access to silicone rubber tubes (inner diameter 1 mm, AMT, Düsseldorf, Germany) distributed throughout the extra-capillary compartment in

which cells are maintained. This port is used for cell inoculation. The cell compartment has a volume of 2 ml. Figure 1c depicts the cell compartment and capillary layers. The bioreactor is connected to a perfusion system and is enclosed in a Plexiglas chamber providing a constant external temperature of 37.5°C. The perfusion system consists of a recirculation pump for medium perfusion, a feed pump for fresh medium supply and a flow regulator for gas supply. The whole system including tubing and connections has a volume of about 30 ml. Bioreactor and tubing system were assembled in sterile conditions under a laminar flow workbench. After assembly, the bioreactor was connected to the perfusion system and rinsed with PBS. Schemes of the 3D bioreactor system, the capillaries and the cell compartment are shown in figure 1a, b and c respectively. Before cell inoculation, the PBS was replaced by culture medium supplemented with 2.5% FCS and equilibrated for 24 hours.

### **2.2.3 Primary human hepatocytes and 3D bioreactor**

Hepatocytes from resected liver tissues from patients with primary and secondary tumors were used. Tissue collection was done according to the institutional guidelines and with the patient's written consent. The liver tissues used for hepatocyte isolation were selected under stringent control with the surgical resection area left untouched. Chosen tissue material was regularly checked for small satellite tumors and the isolation was aborted upon finding these. Therefore, only tumor free tissue was used on the basis of visual and physical check up. Hepatocytes were isolated using a two-step collagenase P (from *Clostridium histolyticum*) perfusion technique, followed by a Percoll density gradient centrifugation (Nussler *et al.*, 2009). The purity and viability was determined under light microscopy using trypan blue exclusion. The non-parenchymal contribution was estimated to be 5-10% from cell size and shape under the microscope. 90-95% cells were large polygonal binucleated hepatocytes.

Prior to inoculation into the bioreactor, cells were again counted and viability assessed using trypan blue exclusion method.  $1.0-1.1 \times 10^8$  viable PHH were re-suspended in 7 ml Heparmed medium supplemented with 2.5% FCS and transferred to a 10 ml syringe which was afterwards connected to the cell inoculation port of the bioreactor via Luer-Lok connection. Cell suspension was injected into cell compartment slowly and 5 ml culture medium was injected afterwards bringing all cells into the cell compartment. Heparmed was used as cultivation medium during the whole bioreactor run. After cell inoculation, medium was continuously circulated through the bioreactor system with a recirculation rate of 7 ml/min. This flow rate was chosen to ensure retention of the medium in the 3D bioreactor for the measurement of the oxygen differences between the bioreactor in- and outlet and at the same time avoiding oxygen

limitation. Fresh medium was fed into the system with a feed rate of 1.5 ml/h resulting in an identical effluent flow rate. However, during Cytochrome P450 activity assays no fresh medium was supplied. The bioreactors were switched to serum free conditions after day 9-10. Daily samples were taken via sample port and effluent medium.

#### **2.2.4 Oxygen consumption**

Oxygen partial pressures were monitored and measured automatically using the oxygen sensors connected to a 4-channel fiber optic meter (OXY-4) with Oxy4v2-software (PreSens, Regensburg, Germany). During cultivation, measurements were carried out in time intervals of 5 minutes. Data was obtained as % air saturation or dissolved oxygen values. Oxygen uptake rates were calculated using the following equation:

$$OUR = F_r \times (c_{O_2,in} - c_{O_2,out}) = F_r \times \Delta c_{O_2}$$

where *OUR* is the oxygen uptake rate,  $F_r$  represents the medium recycle flow rate through the bioreactor (7 ml/min),  $c_{O_2,in}$  and  $c_{O_2,out}$  are the dissolved oxygen concentrations in front and behind the bioreactor respectively (figure 1a).

#### **2.2.5 AST and LDH activities**

The activity of liver-specific aspartate aminotransferase (AST) in the culture supernatant was determined using a kinetic UV assay kit (Hitado, Möhnesee-Delecke, Germany) according to manufacturer's instructions. The activity of lactate dehydrogenase (LDH) in the culture supernatant was determined using a colorimetric enzymatic assay kit (Cytotoxicity Detection Kit; Roche, Grenzach, Germany). For both a dilution series of standard serum (NobiCal-Multi, Hitado, Möhnesee-Delecke, Germany) was measured in parallel for quantification.

#### **2.2.6 Quantification of substrates, organic acids and amino acids**

D-glucose, D-galactose, D-sorbitol and L-lactate concentrations in recirculation and effluent samples were determined using routinely utilized enzymatic kits (R-Biopharm, Darmstadt, Germany). The assays were performed according to the instructions of the manufacturer. Amino acids were quantified by high performance liquid chromatography (HPLC, Agilent 1100, Agilent Technologies, Germany) equipped with a C18-RP-column (Gemini® 5uC18 110°A, 150x4.6mm, Phenomenex, Aschaffenburg, Germany) and with automated *on line* derivatization (Kromer *et al.*, 2005). 40 mM NaH<sub>2</sub>PO<sub>4</sub> (pH=7.8) was used as eluent A and a mixture of

acetonitril-methanol-water (45:45:10) was used as eluent B in a gradient elution. Flow rate was adjusted to 1 ml/min; the column temperature was set at 40°C. Peaks were detected using a fluorescence detector at 340 nm excitation and 450 nm emission wavelengths.  $\alpha$ -amino butyric acid was used as internal standard for quantification.

### **2.2.7 Urea and albumin**

Urea was quantified in recirculation and effluent samples using a colorimetric enzymatic test kit (Hitado, Möhnese-Delecke, Germany). Albumin concentration was determined via an enzyme-linked immunosorbent assay (ELISA) (Albuwell II; Exocell, Philadelphia, USA). Both assays were performed according to manufacturer's instructions.

### **2.2.8 Cytochrome P450 activity assay**

The functional enzyme activity test for CYP1A2, CYP2B6, CYP2C9 and CYP3A4 was performed in a cassette approach based on probe reactions. Samples were taken until 6 hours after injection. The system was kept in recirculation mode without feeding during the CYP activity assays. After 6 hours feed mode was adjusted. The probe substrates, their test concentrations and the products used for the quantification of the enzyme reactions are summarized in table 2-1.

**Table 2-1: Substrates, products and metabolizing enzymes used for Cytochrome P450 activity assay**

<b>Substrate</b>	<b>Product</b>	<b>Enzyme</b>	<b>c (Substrate) [<math>\mu</math>M]</b>	<b>LC/MS-MS transition reaction [<math>m/z \rightarrow m/z</math>]</b>
Phenacetin	Acetaminophen	CYP1A2	26	152.1 $\rightarrow$ 65.0
Bupropion	OH-bupropion	CYP2B6	100	256.2 $\rightarrow$ 139.0
Diclofenac	4-OH-diclofenac	CYP2C9	9	312.1 $\rightarrow$ 231.0
Midazolam	1-OH-midazolam	CYP3A4	3	342.1 $\rightarrow$ 203.0

### 2.2.9 Quantification of metabolites by LC-MS/MS

The HPLC system consisted of an MS Plus pump (Surveyor) and an AS Plus auto sampler (Surveyor). Mass spectrometry was performed on a TSQ Quantum Discovery Max triple quadrupole mass spectrometer equipped with either a heated electrospray (H-ESI) interface (for analysis of hydroxybupropion, 1-hydroxymidazolam and 4-hydroxydiclofenac) or an APCI probe (for analysis of acetaminophen), respectively, connected to a PC running the standard software Xcalibur 2.0.7 (Thermo Fisher Scientific, USA). The flow rate was set to 300  $\mu$ l/min and the compounds were separated on an Uptisphere OBD, 3  $\mu$ m, 100x2.1 mm (Interchim, France) analytical column with a pre-column (Uptisphere OBD, 3  $\mu$ m, 10x2.0 mm, Interchim, France). Gradient elution with acetonitrile/0.1% formic acid as organic phase (A) and 10 mM ammonium formate/0.1% formic acid as aqueous phase (B) was performed using the following gradient: % A (t (min)): 5(0-0.2)-97(1.8-4.3)-5(4.5-7.0). The MS-MS identification of characteristic fragment ions was performed using a generic parameter set: ion source temperature 350°C, capillary voltage 3.8 kV, collision gas 0.8 mbar argon, spray and sheath gas, 20 and 8 (arbitrary units), respectively. The stable product ions with the highest S/N ratio were used to quantify the analyte in the selected reaction monitoring mode (SRM). The transitions used for MS/MS analysis are given in table 2-1.

### **2.2.10 Calculation of metabolite consumption/production rates**

Following equation was used for the calculation of substrate consumption and product formation rates:

$$V_r \frac{dc_r}{dt} = F_m (c_m - c_e) + r$$
$$\Leftrightarrow r = V_r \frac{c_{r,tx} - c_{r,tx-1}}{\Delta t} - F_m (c_m - c_e)$$

where  $r$  = specific production/consumption rate;  $V_r$  = recirculation volume;  $tx$  = timepoint  $x$  [d];  $tx-1$  = timepoint  $x - 1$  [d];  $F_m$  fresh medium inflow rate (1.5 ml/hr);  $c_r$ ,  $c_m$  and  $c_e$  represent the concentration of a respective metabolite in recirculation, fresh and effluent medium.

## **2.3 Results**

### **2.3.1 Long-term stability of the 3D bioreactor**

Viability of PHH before inoculation into the bioreactor was assessed by trypan blue exclusion method. The viability of the inoculated cells from three donors was 62, 72 and 81% for the respective bioreactor runs.  $1.0 - 1.1 \times 10^8$  viable cells were inoculated into the 3D bioreactor. The 3D bioreactors were run for 3-4 weeks. Liver specific functions i.e. urea and albumin production were monitored and quantified for two weeks (figure 2-2a and b) to determine long-term stability of the PHH within the bioreactor. The three time points day 1, 6-7 and 14 were chosen because no system disturbances such as CYP 450 activity assay were carried out around these days.

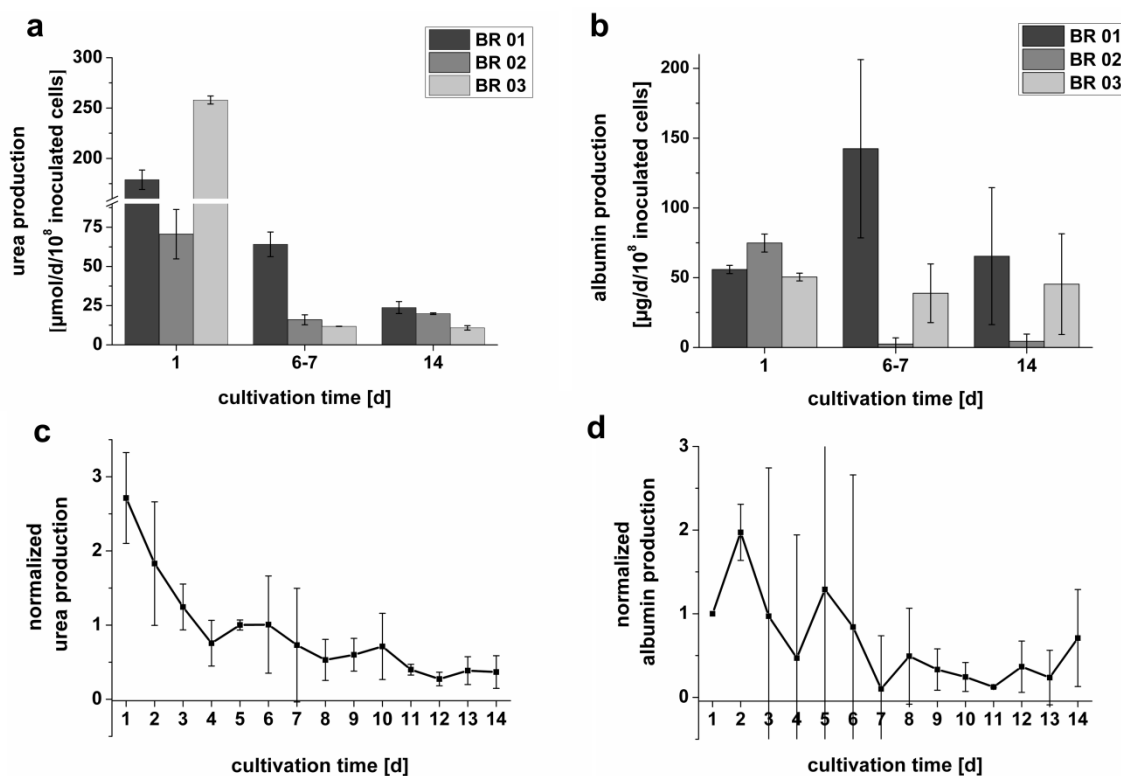


**Figure 2-2:** Liver specific parameters of primary human hepatocytes from three different donors cultivated in 3D bioreactors a) Urea production rates at days 1, 6-7 and 14 for BR 01–03, error bars indicate standard deviation ( $\pm$ SD, n=3) b) albumin production rates at days 1, 6-7 and 14 for BR 01–03, error bars indicate standard deviation ( $\pm$ SD, n=2) c) mean urea production in three bioreactor runs during two weeks of cultivation, normalized to starting value (day 3-4). Error bars indicate standard deviation ( $\pm$ SD, N=3, n=3) d) mean albumin production in three bioreactor runs during two weeks of cultivation normalized to starting value (day1). Error bars indicate standard deviation ( $\pm$ SD, N=3, n=2).

It was observed that the three bioreactors (BR 01-03) produced urea and albumin over two weeks of cultivation, but with high differences in absolute values between the single runs. The differences in viability of the inoculated cells, as well as the individual phenotypes and case history of the respective patient lead to high variance in cellular performance. Normalization to the starting values (day 3 and 4 for urea, day 1 for albumin), as seen in figure 2-2c and d, indicates long-term viability of PHH in the 3D bioreactors. For urea production, days 3 and 4 were chosen as starting values for normalization since during first two days of inoculation high extracellular urea production was observed mostly due to cell death releasing enzymes in the medium. Because of high donor to donor differences, we present in detail a single bioreactor (BR 03) including measurements for oxygen uptake rates, viability parameters,

consumption/production rates, amino acid metabolism and CYP activity in PHH in this bioreactor.

### 2.3.2 Viability parameters

Oxygen measurements showed significant differences between bioreactor in- and outlet soon after inoculation indicating rapid oxygen consumption by the cells in the presented bioreactor (figure 2-3).

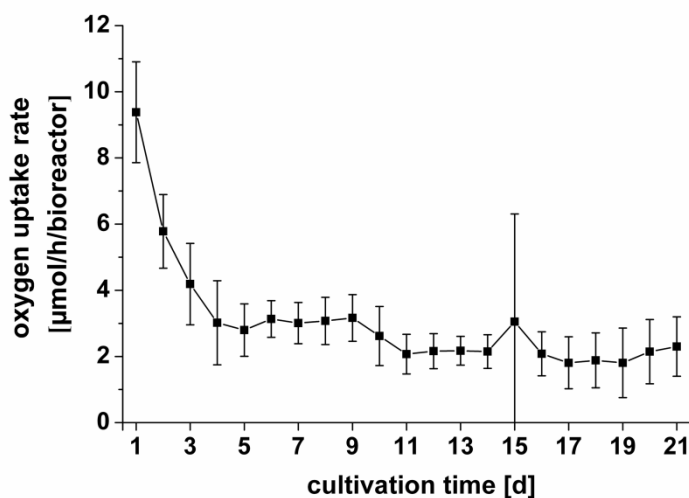


**Figure 2-3: Mean oxygen uptake rates in primary human hepatocytes in a 3D bioreactor system monitored for 21 days after inoculation.  $1.1 \times 10^8$  viable cells were inoculated in the bioreactor. Measurements were carried out at intervals of 5 minutes. Error bars indicate standard deviation of daily mean values (total of 288 measurements per day).**

At cultivation day 1, specific oxygen uptake rate reached a mean value of 9.4  $\mu\text{mol/h}$  which stabilized to a nearly constant value of about 3  $\mu\text{mol/h}$  at day 4 until day 21.

As further viability parameters, liver-specific AST activity as well as LDH activity in effluent samples was measured for two weeks (figure 2-4 a and b).

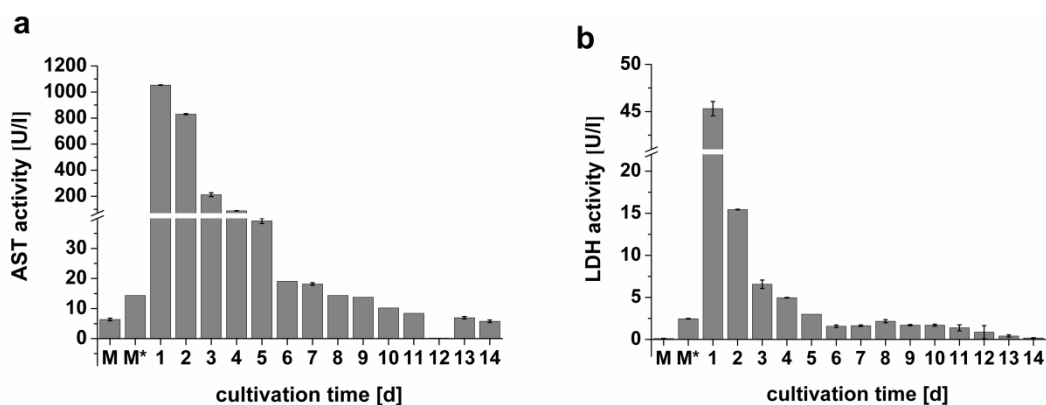


**Figure 2-4: a) AST activity b) LDH activity, both measured in effluent samples during two weeks of cultivation of primary human hepatocytes in single 3D bioreactor inoculated with  $1.1 \times 10^8$  cells. M = medium w/o FCS; M\* = medium supplemented with 2.5% FCS. Error bars indicate standard deviation of duplicate measurements.**

The culture medium shows an intrinsic AST activity of 14 U/l when supplemented with 2.5% FCS. The AST activity was highest at cultivation day 1 (1053 U/l) after inoculation and decreased afterward. At day 8, basal activity levels due to FCS, were reached in the bioreactor.

The LDH activity was highest (45 U/l) on the first day of cultivation which decreased continuously to the basal level (2.5% FCS) within a few days. Upon switching to FCS free conditions (day 9), both AST and LDH activities further decreased to non detectable levels (figure 2-4 a and b).

### 2.3.3 General cellular parameters

General cell functions including substrate consumption (medium contained glucose, galactose and sorbitol) and lactate production at day 1, 7 and 14 are depicted in figure 2-5.

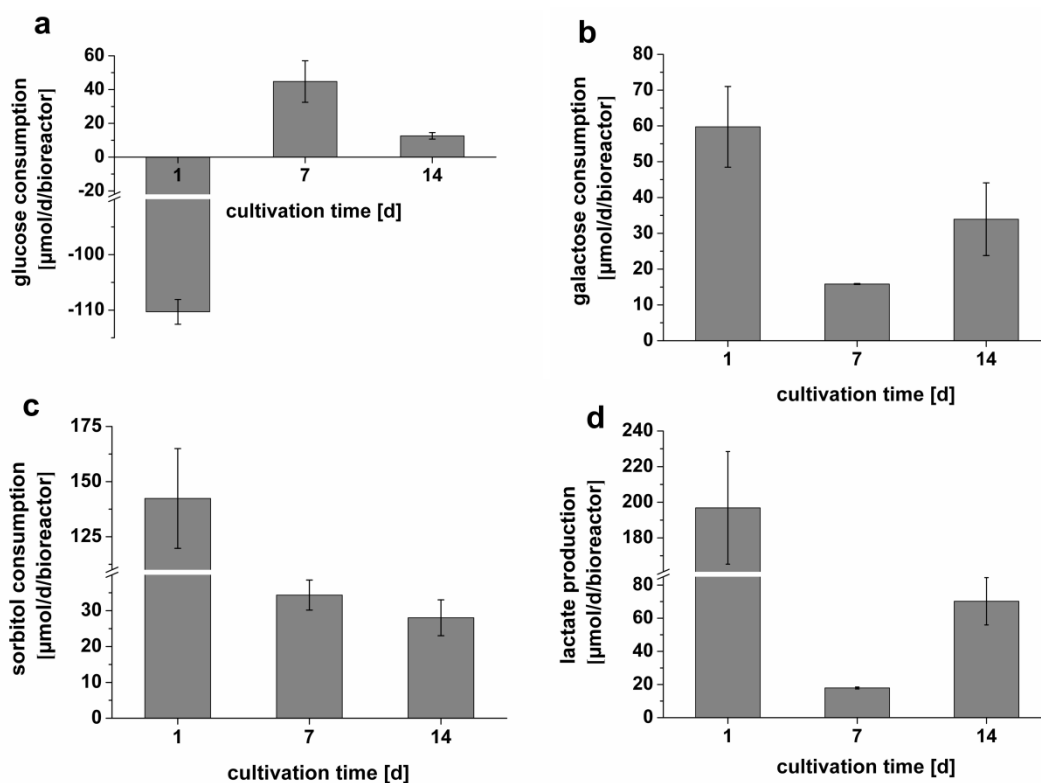


Figure 2-5: General cellular parameters of primary human hepatocytes cultivated in single 3D bioreactor inoculated with  $1.1 \times 10^8$  cells a) glucose consumption rates b) galactose consumption rates c) sorbitol consumption rates d) lactate production rates; at cultivation days 1, 7 and 14 respectively. Rates were calculated from recirculation and effluent samples. Error bars indicate standard deviation ( $\pm$ SD, n=3).

At the first cultivation day, glucose was released by the cells with a secretion rate of  $110 \mu\text{mol/d}$ . At cultivation day 7, glucose was net consumed at a rate of  $45 \mu\text{mol/d}$  which decreased to a value of  $13 \mu\text{mol/d}$  at cultivation day 14. The glucose isomer galactose as well as sorbitol, the polyolform of glucose, were both consumed in the 3D bioreactor during cultivation. Concentrations of lactate were determined, showing a lactate production rate of  $197 \mu\text{mol/d}$  at the first cultivation day, whereas  $18 \mu\text{mol}$  and  $70 \mu\text{mol}$  lactate were produced at day 7 and 14 respectively. For the investigation of amino acid metabolism, 19 proteinogenic amino acids (contained in the culture medium) as well as ornithine were quantified in bioreactor recirculation samples. Table 2-2 summarizes the specific rates of all investigated general metabolites.

**CHAPTER 2: IN-DEPTH PHYSIOLOGICAL CHARACTERIZATION OF PRIMARY HUMAN HEPATOCYTES IN A 3D HOLLOW FIBER BIOREACTOR**

**Table 2-2: Metabolite uptake and secretion rates in  $\mu\text{mol/d} \pm\text{SD}$  (n=3). Negative values indicate net release.**

<b>Metabolite</b>	<b>day 1</b>	<b>day 7</b>	<b>day 14</b>
Arginine	302.40 $\pm$ 0.55	24.68 $\pm$ 4.96	16.63 $\pm$ 1.13
Histidine	70.75 $\pm$ 3.47	15.93 $\pm$ 2.16	13.77 $\pm$ 0.79
Aspartate	63.89 $\pm$ 10.13	16.38 $\pm$ 3.06	10.42 $\pm$ 1.34
Asparagine	28.71 $\pm$ 5.33	11.71 $\pm$ 3.98	10.52 $\pm$ 1.22
Glycine	26.89 $\pm$ 5.45	8.65 $\pm$ 1.10	4.56 $\pm$ 0.11
Proline	14.41 $\pm$ 1.03	6.40 $\pm$ 1.19	1.84 $\pm$ 0.05
Phenylalanine	12.00 $\pm$ 1.44	5.97 $\pm$ 1.90	2.76 $\pm$ 0.46
Leucine	6.85 $\pm$ 2.66	3.76 $\pm$ 1.86	4.76 $\pm$ 0.85
Glutamine	2.95 $\pm$ 0.84	3.64 $\pm$ 1.45	-2.36 $\pm$ 0.60
Tryptophan	0.20 $\pm$ 1.28	0.82 $\pm$ 0.55	1.70 $\pm$ 0.42
Lysine	-0.11 $\pm$ 1.85	0.07 $\pm$ 1.23	-0.43 $\pm$ 0.22
Methionine	-2.76 $\pm$ 1.15	-0.85 $\pm$ 0.72	-0.96 $\pm$ 0.29
Isoleucine	-4.23 $\pm$ 2.50	-0.49 $\pm$ 1.73	-0.46 $\pm$ 0.08
Valine	-7.66 $\pm$ 3.80	-3.66 $\pm$ 2.26	-3.25 $\pm$ 0.17
Threonine	-8.50 $\pm$ 4.22	-1.25 $\pm$ 2.76	-1.27 $\pm$ 0.16
Serine	-10.18 $\pm$ 4.30	-2.51 $\pm$ 2.07	-2.36 $\pm$ 0.17
Glutamate	-22.34 $\pm$ 8.13	6.04 $\pm$ 2.14	5.32 $\pm$ 0.87
Alanine	-22.48 $\pm$ 2.06	-2.62 $\pm$ 1.14	-0.41 $\pm$ 0.06
Tyrosine	-53.48 $\pm$ 9.28	-19.87 $\pm$ 1.51	-28.10 $\pm$ 3.24
Ornithine	-75.3 $\pm$ 4.31	-5.15 $\pm$ 1.32	-1.44 $\pm$ 0.47
Glucose	-110.33 $\pm$ 2.24	44.78 $\pm$ 12.28	12.60 $\pm$ 1.93
Galactose	59.73 $\pm$ 11.28	15.84 $\pm$ 0.13	33.94 $\pm$ 10.15
Sorbitol	142.32 $\pm$ 22.62	34.35 $\pm$ 4.20	28.02 $\pm$ 5.01
Lactate	-196.85 $\pm$ 31.59	-17.93 $\pm$ 0.59	-70.20 $\pm$ 14.18

A net consumption of 9 proteinogenic amino acids from culture medium was found at cultivation day 1. Arginine was found to be consumed at a highest rate of 302  $\mu\text{mol/d}$ . Ornithine was produced at a rate of 75  $\mu\text{mol/d}$ . Aspartate, asparagine and histidine were also taken up whereas glutamate, alanine and tyrosine were net produced at day 1. On day 7, arginine consumption decreased tremendously to a rate of 25  $\mu\text{mol/d}$ . In parallel, ornithine production also decreased. Overall, a similar amino acid profile was observed from day 7 and onwards. For methionine and tryptophan, no significant net uptake or release could be detected during cultivation.

#### **2.3.4 Liver specific drug-metabolizing function**

To assess liver specific drug-metabolizing function, CYP 450 activity assay was performed at cultivation day 5 and 18, i.e. metabolizing capacities at the beginning and at the end of the culture. Activities of CYP2B6, CYP1A2, CYP2C9 and CYP3A4 in terms of product formation rates are shown in figure 2-6.

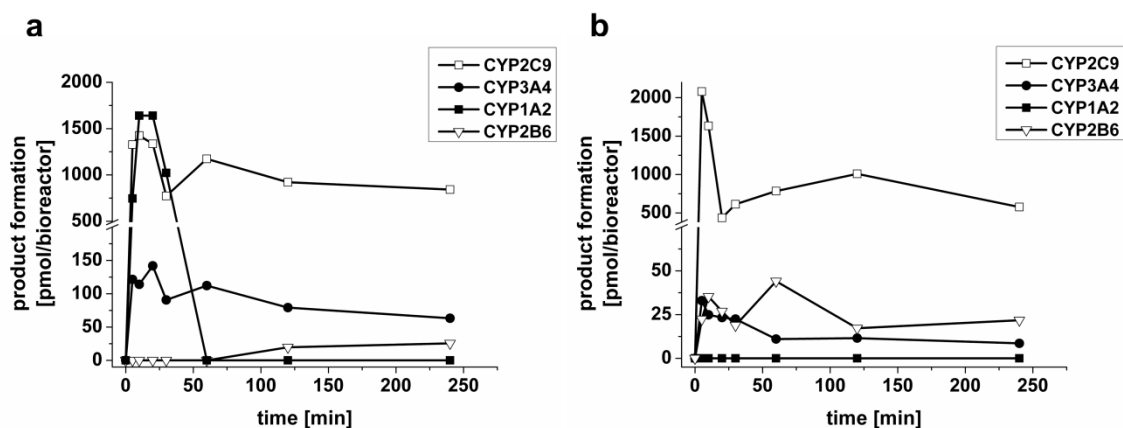


Figure 2-6: Activity of CYP 450 isoenzymes in a single 3D bioreactor a) at cultivation day 5 b) at cultivation day 18. Activity was determined by the formation rate of 1-OH-midazolam (CYP3A4), 4-OH-diclofenac (CYP2C9), OH-bupropion (CYP2B6) and acetaminophen (CYP1A2). Assay duration was 6h.

Rates of formation of the investigated CYP isoform products after 6 hours assay time and the comparison of activities between cultivation day 5 and 18 are shown in table 2-3.

Table 2-3: Formation of specific CYP products at the end of assay (6h) at cultivation day 5 and 18 showing % remaining activities.

CYP 450 isoform	pmol formation		remaining activity [%]
	day 5	day 18	
CYP2C9	842	577	69
CYP3A4	63	9	13
CYP2B6	25	22	86
CYP1A2	_*	_*	-

\*product substrate of CYP3A4 and CYP2C9

The comparison between day 5 and day 18 shows remaining activities of 13%, 69% and 86% for the respective CYP isoforms almost 3 weeks after isolation.

## 2.4 Discussion

In-depth characterization of PHH in a miniaturized 3D hollow fiber bioreactor was carried out in this study monitoring viability as well as general cellular and liver specific functions for long-term cultivation. Three individual 3D bioreactors using cells from different donors were compared. Urea, as marker for intracellular ammonia detoxification, was steadily produced in the 3D bioreactors with highest rates at the start of the culture. The high urea production during first two days of cultivation is mainly due to the release of intracellular urea through damaged cell membranes during inoculation as well as the extracellular production of urea by arginase I which was accompanied by the production of ornithine. After this initial phase, the average urea production in three bioreactors was quite constant with donor to donor variability resulting in large standard deviations. Since the viability (ranging from 62% - 81%) at inoculation into the bioreactors was different for each run, it is quite difficult to compare all measured parameters due to high variations in values for each of the three bioreactors. We therefore focus on a single bioreactor with an initial viability of 72%, which was observed to be sufficient for a stable bioreactor run as shown by constant oxygen uptake rates. In this bioreactor constant urea production rates were observed during 2 weeks of cultivation. An *in vivo* urea production of 260  $\mu\text{mol/d}/10^8$  cells was previously reported (Bhatia *et al.*, 1999). In an *in vitro* two-dimensional culture, a urea production of  $15 \pm 7.5 \mu\text{mol/d}/10^8$  cells after 3 days of isolation and  $6 \pm 8 \mu\text{mol/d}/10^8$  cells after 17 days of isolation was recently reported using cells of 6 different donors (Lubberstedt *et al.*, 2010). In the presented study, average urea production rates of  $44 \pm 21 \mu\text{mol/d}/10^8$  inoculated cells at cultivation day 4 and  $18 \pm 7 \mu\text{mol/d}/10^8$  inoculated cells at cultivation day 14 in the 3D bioreactor (N=3) lie between *in vivo* and 2D-*in vitro* values. However, the inoculated cell number in the 3D bioreactor system which was used for normalization does not represent the actual number of living cells within the bioreactor because of initial certain loss of cells due to inoculation. As such, specific urea production per cell is probably higher than the above calculated values and therefore even closer to physiological *in vivo* situation. Albumin is produced *in vivo* at a rate of  $4.8 - 7.2 \text{ mg/d}/10^8$  cells (Bhatia *et al.*, 1999). Compared to production rates in presented 3D bioreactor system, this *in vivo* rate is 30-500 times higher, depending on cultivation time and cell performance. Again, the inoculated cell number used for normalization does not reflect actual number of viable cells. However, the low calculated albumin production rates is probably due to the binding of the protein to the capillaries within the 3D bioreactor resulting in its retention in the cell compartment, so that lower concentrations were observed in the ex-bioreactor samples. This inherent limitation of the presented bioreactor system poses a problem in proteomics based assays.

In addition, reported 3D bioreactor cultivation systems often lack a possibility of direct cell viability monitoring. Commonly, this is done by indirect methods such as calculation of substrate consumption or LDH release. Measuring oxygen concentrations with optodes is a sensitive and non-invasive tool not only for viability assessment but also for respiration studies in terms of metabolic state of the cells. We demonstrate the integration of oxygen concentration monitoring by modifying the system and establishing a method of *on-line* oxygen monitoring allowing *in situ* estimation of cell viability over the whole period of 3D bioreactor cultivation. Figure 3 depicts the oxygen uptake rate in a single bioreactor. At the first day of cultivation, the highest oxygen consumption was observed. This indicates a hypermetabolic state during culture equilibration phase. In this phase, cell attachment and spreading takes place which strongly depends on oxygen supply (Rotem *et al.*, 1994). The energy required for this cellular process leads to high oxygen uptake rates in this phase. During cultivation, constant oxygen consumption was recorded from day 4 until day 21. Our results show that exact monitoring of oxygen is very important for gaining insights on the actual physiological state of the cells during different phases of cultivation and for identifying changes in metabolic activity due to physiological or environmental challenges, e.g. exposure to a drug or toxic compound. The continuous monitoring of oxygen upon and during exposure to a test compound will also allow determining the kinetics of a toxic response. This in turn is of extreme usefulness when a long-term response is evaluated. As the presented bioreactor system can be run in recirculation and feed mode, this allows the possibility of repeated dose testing which more closely reflects the *in vivo* situation when compared with other systems. Moreover, since mitochondrial effects are one of the major causes of idiosyncratic hepatotoxicity (Labbe *et al.*, 2008), the measurement of respiration is assumed to provide valuable help in identifying toxicity potential of test compounds that affect the mitochondria resulting in altered respiratory chain activity. Regarding AST and LDH enzyme activity, in the same bioreactor, as indicator of cell viability, inoculation of the liver cells into the bioreactor caused a certain loss of viable cells resulting in activity maxima at the first cultivation day. After the equilibration phase of 4-5 days, activities of both enzymes were at low levels corresponding to the basal activity of medium containing 2.5% FCS. The switch to serum-free conditions at cultivation day 9 further decreased these activities showing constant viability of the liver cells for the rest of the cultivation period. It was observed (data not shown) that complete removal of FCS from the bioreactor is gradual. The proteins in FCS seem to bind within the bioreactor system and could be detected days after the system is switched to serum free medium. This again poses a challenge to proteomics based studies.

As general cellular functional parameter, specific consumption rates of three substrates (glucose, galactose and sorbitol) as carbon sources were analyzed. Glucose was released extensively at the first cultivation day. A release of glucose soon after isolation has been previously reported (Pless *et al.*, 2006). It can be explained by the release of intracellular glycogen in form of monomeric glucose. The other two substrate (galactose and sorbitol) consumption rates were highest at day 1. Correspondingly, lactate production reached its maximum on the first day. These high substrate consumption and product formation rates also indicate a hypermetabolic state at the beginning of the culture. At day 7 and 14, a low consumption of glucose as well as consumption of galactose and sorbitol as additional energy sources was observed. Hereby, the uptake of sorbitol is insulin-independent and it was recently shown that both galactose and sorbitol consumption could be used for the assessment of cell performance in liver bioreactors (Gerlach *et al.*, 2010a).

The quantification of amino acids reveals a net uptake of 9 proteinogenic amino acids by the PHH at cultivation day 1. Arginine showed the highest consumption rate of all amino acids. This can partly be explained by extracellular degradation of arginine by arginase I which converts arginine to urea and ornithine (Peters *et al.*, 2008). The high ornithine production measured at day 1 supports this assumption. The enzyme is released into the extracellular environment after cell death during the inoculation procedure. This is further supported by AST and LDH activity measurements. The decrease in both enzyme activities to the basal-level of the medium control and finally to almost non-detectable values shows that after initial stress, the viability of the surviving inoculated cells is ensured during the investigated cultivation time of two weeks. However, arginine is an important precursor not only for protein synthesis but also for several intracellular pathways. It plays a major role in urea cycle as well as in creatine synthesis and can also be converted to nitric oxide (NO) by inducible NO synthase (iNOS). NO is a signaling molecule involved in a wide range of biological processes, both protective and toxic. In liver cells, NO can carry out a cytoprotective effect *in vitro* by the inhibition of caspases (Diesen and Kuo, 2009). It was also reported that NO generation is stimulated by shear stress (Ulker *et al.*, 2010), which also occurs during 3D bioreactor inoculation. This increased cellular need for arginine as precursor could also contribute to the high arginine uptake rate during equilibration phase. The high aspartate consumption at day 1 can be explained by AST activity in the 3D bioreactor after cell inoculation. For cultivation day 7 and 14, the overall pattern of amino acid metabolism was constant. This shows again the functionality and stable phenotype of the PHH during longer cultivation times. Further analyses

focusing on metabolic flux analysis to get a more detailed insight into the amino acid metabolism in primary hepatocytes in the 3D bioreactor system is underway in our laboratory. CYP activity assay shows that all investigated CYP 450 isoforms were active at cultivation day 5 including CYP3A4, the major isoform involved in the metabolism of a large number of xenobiotics in the liver. At cultivation day 18 (day 20 after cell isolation), CYP2C9, CYP3A4 and CYP2B6 basal activities, i.e. without induction, could still be detected. Their respective activities compared to day 5 were 69% for CYP2C9 and 14% for CYP3A4 after 6 hours of assay. CYP2B6 activity after 6 h assay time at day 18 was 86% of day 5 activity. For CYP1A2, no activity could be detected after 18 days of cultivation. It should be noted that the product of the used substrate of CYP1A2 (Phenacetin) is itself a substrate for other multiple CYP enzymes. Figure 6 shows a rapid formation of the CYP1A2 product within 30 minutes of the assay. The product concentration goes down after one hour of incubation. It can be assumed that the product formed (Acetaminophen) is rapidly metabolized by other CYP enzymes as well as the phase II enzymes. If this is the case, then the CYP1A2 activity at day 18 of cultivation in the bioreactor is probably low and the product formed is rapidly metabolized resulting in undetectable level of CYP1A2 enzyme activity. Nonetheless, the possibility for long-term studies could be proved by showing CYP 450 activity even after 18 days of cultivation within the 3D bioreactor system.

In this study, we have shown the long-term cultivation of PHH in a 3D hollow fiber bioreactor system. This is a useful alternative to conventional 2D culture ensuring hepatocyte functionality and therefore better assay system. General cellular and liver specific parameters were stable after equilibration phase for almost 3 weeks. Quantification of amino acids gave a good insight into cellular metabolism and extracellular events which could be further supported in future by metabolic flux analysis. *On line* oxygen measurements improved the estimation of system performance as well as gave an opportunity of *in situ* kinetic viability assessment. This could be very useful for kinetic toxicity studies in pharmacological screening. In addition, the possibility to precisely monitor and control oxygenation will be of use concerning the metabolizing capacity as well as the polarity of the hepatocytes. Activity of CYP enzymes could be detected at cultivation day 18. The feasibility of using the 3D hollow fiber bioreactor for long-term cultivation and application is demonstrated in the presented study. The bioreactor is a closed system, therefore a modification allowing visual microscopic inspection of cells during cultivation would be an additional advantage. Further miniaturization of the bioreactor would allow working with lesser number of cells which is a critical issue with regard to availability of human primary material. This would also allow including replicates from a single donor for

comparison. Donor to donor variability could also be assessed when the initial viability of cells at inoculation is similar. In the presented study, the aim was to run the bioreactor for a maximum of time. The histological studies at the end of cultivation (more than 3 weeks) were not carried out since these do not reflect the fitness of cells during the first two weeks of cultivation when all characterizing assays were carried out. However, previous studies have shown the formation of tissue like structures within these 3D bioreactors. As suggested further miniaturization would allow running several parallel bioreactors of which some could be used for histological analyses after certain time points during cultivation.

## **2.5 Conclusion**

The 3D bioreactor system described in this study could be used for 3D cultivation of liver cells allowing cultivation and maintenance of the cells for physiological, pharmacological and toxicological applications. Further miniaturization will improve the throughput. It can especially play an important role in the assessment of long-term and repeated dose toxicity. In addition, the system can be adapted to any other cell/organ type culture for characterization of biological and/or pathophysiological parameters.

## **Acknowledgements**

This study was funded by the German BMBF project “3D-*in vitro* model for hepatic drug toxicity” (Hepatox project numbers 01GG0730-01GG0733). We thank Michel Fritz for his most valuable assistance concerning the HPLC analysis.

**CHAPTER 3: REAL-TIME *IN SITU* VIABILITY  
ASSESSMENT IN 3D BIOREACTOR WITH  
HUMAN LIVER CELLS USING RESAZURINE  
ASSAY DURING DRUG EXPOSURE**

This chapter has been accepted for publication as:

**Mueller D**, Tascher G, Damm G, Nüssler AK, Heinzle E and Noor F (2012):

**Real-time *in situ* viability assessment in 3D bioreactor with liver cells using resazurin assay during drug exposure**

*Cytotechnology*, in press

## **Abstract**

Three-dimensional cultivation of human cells is promising especially for long-term maintenance of specific functions and mimicking *in vivo* tissue environment. However, direct viability assessment is very difficult in such systems. Commonly applied indirect methods such as glucose consumption, albumin or urea production are greatly affected by culture condition, stress and time of cultivation and may not reflect the viability of the cells. In this study we established a real-time *in situ* viability assay namely; resazurin assay, in a 3D hollow-fiber bioreactor using human liver cells. Resazurin assay is based on the conversion of resazurin to a fluorescent dye by cytoplasmatic and mitochondrial enzymes. We show that the resazurin reagent in concentrations used in this study is non-toxic and could be rapidly removed out of the system. We optimized the assay on HepG2 cells and tested it with primary human hepatocytes. Moreover, we maintained primary human hepatocytes in the 3D bioreactor system in serum-free conditions and also assessed viability before and after the exposure to amiodarone using the resazurin assay. It was shown that this approach is applicable during long-term cultivation of cells in bioreactors under different conditions and can moreover be applied to pharmacological studies, e.g. investigation of chronic drug effects in such 3D bioreactors.

### 3.1 Introduction

The cell viability is routinely assessed during maintenance and testing of cell culture systems. A palette of established and validated assays based on diverse endpoints is available. Examples include assays such as the MTT and WST-1 assays which are based on metabolic activity, Trypan-Blue exclusion method which relies on membrane integrity and Sulforhodamine B and crystal violet assays that quantify protein content among many others. Other non-invasive methods such as measurement of respiration in 2D multiwell plates equipped with oxygen sensors have been reported to show high correlations to other endpoint assays (Noor *et al.*, 2009). The resazurin assay, well-known under the trade name Alamar Blue®, is based on the reduction of the non-fluorescent substrate resazurin into the fluorescent dye resorufin by mitochondrial and cytosolic enzymes. The reduced form of the fluorescent dye is soluble and the cells can be further cultivated after the assay (O'Brien *et al.*, 2000).

Although 2D cultivation systems are easy to maintain and handle, these do not reflect the three-dimensional *in vivo* tissue environment. Alternative cell culture systems are 3D cell culture techniques mimicking the microenvironment of tissues or organs. These include gel-based systems imitating extracellular matrix (Sodunke *et al.*, 2007), spheroids (Abu-Absi *et al.*, 2002), micro scaffolds (Bokhari *et al.*, 2007) or various types of hollow fiber bioreactors (Schmitmeier *et al.*, 2006; Schmelzer *et al.*, 2010). Hollow fiber 3D bioreactors were applied as bioartificial liver for clinical application (Gerlach *et al.*, 2003a) and were down-scaled for analytical purposes. Liver cells form three-dimensional aggregates around the hollow-fibers including the formation of liver-specific structures (Zeilinger *et al.*, 2004). It was shown that the 3D bioreactors are suitable for long-term functional maintenance of primary human hepatocytes indicating high potential of these systems for the assessment of chronic drug-induced effects (Mueller *et al.*, 2011). However, one main disadvantage of this hollow-fiber bioreactor is its black-box character, since direct cell counting methods as well as microscopic observation of cells is not possible and only indirect methods such as monitoring of substrate consumption rates are used so far for viability assessment. A real-time *in situ* viability assay would be very helpful for evaluating cellular state over extended periods of culture. Gloeckner and colleagues applied the resazurin assay to a miniaturized 3D hollow-fiber bioreactor monitoring proliferation of human leukemic cell lines (Gloeckner *et al.*, 2001). Using suspension cell lines, they found a higher sensitivity of their method compared to indirect methods such as monitoring of glucose consumption.

In this study, we extended this method to adherent cells and used resazurin based assay for viability assessment of the HepG2 cell line as well as of primary human hepatocytes in a 3D-hollow fiber bioreactor system. Moreover, we determined the concentration of the reagent that can be safely used in the bioreactor without causing toxicity and at the same time giving a measurable signal. We also assessed the retention of the reagent inside the bioreactor and determined the time needed to wash out the reagent from the system. In case of primary human hepatocytes, the cells were exposed to a clinically relevant concentration of amiodarone for 4-6 days. Viability was assessed in the early and late phase of the cultivation (i.e. before and after drug exposure). Although we used human liver cells, other cell types like kidney cells (Iwahori *et al.*, 2005) or cardiac cells (Hosseinkhani *et al.*, 2009) could also be maintained in a 3D bioreactor system. In all cases, viability assessment is fundamental. The real time assay described in our study could be extended to these other cell types in various 3D bioreactor settings. This would additionally support studies on cell physiology and phenotype and can be also applied to drug toxicity assessment studies.

## **3.2 Materials and Methods**

### **3.2.1 Culture medium and cells**

The human hepatoblastoma cell line, HepG2, was obtained from the German collection of microorganisms and cell cultures (DMSZ, Braunschweig, Germany). Cells were routinely maintained in Williams Medium E (WME)(PAN Biotec, Aidenbach, Germany) supplemented with 100 U/ml penicillin, 100 µg/ml streptomycin and 10% fetal calf serum (FCS; PAN Biotec, Aidenbach, Germany) at 37°C in a cell incubator (Mettler GmbH, Schwabach, Germany) at 95 % relative humidity with 5 % CO<sub>2</sub> supply.

Primary human hepatocytes were isolated from resected liver tissues from patients with primary and secondary tumors. Tissue collection was done according to the institutional guidelines and with the patient's written consent. Isolation and purification of non-tumor cells was performed as described previously (Mueller *et al.*, 2011).

In the 3D bioreactor system, cells were maintained in Heparmed Vito 143 (Biochrom AG, Berlin) medium supplemented with insulin (20 IU/l), transferrin (5 mg/l) and glucagon (3 µg/l), all from Biochrom AG.

### **3.2.2 3D bioreactor system**

The 3D bioreactors were purchased from Stem Cell Systems GmbH, Berlin, Germany (figure 3-1b). They consist of three interwoven hollow fiber capillary bundles that form four different compartments which are integrated into a polyurethane housing as recently described (Mueller *et al.*, 2011).

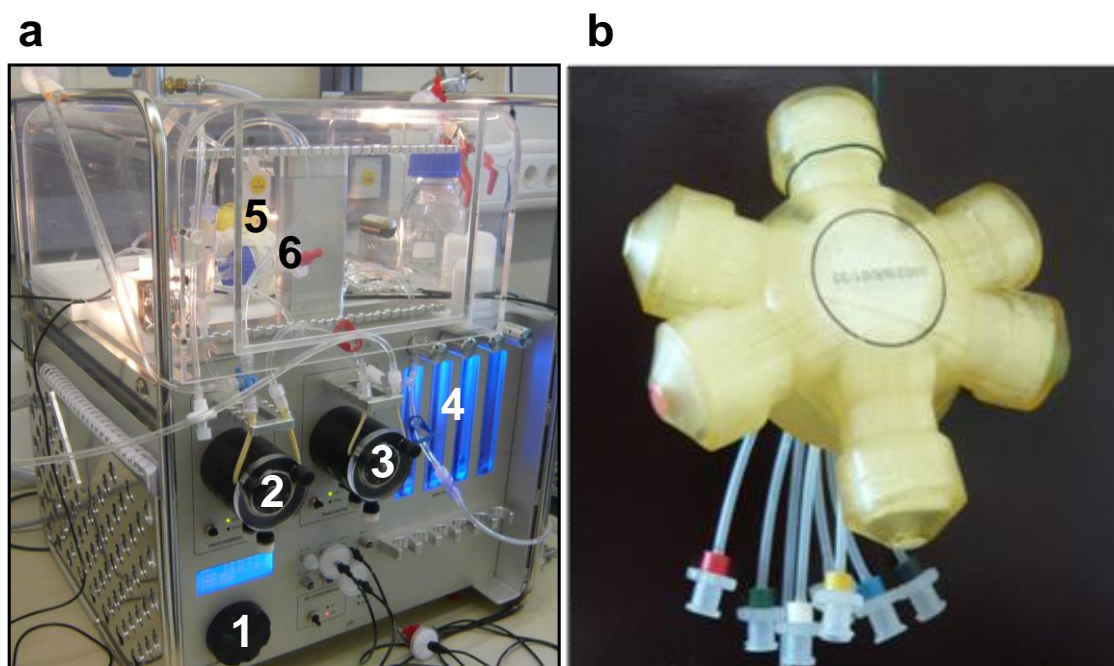


**Figure 3-1: a) Perfusion system for 3D bioreactor: 1 pump control, 2 recirculation pump, 3 feed pump, 4 gas rotameters, 5 bioreactor and 6 sample port b) 3D bioreactor with tubing for medium in- and outflow as well as cell inoculation.**

The bioreactor is kept in a chamber maintained at a temperature of 37.5°C and is connected to a perfusion system (figure 3-1a). The perfusion system includes a recirculation pump for medium perfusion, a feed pump for fresh medium supply and a flow regulation for gas supply. Recirculation flow rate was adjusted to 7 ml/min with a feed rate of 1.5-2 ml/h. The system can be easily kept in recirculation mode when the feed pump is switched off allowing recirculation of the medium in the system, e.g. during cell assays. Bioreactor and tubing system were assembled in sterile conditions under a laminar flow workbench. After assembly, the bioreactor was connected to the perfusion system.

In case of HepG2 cells,  $3 \times 10^7$  viable cells were resuspended in 7 ml Heparmed Vito medium supplemented with 2.5% FCS and inoculated into the 3D bioreactor. Whereas in case of primary human hepatocytes (PHH),  $10^8$  cells were inoculated using Heparmed Vito medium supplemented with 2.5% FCS. At day 10, serum-free conditions were adjusted in this system.

### 3.2.3 Assessment of applicable resazurin concentrations

Resazurin reagent was purchased as CellTiter-Blue® Cell Viability Assay from Promega GmbH, Mannheim, Germany. For the assessment of applicable resazurin concentrations giving

sufficient signals,  $5 \times 10^4$  HepG2 cells per well were seeded in a 96 well plate in Williams Medium E with 10% FCS. After cell adhesion overnight, the cells were washed and 200  $\mu$ l of serum free medium was added. Different resazurin concentrations, ranging from 0.1%-20% in triplicates were added. The plate was incubated at 37°C and fluorescence was measured every hour (in total 6 hours) at ex/em 540 / 590 nm using a Fluoroskan Ascent CF fluorescence reader (Thermo Labsystems, Vantaa, Finland). Medium samples without cells were used as background controls.

### **3.2.4 Assessment of resazurin toxicity**

A dose-response curve of the resazurin reagent was generated to determine its toxicity.  $5 \times 10^4$  HepG2 cells were seeded per well in a 96 well plate in Williams Medium E containing 10% FCS and incubated over night for cell adhesion. Afterwards, cells were washed twice and serum-free medium was added. The cells were exposed to different concentrations of resazurin, ranging from 1% to 100% (v/v) culture medium in triplicates. After 24 hours (h), supernatant was aspirated off and cells were washed twice with PBS. 200  $\mu$ l medium and resazurin reagent (20% v/v) was added to each well. The cells were incubated for 5 hours in the incubator. Fluorescence was measured as described above. Untreated cells were used as positive control while cells treated with 20% DMSO as negative control. Medium samples without cells were used as background controls.

### **3.2.5 Resazurin assay in 3D bioreactor**

Resazurin reagent was slowly injected into the bioreactor system *via* sample port, resulting in a final concentration of 2% (v/v). A 1 ml syringe with Luer-Lok connections was used for injection. Recirculation mode without medium feeding was adjusted. Samples were taken using two 1 ml syringes at the same time, adapted to a 3-way stopcock using Luer-Lok connections. First, about 1 ml of dead volume was drawn using one syringe. After that, 0.5 ml of sample was collected with the other syringe and dead volume was put back into the system. Using this sampling technique, accurate sampling was guaranteed. 50  $\mu$ l samples were transferred into 96-well plates. Fluorescence was measured at ex/em 540 / 590 nm as described earlier. Medium samples without cells were used as background controls.

### **3.2.6 Investigation of artifacts due to extracellular components**

200  $\mu$ l of medium and effluent sample taken from the 3Dbioreactor were transferred into a 96 well plate. 40  $\mu$ l of resazurin reagent were added and the plate was incubated at 37°C in a cell incubator for 24 hours. Fluorescence was measured at ex/em 540 / 590 nm. As positive control, a sample of the resazurin assay within the 3D HepG2 bioreactor (incubation time 6 hours) was used.

### **3.2.7 Drug exposure in 3D bioreactor cultures**

Amiodarone was injected slowly in the 3D bioreactor system, in a similar way to resazurin, preventing oscillative overconcentration. End concentration was 1.2  $\mu$ M. Resazurin assay was performed in the early and late phase of cultivation (i.e. before and after drug exposure) to investigate effects of the drug.

### 3.3 Results

#### 3.3.1 Assessment of applicable resazurin concentrations

To determine the linearity between reagent concentration and fluorescence increase, different resazurin concentrations ranging from 0.5%-20% were added to HepG2 cells in 96 well plates and fluorescence was measured over 6 hours as shown in figure 3-2a.

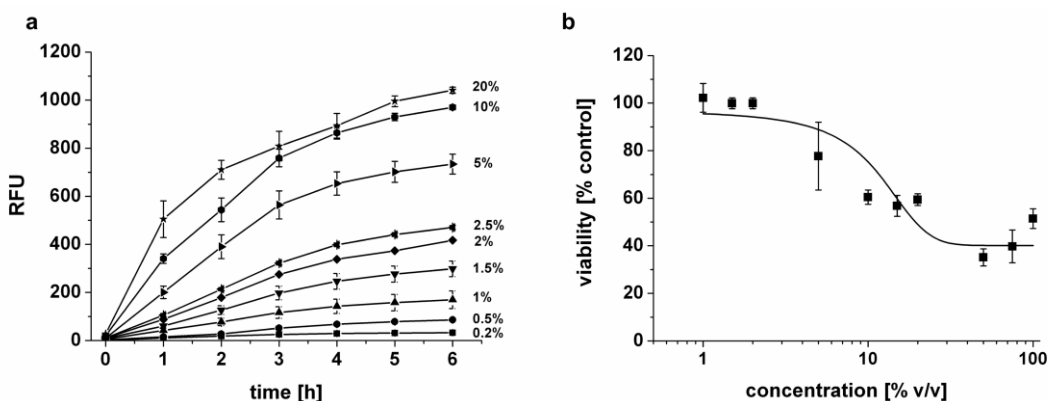


**Figure 3-2:** a) Signal intensity of different resazurin concentrations tested on Hep G2 cells.  $5 \cdot 10^4$  cells were seeded in 96-well plate format and incubated over night. Different resazurin concentrations were added, ranging from 0.5% - 20% (v/v) as indicated. Fluorescence was measured over 6 hours. Error bars indicate  $\pm$ standard deviations ( $n=3$ ). RFU= relative fluorescence units. b) Concentration-response curve for resazurin reagent giving percentage viability of Hep G2 cells. Cell viability was assessed relative to untreated control. Concentration of resazurin reagent in the medium (v/v) is given in percentage of culture medium. Error bars indicate  $\pm$ standard deviations ( $n=3$ ).

All tested resazurin concentrations show a significant increase of fluorescence during 6 hours of incubation. The highest correlation coefficients were found at concentrations between 1 % and 2.5 % (v/v). The higher concentrations [ $\geq 5$  % (v/v)] show a linear range at the first hours of incubation, whereas saturation was observed after 4 hours. Even the lowest concentration of resazurin reagent [(0.2% v/v)] showed significant increase of fluorescence over time.

#### 3.3.2 Assessment of the toxicity of resazurin

For optimization of resazurin assay for its use in the 3D bioreactor, dose-response was assessed using HepG2 cells. As shown in figure 3-2b, cells exposed to higher concentrations of resazurin (i.e. > 10% v/v) for 24 h showed a lower viability as compared to control cells. It was also

observed that lower resazurin concentrations ( $\leq 2\%$  v/v) had no effect on cell viability as the viability remained 100%.

### **3.3.3 Resazurin assay for viability assessment in 3D bioreactor using HepG2 cells**

Based on the above results, we chose 2 % (v/v) resazurin concentration for viability assessment in the 3D bioreactor system. A direct injection of the Alamar Blue dye would lead to an oscillation of the concentration. To prevent this, reagent injection was carried out slowly *via* the sample port of the tubing system and slight mixing within the injection syringe was performed. The resazurin assay was performed at day 3 after cell inoculation (figure 3-3a). At the start of the assay, only background fluorescence was observed which was 21 ( $\pm 1$ ) RFU was observed. Over 6 hours, linear increase of fluorescence was detected (figure 3-3a), with regression coefficients of 0.992. After 6 hours of resazurin incubation maxima of 102 were reached and the slope of the straight line was 12.9.

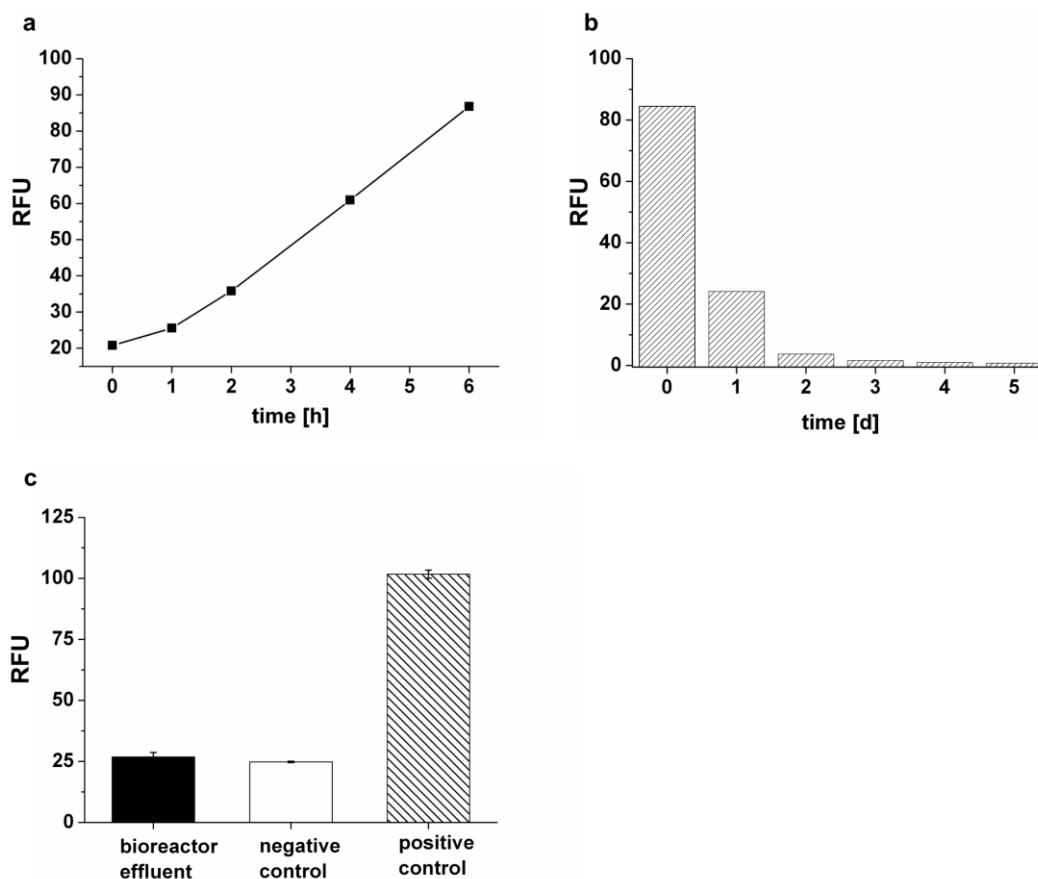


Figure 3-3: a) Resazurin assay on Hep G2 cells in 3D bioreactor system at cultivation day 3 for 6h, b) Fluorescence measurements on effluent samples after resazurin application to determine the removal of the reagent product from the 3D bioreactor. Samples were transferred into 96 well plates and intrinsic fluorescence was measured at ex/em at 540 nm and 590 nm. Day 0 represents the day of the actual resazurin assay after medium change, day 1–5 after the resazurin assay. These samples were effluent samples collected over 24 hours. The dye was washed out with a flow rate of 2 ml/h. RFU=relative fluorescence units, c) Fluorescence measurements on effluent sample of 3D-bioreactor and fresh medium to exclude possible artifacts due to extracellular components. Samples were transferred into 96 well plates and incubated with resazurin reagent (20% v/v) at 37°C for 24 hours. Fluorescence was measured at ex/em at 540 nm and 590 nm. Negative control represents fresh medium incubated with resazurin reagent, positive control represents a sample of the resazurin assay within the 3D-bioreactor at time point 6 hours. Error bars indicate  $\pm$ standard deviations ( $n=3$ ). RFU=relative fluorescence units

### **3.3.4 Washout of resazurin assay product and investigation of artifacts**

Removal of the fluorescent product out of the 3D bioreactor system should occur as fast as possible to prevent any interference in other studies or assays. Effluent samples after wash out of the resazurin assay were collected and intrinsic fluorescence was measured. It was observed that the product could be washed out of the system just by feeding one reactor volume of the fresh medium and turning the system into feed mode, whereby 2 ml/h fresh medium was added. Effluent flowed out with the same rate. As depicted in figure 3-3b, only negligible fluorescence was observed at day 3 while at day 4 all resazurin assay product was washed out and removed from the bioreactor system.

As mentioned before, resazurin reagent is reduced to a fluorescent dye by both, mitochondrial and cytosolic enzymes. Possible artifacts due to extracellular components would lead to false positive values. To exclude this, both effluent sample of the 3D bioreactor, which has been in contact with the cells before, and fresh medium as negative control were incubated with resazurin reagent for 24 h. As shown in figure 3-3c, both effluent sample as well as fresh medium (negative control) show only intrinsic reagent fluorescence ( $26 \pm 1$ ).

### **3.3.5 Resazurin assay for viability assessment in 3D bioreactor of PHH during drug exposure**

After optimization with HepG2 cells we proceeded with PHH in the 3D bioreactor. For primary human hepatocytes, viability was assessed in the early phase after adjusting serum-free conditions (figure 3-4a). Amiodarone was then injected into the 3D bioreactor system as described above. After exposure, amiodarone was washed-out by feeding fresh drug-free medium. Viability was again assessed in the late cultivation phase using the described resazurin method (figure 3-4b).

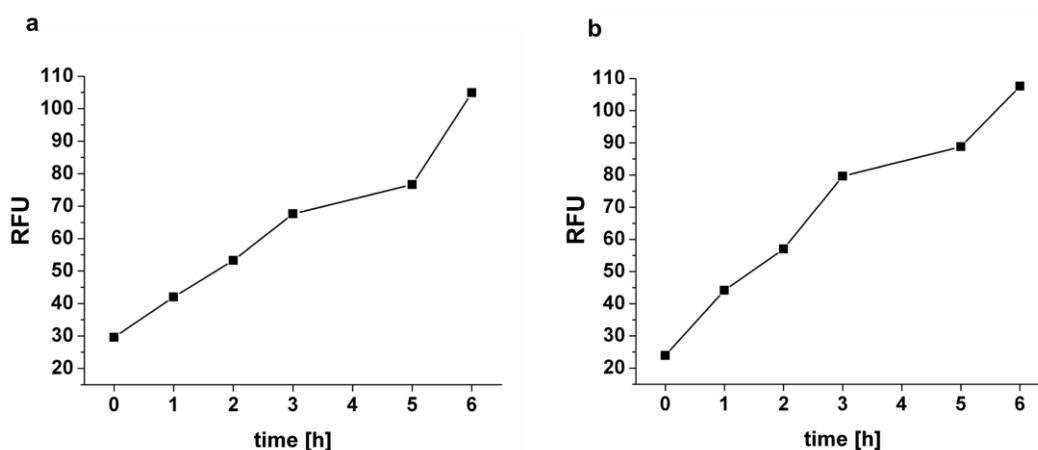


Figure 3-4: Resazurin assay on primary human hepatocytes in 3D bioreactor system at a) day 10 b) day 27. Resazurin concentration was 2 % (v/v). Samples were taken over 6 hours, transferred into 96 well plates and fluorescence was measured at ex/em 540 nm and 590 nm. RFU=relative fluorescence units

At both time points, increase of fluorescence was observed within the assay time. Fluorescence value at assay start was  $27 \pm 4$ . After 6h, RFU was 105 ( $R^2=0.955$ ) for the first assay in the early (day 11) and 108 ( $R^2=0.959$ ) for the second assay in the late cultivation phase (day 27) as shown in table 3-1.

Table 3-1: Results of resazurin assay in the 3D bioreactor system. Table shows relative assay values after 6h, as well as linearity and slope of fluorescence over time. For both HepG2 cells as well as primary human hepatocytes, two assays were performed in the early and late cultivation phase, i.e. before and after drug exposure.

	Primary human hepatocytes	
	Early phase (day 10)	Late phase (day 27)
RFU after 6h	105	108
Linearity ( $R^2$ )	0.955	0.959
slope	11.3	13.0

### 3.4 Discussion

A variety of assays are used for viability assessment in two-dimensional cultures. The 2D systems and assays are adequate and sufficient for most *in vitro* applications. Nevertheless, 2D monolayer cultures differ in their architecture, in the environment and in the phenotype from the *in vivo* tissue. Various 3D bioreactors offer an alternative for maintenance of cells in a tissue like environment. This is especially important for long-term cultivation while maintaining the phenotype and the functionality of the test system. The possibility of long-term cultivation has an impact on the testing of compounds in preclinical screening as well as in safety pharmacology for e.g. chronic liver toxicity assessments. As a prerequisite to any study, cell viability must be assessed over extended culture periods without disturbing the cells. As such non-invasive and real time assay is required. We recently demonstrated long-term cultivation of primary human hepatocytes in a 3D bioreactor system (Mueller *et al.*, 2011) for 3 weeks. We used biochemical parameters such as galactose consumption and lactate production as well as production of the liver-specific markers albumin and urea for an indirect estimation of cellular viability since a direct, microscopic observation of the cells is not possible in this bioreactor. We however, modified the system by incorporating an *on-line* respiration measurement device allowing the monitoring cell viability. However, a technically less challenging assay for viability assessment would be very useful.

In this study, we used a resazurin based viability assay, to directly monitor cell viability within 3D bioreactor. This method allows direct *in situ* real time monitoring of viability of cells despite the black-box character of the bioreactor system. Based on the results on 2D monolayer system using HepG2, we chose a concentration of 2% (v/v) of resazurin since this had no effects on the viability of the cells and gave linear signal for 6 hours. We assessed the viability of HepG2 cells maintained in the 3D bioreactor at day 3 of inoculation. Linear increase of the fluorescence signal was detected during 6 hours of incubation time. It was further demonstrated that wash-out of the product is possible and easy to carry out without perturbing the cells. The short incubation time is moreover helpful since the whole assay can be carried out within a few hours. Reduction of the substrate by medium compounds or released cellular enzymes due to cell death, which would lead to false-positive values was also excluded experimentally. It was concluded that the reagent reduction was exclusively caused by living cells in the 3D bioreactor. Future studies focusing on the proliferation profiles of HepG2 in the 3D bioreactor over time would be very useful to improve the functionality of the HepG2 cells. Some studies have shown

a more differentiated cellular phenotype for HepG2 cells when grown in a three-dimensional manner (Altmann *et al.*, 2008; Lan and Starly, 2011).

A step further, we investigated another 3D bioreactor with primary human hepatocytes. In this system, we started the cultivation using 2.5 % fetal calf serum and adjusted to serum-free conditions at day 10. Serum free cultivation is especially important regarding pharmacological as well as physiological studies such as proteomics. Use of serum limits pharmacological and “-omics” relevant studies due to the non-defined composition, batch-to batch variations and high endogenous protein content of the serum. In our previous study, we showed the serum free cultivation of PHH in these 3D bioreactors for 11 days. Serum free cultivation of PHH is of particular interest since it was reported that FCS induces dedifferentiation and therefore loss of functionality of these cells (Tuschl *et al.*, 2009). After adjusting to serum free conditions, we continuously exposed the PHH to therapeutic concentration of amiodarone for 4 days. The system was washed over 3 days. In the late cultivation phase (day 27), viability was again assessed using resazurin assay. By comparing fluorescence values at the end of both assays (105 RFU and 108 RFU) it was observed that viability was maintained even after drug exposure in serum-free conditions. Therefore we could conclude that the exposure to clinically relevant concentrations of amiodarone did not affect cell viability in this experiment. This also proves the non-invasiveness of the assay. However, future studies should include determination of free drug concentration within the 3D bioreactor system since drug binding to the capillaries inside the bioreactor could occur. This may partly explain why we did not observe any toxic effects of the drug in our system.

We show that the resazurin based assay is applicable to 3D bioreactor systems using adherent cells. This real time *in situ* assay will be of tremendous importance in monitoring long-term cultivation of cells. This will also facilitate the monitoring of drug/test compound induced effects on the cells. The application of this bioreactor system allowing tissue like environment and functionality for physiological and eventually pharmacological studies would be greatly enhanced. Serum free cultivation is an added advantage.

The established assay in our 3D bioreactor would further support future cellular physiological as well as pharmacological studies in terms of the assessment of drug effects on cellular metabolome, fluxome, proteome or peptidome, where accurate assessment of viability is essential for qualitative and quantitative analyses. Moreover, toxic effects of drugs can be assessed and the assay could also be applied to any other cell type in 3D bioreactors supporting different research fields.

## **Acknowledgements**

The study was carried out as a part of the Project “3D-*In vitro* Model for Hepatic Drug Toxicity” (Project numbers 01GG0732; 01GG0733) funded by the Bundesministerium für Bildung und Forschung (BMBF).

# CHAPTER 4: ORGANOTYPIC CULTURES OF HEPG2 GENERATED BY HANGING DROP METHOD AS *IN VITRO* MODEL FOR TOXICITY STUDIES

This chapter has been published as:

**Mueller D**, Koetemann A and Noor F (2011):

**Organotypic cultures of HepG2 generated by hanging drop method as *in vitro* model for toxicity studies**

*Journal of Bioengineering and Biomedical Sciences*, DOI: 10.4172/2155-9538.S2-002

## **Abstract**

Tissue engineering of human liver cells in a three dimensional cell culture system could improve pharmacological studies in terms of drug metabolism, drug toxicity or adverse drug effects by mimicking the *in vivo* situation. In this study, we produced 3D organotypic cultures of HepG2 cells using the hanging drop method. 250 – 8000 seeded cells formed organotypic cultures within 2 – 3 days which increased in size during the first week. Viability and metabolic parameters (glucose, lactate) were analyzed during almost three weeks of cultivation. Liver specific albumin production was higher in the organotypic cultures as compared to both monolayer and collagen-sandwich cultures. Amino acid quantification revealed high production of glutamate as well as uptake of glutamine, alanine and branched-chain amino acids. CYP1A induction capacity was significantly improved by organotypic cultivation. The acute toxicity (24 h) of tamoxifen, an anti-cancer drug, was lower in the 3D cultures as compared to monolayer and collagen-sandwich cultures. This could be explained by a higher drug efflux through membrane transporter (MRP-2). We conclude that the engineered HepG2 cultures could be used for the investigation of CYP450 induction, anti-cancer drug effects and for the study of chemotherapy resistance. Applied to other cell types such as the human primary cells these 3D organotypic cultures may have potential in toxicity screening of compounds.

## 4.1 Introduction

The field of tissue engineering has advanced tremendously in recent years. In preclinical drug development the challenge remains the design and manufacturing of cellular structures which mimic the *in vivo* situation. In a tissue, cell-cell interactions as well as cell contacts to the extracellular matrix and extracellular factors like signal molecules are promoted. The interactions between the cells and the environment strongly influence the behavior and functionality of the whole tissue. Focal adhesions anchor the cytoskeleton to the plasma membrane and transport extracellular signals from the matrix into the cell (Cukierman *et al.*, 2001; Cukierman *et al.*, 2002). In experimental 2D culture, this complex network is lost and an artificial cellular architecture is built up. Moreover, an unnatural polarity is formed since the upper cell side contacts the culture medium and the lower is attached to cell culture surfaces, resulting in a polar distribution of adhesion factors (Tibbitt and Anseth, 2009).

Different 3D cell culture techniques show the improvement of function, differentiation and viability as compared to conventional 2D cultures (Godoy *et al.*, 2009). Biodegradable polymers such as poly(glycolic acid), poly(lactic acid) or their copolymer poly (lactic-*co*-glycolic acid) were successfully used to enhance cellular function (Mikos *et al.*, 1993) and were applied to tissue engineering (Temenoff and Mikos, 2000). Alternatively, hydrogels, a network of hydrophilic polymer chains dispersed in water, were used to setup a 3D environment for various cell types such as liver cell, bone and cartilage (Fisher *et al.*, 2004; Park *et al.*, 2005; Liebmann *et al.*, 2007; Shim *et al.*, 2011). Alginate microencapsulation of hepatocytes was recently shown to enhance long-term cultivation (Miranda *et al.*, 2010) and continuous perfusion of these aggregates further improves liver-specific functions (Tostoes *et al.*, 2011b). Matrigel-based systems are another alternative for 3D cultivation. Containing ingredients of the extracellular matrix such as collagen, laminin, fibronectin or elastin, they can at least partly replace its functions (Frisk *et al.*, 2007). Although these gel-based systems are useful tools to facilitate a 3D environment, gel preparation, storage, batch to batch differences and insufficient chemical composition for matrigels and xenogenic origin compromise their application.

Complex systems such as 3D bioreactors were developed as extracorporeal liver support (Sauer *et al.*, 2002; van de Kerkhove *et al.*, 2002; Gerlach *et al.*, 2003a; van de Kerkhove *et al.*, 2003). These systems were down-scaled for experimental purposes and it was shown that primary hepatocytes form 3D tissue-like structures within the bioreactors and could be kept viable and functional for three weeks (Mueller *et al.*, 2011). Moreover, the cultivation of spheroids in stirred bioreactors also improves liver-specific functionality compared to monolayers (Miranda

*et al.*, 2009). Again these systems require high technical expertise and are not always reproducible.

As a further 3D cell culture approach, multi-cellular spheroids represent a promising tool in tissue engineering since it was shown that cellular reorganization and 3D architecture in such spheroids better reflect *in vivo* situation but also mimic solid tumors in case of oncological studies (Li *et al.*, 2008). Liver cells are of main interest for the investigation of drug-induced effects and drug metabolism and the improvement of *in vitro* test methods for hepatotoxicity is still needed (Mandenius *et al.*, 2011a). The HepG2 cell line was successfully applied for the investigation of the effects of drugs in subtoxic concentrations in terms of respiration and cell metabolism (Niklas *et al.*, 2009; Noor *et al.*, 2009; Beckers *et al.*, 2010). Moreover, when grown in 3D systems, HepG2 cells showed enhanced viability and functionality (Bazou *et al.*, 2008; Corstorphine and Sefton, 2011; Lang *et al.*, 2011; Nakamura *et al.*, 2011). In spheroid cultures, it was observed that HepG2 cells have higher drug efflux activity compared to monolayers (Oshikata *et al.*, 2011). Multi drug resistance (MDR) is shown by tumor cells and leads to a high drug efflux *via* transporters such as MDR-1 or MRP.

In general, the HepG2 cell line has the advantages of reproducibility, easy handling and availability, but is limited in its drug metabolism capacities. For example, CYP3A4 as the most important phase I enzyme is not expressed in HepG2 cells and only CYP1A1 and CYP2D6 shows expression rates approximately in the range of primary human hepatocytes (Wilkening *et al.*, 2003). Recently, it was proposed that engineering the cell culture environment for a better reflection of the *in vivo* situation would improve drug development at an early stage (Bhadriraju and Chen, 2002). HepG2 spheroid cultures therefore seem to be promising as *in vitro* assay system, at least for acute and parent compound toxicity screening.

In this study, we used a commercially available 96 well plate system for the generation of 3D spheroids using the hanging drop method. We investigated the HepG2 spheroid formation over time including growth in size. We cultivated the spheroids in low-serum conditions for more than two weeks and assessed cell viability, albumin production and metabolism in the 3D cultures. Moreover, we investigated drug metabolism capacities by CYP1A induction and tested the effects of tamoxifen on the 3D HepG2 spheroids. Tamoxifen is a non-steroidal selective estrogen-receptor (ER) modulator applied in the therapy of ER-positive breast cancer. Tamoxifen is mainly metabolized by CYP3A4 and CYP2D6 to active metabolites (Holmes and Liticker, 2005). However, it was reported that tamoxifen is cytotoxic in non-metabolizing cell lines, implicating parent compound toxicity (Petinari *et al.*, 2004). We tested tamoxifen on the

HepG2 organotypic cultures and compared the results with those obtained with 2D monolayer and collagen-sandwich cultures. We also investigated the activity of MRP-2 transporters. Our results demonstrate the potential of engineered HepG2 spheroids as *in vitro* model to screen anti-cancer drugs and their effects on cancer tissue as well as for the investigation of MDR activity in chemotherapy resistance. In addition, such organotypic cultures of other cells (including co-cultures) such as primary human cells (e.g. liver) can also be used to develop *micro-tissues* which may be used in toxicological screening of compounds.

## **4.2 Material and methods**

### **4.2.1 Cell culture**

The human hepatoblastoma cell line (HepG2) was obtained from the German collection of microorganisms and cell cultures (DMSZ, Braunschweig, Germany). Cells were maintained in Williams Medium E supplemented with penicillin/streptomycin (100 U / 100 µg/ml) and 10% FCS. The cells were kept at 37°C in a cell incubator (Mettler GmbH, Schwabach, Germany) at 95% relative humidity with 5% CO<sub>2</sub> supply. Viability was assessed by the trypan blue exclusion method. Cells were counted using an automated cell counter (Countess, Invitrogen, Karlsruhe, Germany).

### **4.2.2 Monolayer / Collagen-Sandwich**

For monolayer culture, cells were seeded in conventional 96-multiwell plates. For collagen-sandwich cultures, the plates were coated with collagen I solution (0.75 mg/ml) for 1 h at 37°C before being seeded. After 4 hours, medium was aspirated and the second collagen layer was added as before. In both cultures, 5\*10<sup>4</sup> cells / well were seeded.

### **4.2.3 Organotypic cultures**

The organotypic cultures were produced using the GravityPlus system (InSphero, Zurich, Switzerland). According to the manufacturer's instructions, 40 µl of cell suspension was given into each well of the plate for the formation of multi-cellular spheroids (250 – 8000 cells). For initial seeding, Williams Medium E supplemented with 10% FCS was used. It was changed by refreshing 50% of the culture volume every 2 -3 days. For the quantification of metabolites, the supernatants were collected, centrifuged and stored at -20°C until analysis. The spheroids were monitored using a 10 x long-working distance objective of an Olympus IX 70 microscope which was connected to an Olympus CC12 Soft Imaging System (Muenster, Germany).

### **4.2.4 Maintenance in low-serum conditions**

The spheroids were produced using medium supplemented with 10% FCS. After spheroid formation, 50% medium volume was replaced three times. This time point was set as day 1 in low-serum conditions. However, due to the fact that the medium cannot be replaced completely in the drop, a small amount of 1.25 % FCS was still present in the medium. After that, medium

was replaced at day 4 reducing the percentage of serum to below 1%. Medium drops without cells were used as controls for each time point.

#### **4.2.5 AST assay**

The activity of liver-specific aspartate aminotransferase (AST) in the culture supernatant as cell viability marker was determined using a kinetic UV assay kit (Hitado, Moehnesee- Delecke, Germany) according to the manufacturer's instructions. A dilution series of standard serum (NobiCal-Multi, Hitado) was measured in parallel for quantification.

#### **4.2.6 Quantification of glucose, albumin and amino acids**

D-glucose and l-lactate concentrations in the supernatants were determined using routinely utilized enzymatic kits (R-Biopharm, Darmstadt, Germany). The assays were performed according to the instructions of the manufacturer.

Albumin concentration was determined by an enzyme-linked immunosorbent assay (ELISA) (Albuwell II; Exocell, Philadelphia, PA) according to manufacturer's instructions.

Concentrations of amino acids in the supernatants were quantified by an high performance liquid chromatography (HPLC) method as previously reported (Mueller *et al.*, 2011).

Medium exchange was performed by refreshing 50 % of the drop volume. The metabolic rates in 3D spheroid cultures were determined using the following equation:

$$r = \left[ (0.5 \times c_m + 0.5 \times c_{dx-1}) - c_{dx} \right] \times \frac{V}{\Delta t}$$

Whereas

$c_m$  = c (metabolite) in medium w/o cells

$c_{dx}$  = c (metabolite) in supernatant at day x

$c_{dx-1}$  = c (metabolite) in supernatant at day x - 1

V = hanging drop volume

#### **4.2.7 Live/dead-assay**

Live/dead-assay was performed using fluoresceindiacetate/propidiumiodide staining (FDA/PI). Cells were incubated with FDA/PI staining solution (25  $\mu$ M FDA / 40  $\mu$ M PI in PBS) for 1 min. After PBS washing (2x), fluorescence was monitored using an Olympus IX70 fluorescence microscope (ex 488 nm).

#### **4.2.8 CYP450 induction assay**

For the induction of CYP1A, the HepG2 cells were incubated with 3-methylcholantren (5  $\mu$ M) for 72 h. EROD assay, based on the conversion of 7-ethoxyresorufin to the fluorescent dye resorufin by CYP1A, was performed. For that, the cells were incubated with the substrate 7-ethoxyresorufin (10  $\mu$ M in serum-free medium) for 3 h. Fluorescence at ex/em 544/590 nm was measured. Fluorescence intensities were corrected for background fluorescence (substrate solution without cells). Fold changes compared to uninduced control were calculated.

#### **4.2.9 Dose response curves**

To assess dose-dependent toxic effects on the cells in the three different cultivation types, stock solution of tamoxifen was prepared in DMSO. Concentrations of 0.1 – 500  $\mu$ M were tested in triplicates. For all experiments, the highest DMSO concentration did not exceed 2%. Cells were incubated with the respective drug concentrations in serum-free medium for 24 h. After 24 h drug exposure, alamar blue assay was performed. For this, alamar blue assay solution (20 % v/v) was added to the cells and incubated for 4 h. Fluorescence was measured using a Fluoroskan Ascent CF fluorescence reader (Thermo Labsystems, Vantaa, Finland) at ex/em 544/590 nm. Three individual experiments were carried out for each cultivation system and mean values of viability related to the respective untreated control were calculated. Dose-response curves were obtained by plotting the logs of the tested concentrations against the viability as percentage of untreated control. EC<sub>50</sub> values and standard deviations were determined using the Boltzmann function (Origin 8.1G).

#### **4.2.10 MRP-2 transporter activity**

A fluorescence based assay was used for the investigation of MRP-2 transporter activity in organotypic cultures. Thereby, the membrane permeable and non-fluorescent substrate 5-chloromethylfluorescein diacetate (CMFDA) was used as substrate. CMFDA is converted by cellular esterases to a membrane-impermeable compound, which then reacts with cellular

glutathione to glutathione-methylfluorescein (GSMF). GSMF is a substrate of the membrane transporter MRP-2 and is excreted out of the cell into canaliculi where it accumulates. The organotypic cultures were incubated at day 3 after seeding with 5  $\mu$ M CMFDA for 30 min. Thereafter, dye solution was aspirated and the cells were incubated with dye-free medium for 45 min. Fluorescence was monitored using an Olympus IX 70 fluorescence microscope (Muenster, Germany).

#### **4.2.11 Statistical analysis**

The fold induction in organotypic, monolayer and collagen sandwich cultures relative to respective uninduced controls were compared using student's *t*-test (Matlab R2006a). The EC<sub>50</sub> values in OTC, ML and CS cultures were compared using student's *t*-test (Matlab R2006a).

## 4.3 Results

### 4.3.1 Spheroid formation and growth

Spheroid formation and growth was investigated by seeding different cell numbers (250 – 8000). Morphology was evaluated over seven days as shown in figure 4-1.

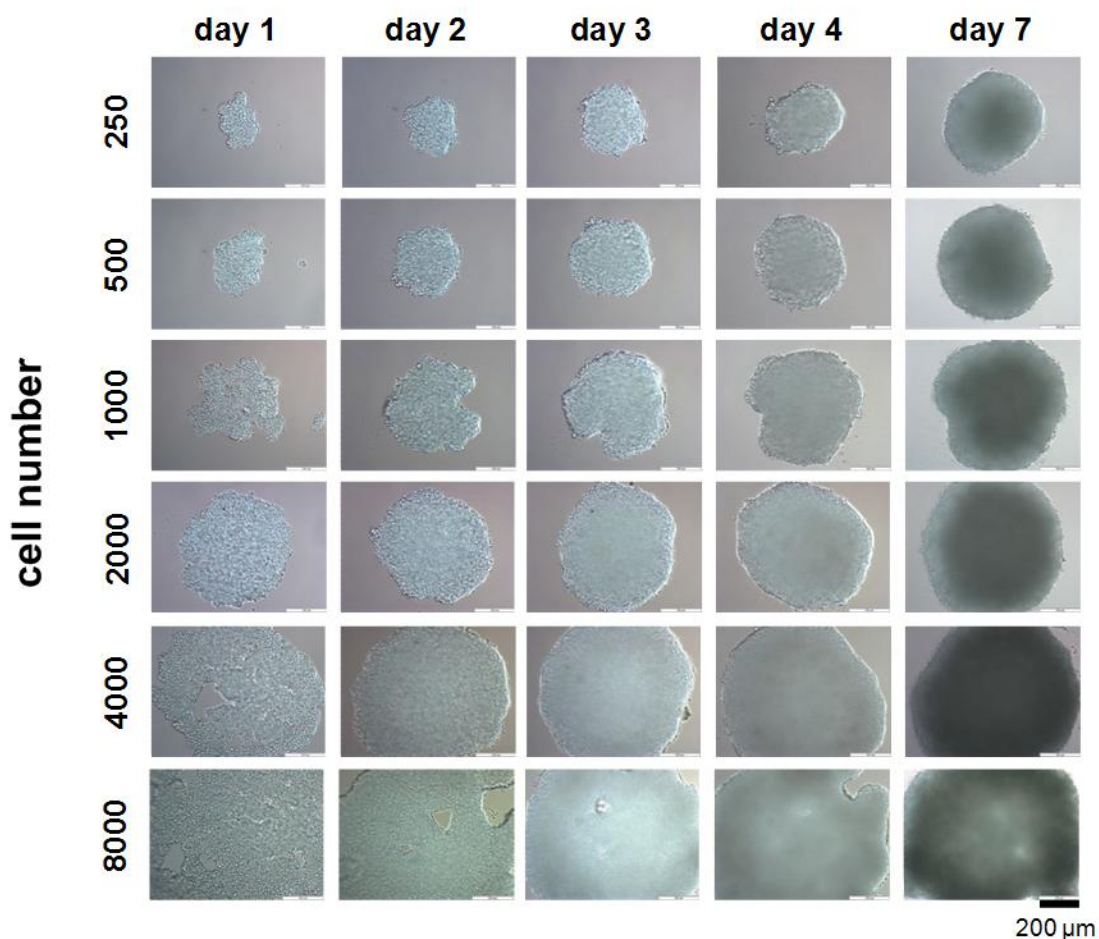


**Figure 4-1: Formation of HepG2 spheroids. Different cell numbers were (250 – 8000) were seeded and cluster formation was monitored over seven days as indicated. Scale bars represent 200 μm.**

Structure reorganization was observed already at day 1 after seeding. Compact organotypic cultures were observed at day 2-3. The used cell numbers all formed compact spheroids of reproducible diameters. Moreover, cell proliferation was observed by increasing cluster sizes. In the group of 250 seeded cells at day 1, diameters of 500 μm were achieved at day 7. In case of 8000 initial seeded cells, the spheroid diameters were around 900 μm at day 7. It was also apparent that the spheroids could freely move in the drop.

Organotypic cultures of 2000 seeded cells were further analyzed regarding time-dependent growth by measuring the diameters over 10 days (figure 4-2).

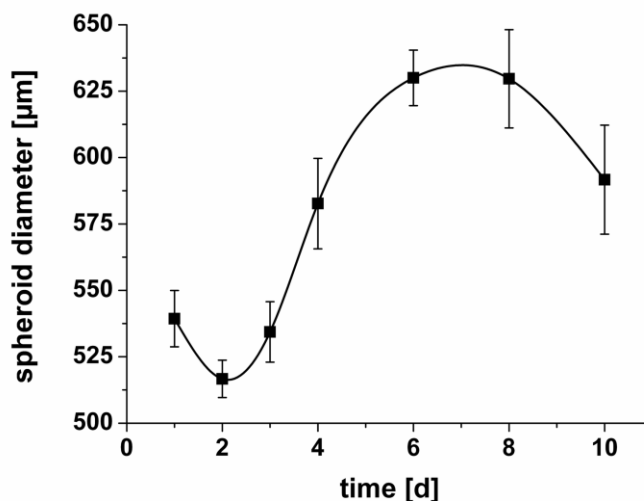


**Figure 4-2: Spheroid growth over time. 2000 cells were seeded (day 0) and the diameter was assessed during 10 days. Error bars represent  $\pm$ SD (n=3).**

After initial seeding, the diameter decreased due to cell reorganization and tissue-like formation. The spheroids were then growing linearly ( $R^2=0.98$ ) to a diameter of  $630 \pm 11 \mu\text{m}$  at day 6. After that, the cluster size then decreased until day 10 to  $592 \pm 21 \mu\text{m}$ . For further experiments, 2000 cells were chosen as initial cell number which gives sufficient signal in viability assay and can be cultivated with high viability for more than two weeks.

### **4.3.2 Maintenance of the spheroids in low-serum conditions**

After structure reorganization, the HepG2 spheroids were maintained in very low-serum medium. For viability, AST release from HepG2 spheroids was measured (figure 4-3a).

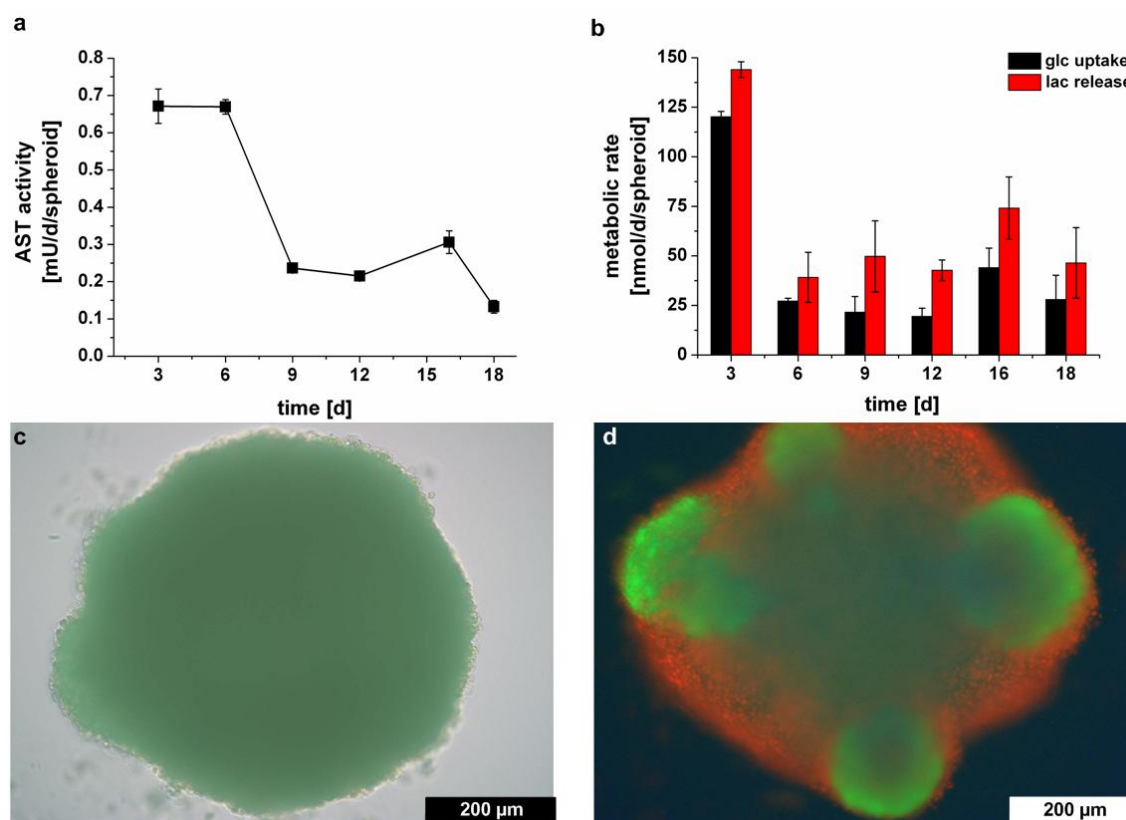


**Figure 4-3: Low-serum, long-term cultivation of HepG2 cells in organotypic cultures a) AST activity b) glucose consumption and lactate production rates c) morphology organotypic culture at day 18 d) viability of organotypic culture at day 18, assessed by Live-Dead staining. Error bars in a) and b) indicate  $\pm$ SD ( $n=3$ , supernatants of 6 spheroids were pooled). Day 1 = 1<sup>st</sup> day in low-serum medium. Scale bars represent 200  $\mu$ m.**

The highest AST activity (0.67 mU/d) was found after adjusting low-serum conditions (day 3) and was constant until day 6 indicating highest cell death in this phase. Thereafter, AST release significantly decreased to stable values in the middle phase of cultivation. At day 18, the lowest AST activity (0.13 mU/d) was found in the spheroid supernatants.

The spheroids consumed glucose with highest rate at day 3 (120 nmol/d). This rate decreased during low-serum maintenance to nearly constant values between day 4 and 18. Similarly, the highest lactate production (144 nmol/d) was measured at day 3 after adjusting serum-free conditions which decreased further on to values between 39 and 74 nmol/d. Lactate yield was highest between days 9 – 12, whereas at the beginning and at the end of the cultivation, lactate yields between 1.2 – 1.7 were observed.

Light microscopy revealed that the organotypic cultures still maintained their 3D structure at day 16 (figure 3c). Though high cell death rate was observed by live/dead staining (figure 3d), some outer parts of the spheroids showed high viability indicating high proliferation rates in these zones.

Albumin production in HepG2 cells in the three cultivation systems was measured (figure 4-4).

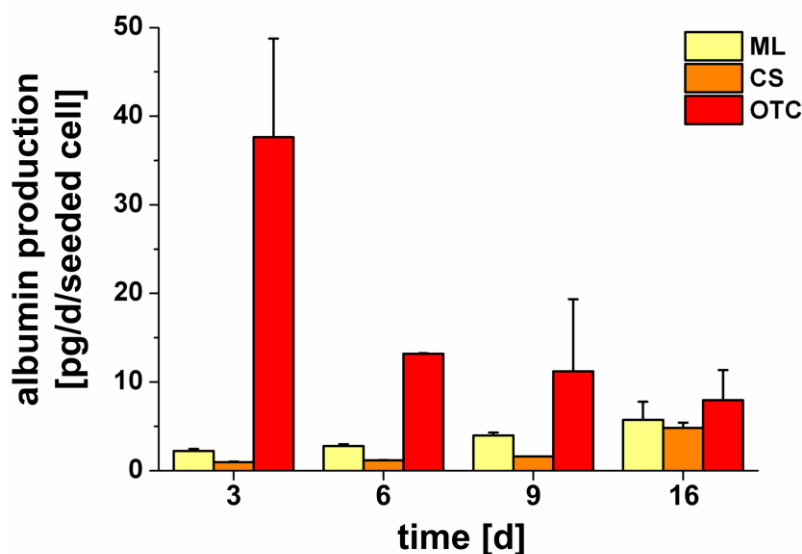


**Figure 4-4: Albumin production rates of monolayer (ML), collagen sandwich (CS) and organotypic (OTC) cultures, expressed in pg/d/seeded cell. Error bars indicate standard deviation (n=2, for OTC supernatants of 6 spheroids were pooled).**

It was observed that the organotypic cultures produced the highest amounts of albumin (normalized to the initial seeded cell number). The albumin production per seeded cell increased in both monolayer- and collagen sandwich cultures over 16 days indicating cell proliferation. The organotypic cultures produced the highest amount of albumin at day 3 (38 pg/d/seeded cell). Between day 6 and day 16 in low-serum medium, the production rates were almost constant (8 – 13 pg/d/seeded cell). Comparing the three cultivation systems, the albumin production rates were 17 or 38 fold higher in the organotypic cultures than in monolayer- or collagen sandwich cultures at day 3. At day 16, fold changes the production rates per seeded cell were more similar (fold changes 1.4 for ML and 1.6 for CS).

Amino acid metabolism in the HepG2 spheroids in low-serum medium was analyzed as shown in figure 4-5.

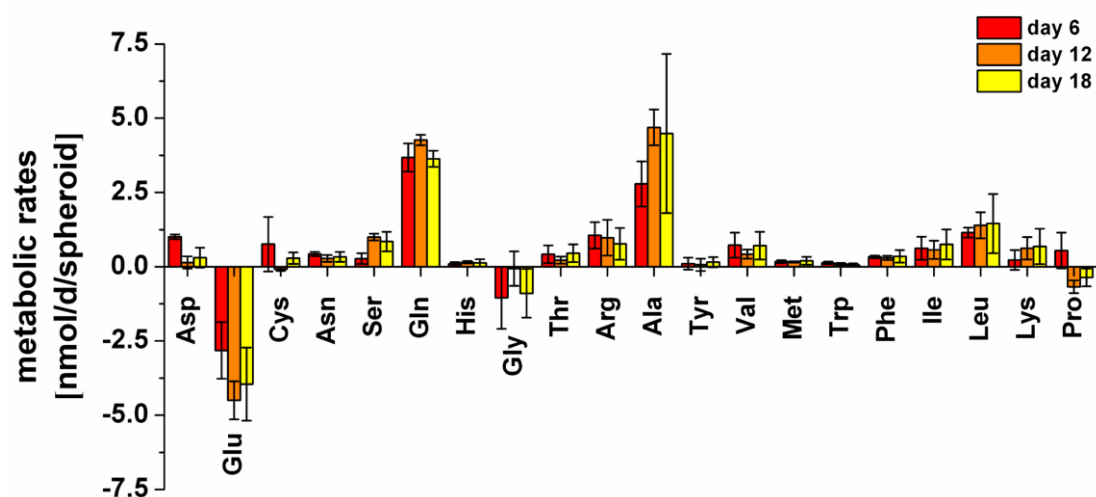
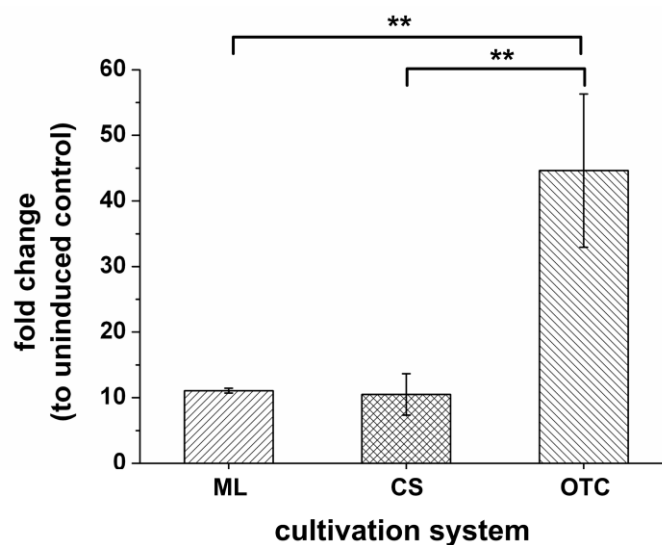


Figure 4-5: Amino acid metabolism of 3D spheroids during low-serum long-term cultivation at day 6, 12 and 18 respectively. Positive values indicate net uptake. Day 1 = 1<sup>st</sup> day in serum-free conditions. Error bars indicate  $\pm$ SD (n=3, supernatants of 6 spheroids were pooled, respectively).

At day 6, glutamine (3.7 nmol/d), alanine (2.8 nmol/d), leucine (1.2 nmol/d) and arginine (1.1 nmol/d) were consumed at highest rates. The spheroids produced high amounts of glutamate between day 6 and 18 (2.8 – 4.5 nmol/d). The consumption of serine increased after the first cultivation week as well as aspartate production decreased over time. For glycine and proline, we found low net production rates in the later phase. The branched-chain amino acids leucine, isoleucine and valine were constantly taken up until day 18. Glutamine was consumed over the whole serum-free cultivation at very stable rates (3.6 – 4.3 nmol/d)

### 4.3.3 CYP450 induction

We analyzed the CYP1A induction capacity of HepG2 cells in monolayer, collagen-sandwich and organotypic cultures using the EROD assay. The organotypic cultures clearly showed the highest fold change (44.6) upon 3-MC induction compared to the uninduced control (figure 4-6).



**Figure 4-6: CYP1A induction assessed by EROD assay. Induction fold change (compared to uninduced control) after 72 h induction with 3-MC is shown for HepG2 cells cultivated in monolayer (ML), collagen-sandwich (CS) or organotypic cultures (OTC). Error bars indicate  $\pm$ SD (n=3). \*\* Significance at  $p < 0.01$**

The induction capacity was significantly higher compared to the other two cultivation systems ( $p < 0.01$ ). Monolayer- and collagen-sandwich-cultures showed similar induction capacities (fold changes 10.6 and 10.5, respectively).

#### 4.3.4 Toxicity of tamoxifen

The toxicity of tamoxifen was assessed in monolayer-, collagen sandwich- and organotypic cultures. Dose-dependent effects of the drug were observed for all three cell culture systems (figure 4-7 a-c).

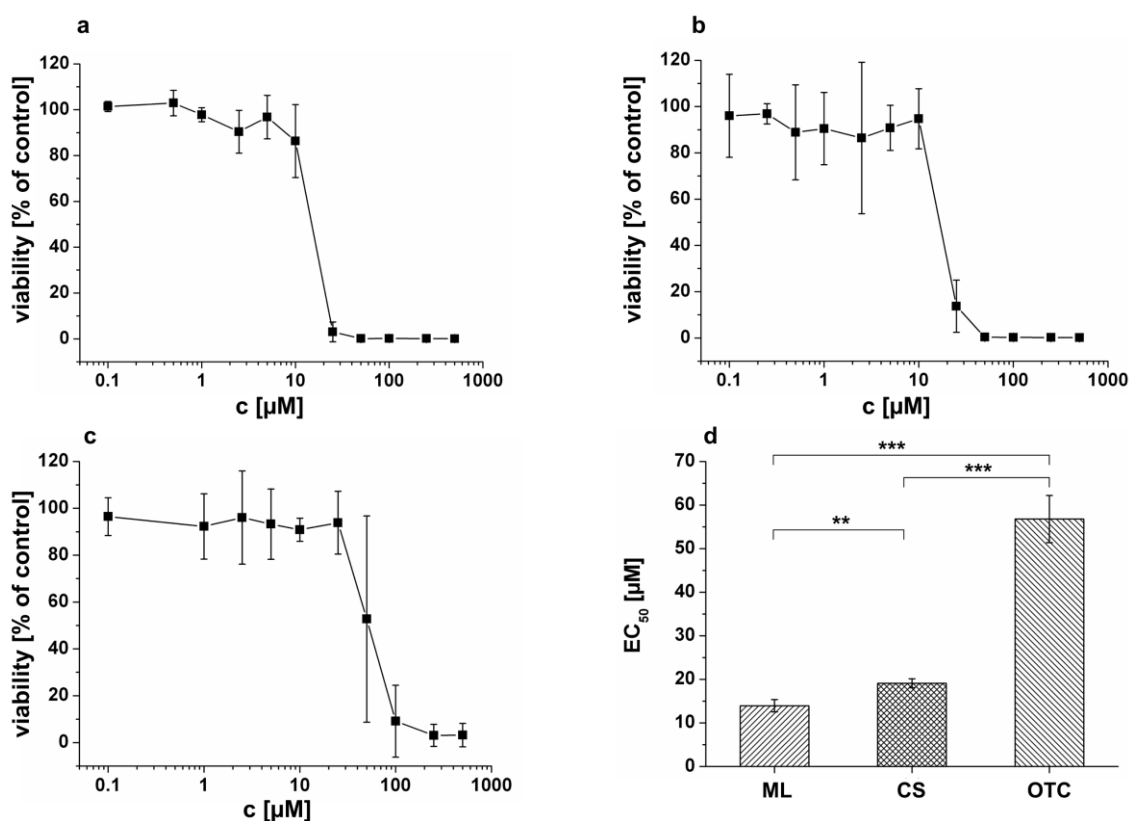
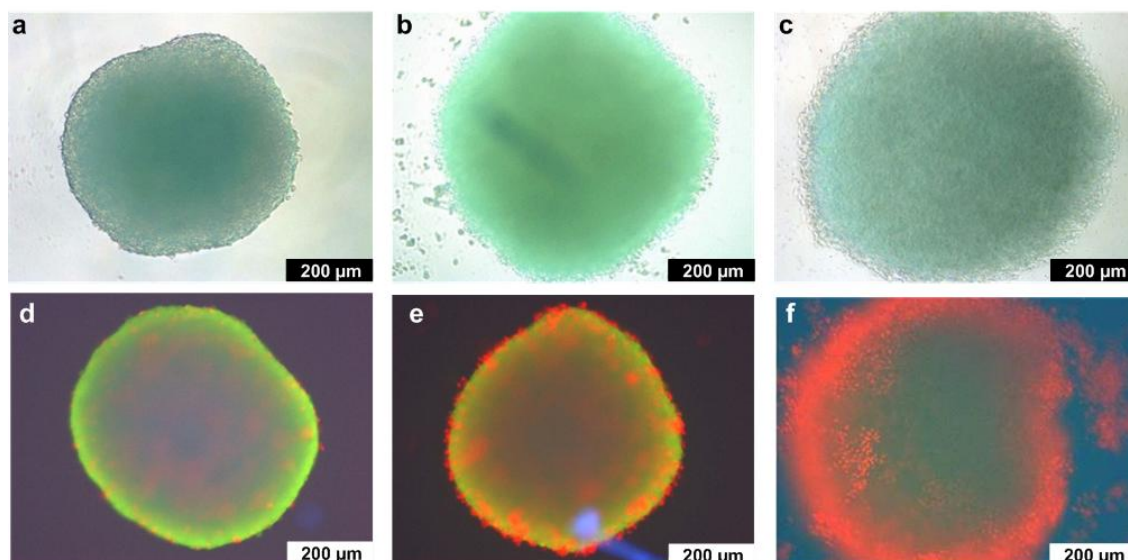


Figure 4-7: Dose response curves and EC<sub>50</sub> values of tamoxifen (24 h exposure) for HepG2 cells cultivated in a) monolayer (ML), b) collagen-sandwich (CS), or c) organotypic cultures (OTC). EC<sub>50</sub> values (d) were calculated using Boltzmann function. Viability was assessed by alamar blue assay and calculated relative to the respective untreated controls. Error bars indicate  $\pm$ SD (N=3, n=3), \*\* significance at  $p < 0.01$ , \*\*\* significance at  $p < 0.001$

The EC<sub>50</sub> value (figure 4-7 d) for monolayer cultures (13.9 µM) was significantly lower as compared to collagen-sandwich culture (19.1 µM). The organotypic cultures showed the highest EC<sub>50</sub> value (56.8 µM) of the three models. The effects of tamoxifen on the HepG2 spheroids were further visualized by live-dead-staining. Untreated control, 50 µM (in the range of EC<sub>50</sub>) and 100 µM as positive control were tested (incubation time 24 h) as depicted in figure 4-7. The untreated spheroids (figure 4-8 a, d) were highly compact and showed only a low number of dead cells around the cluster. After exposure to 50 µM tamoxifen, a higher amount of dead cells were observed in the drop (figure 4-8 b) as well as on the cluster surface (figure 4-8 e).



**Figure 4-8: Morphology and viability of HepG2 organotypic cultures upon 24h exposure to tamoxifen. Morphology: a) untreated control b) 50  $\mu$ M tamoxifen c) 100  $\mu$ M tamoxifen; Viability: d) untreated control e) 50  $\mu$ M tamoxifen f) 100  $\mu$ M tamoxifen. Scale bars represent 200  $\mu$ m.**

Cell debris as shown by light microscopy in figure 4-8b was washed away during the staining procedure. The treatment with 100  $\mu$ M tamoxifen degraded the spheroid structure and its compactness and induced cell death; both at the surface and within the organotypic culture (figure 4-8c, f).

#### **4.3.5 Investigation of MRP-2 activity**

The MRP-2 transporter activity was investigated using CMFDA-based assay. Monolayer cultures of HepG2 show strong intracellular fluorescence and almost no transport of the dye into canaliculi. Likewise high accumulation of the fluorescent dye within the cells was found for the collagen sandwich cultures. In contrast, the organotypic cultures show MRP-2 transporter activity all around the 3D structure. The fluorescent MRP-2 substrate was transported out of the cell. Accumulation within the canaliculi was clearly observed whereas no intracellular fluorescence was detected (Figure 4-9).

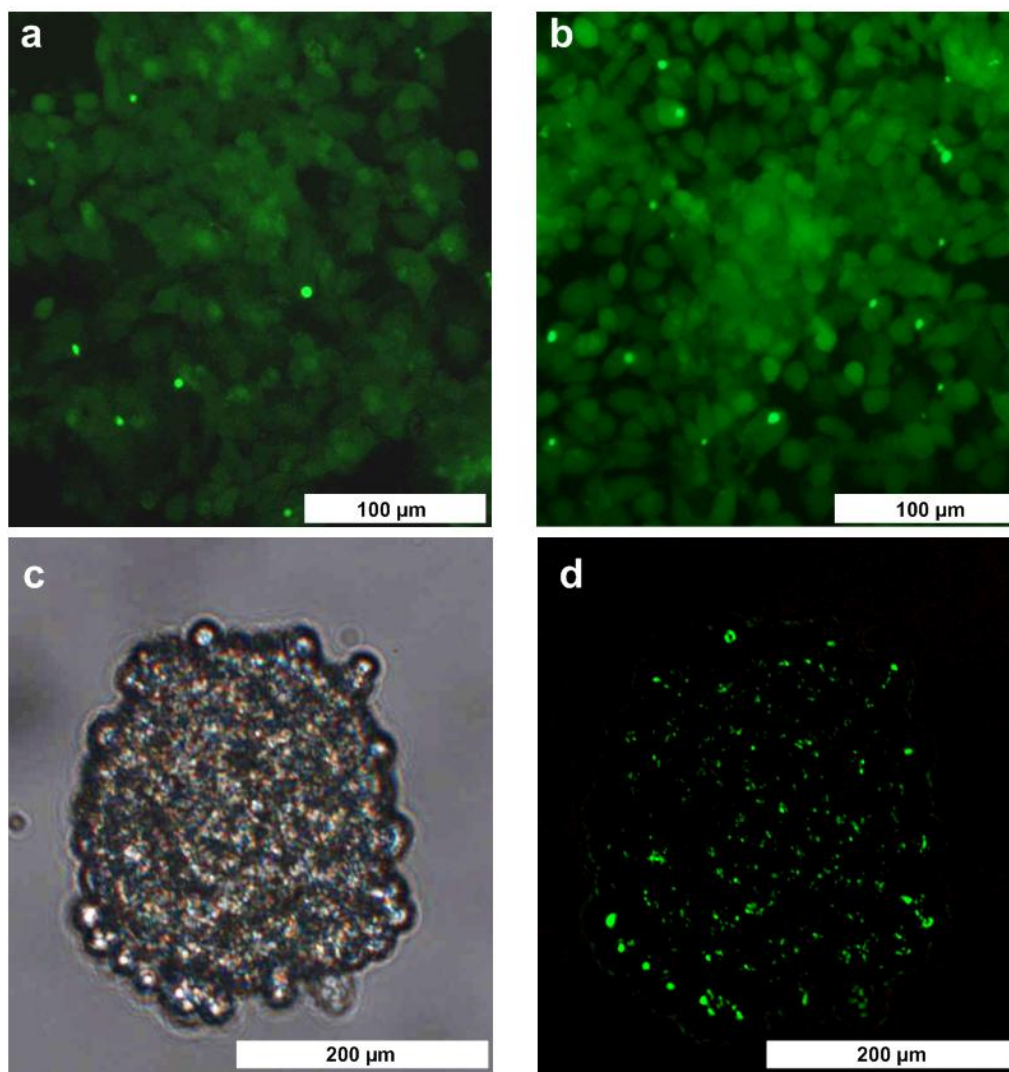


**Figure 4-9:** Investigation of MRP-2 transporter activity by CMFDA-based fluorescence assay a) HepG2 monolayer culture, b) HepG2 sandwich culture, c) light microscopy of HepG2 organotypic culture d) HepG2 organotypic culture.

## **4.4 Discussion**

In this study, 3D organotypic cultivation of HepG2 cells was performed in a scaffold-free system using hanging drop method. The method was already applied for the formation of organotypic cultures of different cell types and cell lines (Kelm *et al.*, 2003; Kelm *et al.*, 2004; Kelm and Fussenegger, 2004; Kelm *et al.*, 2006). Tissue reorganization is facilitated by gravity and as shown in our study, organotypic cultures (OTC) of a wide range of initial cells numbers (250 – 8000) can be produced. Scaffold-free cellular reorganization was observed already at day 1 after seeding and was completed at day 3. The scaffold-free system enables the microtissue formation without any force besides gravity and without xenogenic or synthetic materials. Therefore, biodegradability is not an issue and the produced organotypic cultures can be used as alternative to scaffold-based microtissue building blocks.

Importantly, the sizes of microtissues are reproducible ( $< \pm 10\%$  of mean) and are exactly adjustable for each experiment. In case of toxicity studies, lower cell numbers e.g. 250 – 500 could be used for long-term, chronic experiments ( $> 3$  weeks) in case of proliferating cells and higher numbers (2000 – 8000) could be applied in short-term toxicity studies for which a certain cell number is needed to perform endpoint assays. The low cell numbers required for these organotypic spheroids can moreover enhance throughput by allowing parallel studies in multiwell plates. This is especially advantageous in case of primary human cells which are limited by availability and other costly cell types. In case of hepatotoxicity, adequate replicates from same donor can be included. The change of culture medium is possible and therefore, different conditions are adjustable in the system e.g. the reduction of serum, the exposure to drugs, induction and other activity studies as shown in our study. Supernatant collection moreover allows studies such as metabolite profiling or protein analysis. Therefore, a detailed analysis of single spheroids is possible. If needed, high amounts of spheroids can rapidly be generated, harvested and used for further analysis. We maintained the HepG2 spheroids in low-serum medium since reduction of serum is desirable due to its chemically undefined composition, batch to batch variations and possible interactions of serum components with drug or inducers. The spheroids could be kept viable for more than two weeks at very low-serum conditions. In the late cultivation phase, proliferation zones within the spheroids were detected. This was also confirmed by glucose uptake and lactate production rates, which increased at the end of the cultivation (day 16) probably due to cell proliferation. The activity of AST as marker of cell death was highest directly after adjusting to low-serum medium. This might be due to high cellular stress in this phase because of several medium change steps. Between day 3 -6,

AST release was at constant high level indicating constant number of dying cells during this time. However, growing size indicated proliferation of the cells at the same time which seemed to stop after day 6 and onwards. Thus, AST activity was at a low stable level between day 6 and 16. Albumin production rates in the organotypic cultures were highest (38 pg/d/seeded cell) at day 3 in low-serum medium (representing day 6 after seeding), as seen before for glucose and lactate uptake/production rates. This rate is quite close to *in vivo* values of 48-72 pg/d/hepatocyte (Bhatia *et al.*, 1999). Albumin production in OTC was almost stable between day 6 and 16 and higher than in monolayer (ML) and collagen sandwich (CS) cultures for each time point. As observed by diameter measurements, the spheroids (2000 seeded cells) stopped increasing in size upon achieving diameters of about 625  $\mu\text{m}$ . This is probably due to contact inhibition which usually does not occur in conventional 2D cultures (Maruyama *et al.*, 2007). It was reported that three-dimensionally grown HepG2 cultures show higher cell cycle arrest and therefore lower proliferation than monolayer cultures (Li *et al.*, 2008). This may explain stable albumin production between day 6 and 16 by OTC since HepG2 cells seems to have stopped proliferating. Whereas in case of ML and CS the cells are continuously proliferating and therefore the albumin production per seeded cell number is higher.

Nevertheless, the increased serum protein production show enhanced liver-specific function of the organotypic cultures. The analysis of amino acid metabolism reveals that the spheroids consumed most of the proteinogenic amino acids over the whole low-serum cultivation of 3 weeks. The highest rates were found for glutamine, acting as the main energy source for the spheroids besides glucose. Moreover, mammalian cells use glutamine nitrogen to build nucleotides, amino acids and vitamins. On the other side, the spheroids steadily produced glutamate which plays an important role in the degradation and transamination of various amino acids. BCAAs were constantly consumed over time as additional energy source. These amino acids can be converted to acetyl-CoA or succinyl-CoA, which subsequently enter the TCA cycle. BCAAs moreover induce albumin production in hepatocytes through the mTOR signal pathway (Ijichi *et al.*, 2003). Overall, the consumption and production rates for most of the amino acids were quite constant indicating stable metabolism and viability of the spheroids which is a prerequisite for chronic toxicity assessment. Therefore, these organotypic cultures are well-suited for investigations of long-term drug effects. Moreover, assessing the metabolic profile of the organotypic cultures would help define substrates for  $^{13}\text{C}$  metabolic flux analysis (MFA). This can further give deep insights into the cellular metabolism of the organotypic cultures and contribute to the analysis of drug-induced metabolic effects. The use of MFA in physiological characterization has been recently reviewed (Niklas and Heinzle, 2011; Niklas *et*

*al.*, 2011b; Niklas *et al.*, 2011c). Additionally, analyzing the influence of the initial cell number (250 – 8000) on cellular metabolism would be of high interest for future studies, since differences in nutrient supply, diffusion through the spheroid, oxygen concentration or pH could affect the metabolic rates in the organotypic cultures. Further studies in these directions are underway in our laboratory.

The assessment and prediction of CYP450 enzyme induction by xenobiotics is one of the main tasks in early drug development (LeCluyse, 2001). We tested the CYP1A induction capacity, as the predominant CYP450 isoform in HepG2 cells (Wilkening *et al.*, 2003), and compared organotypic cultures to monolayer and collagen sandwich cultures. Enzyme induction was highest in the OTC and induction in ML and CS culture was similar at lower level. CYP1A enzymes catalyze the oxygenation of polycyclic aromatic hydrocarbons (PAHs) and heterocyclic aromatic amines /amides (HAAs) which can result in the formation of carcinogens (Jerina, 1983). Therefore, CYP1A induction is still of main interest in cancer research but also in drug development (Ma and Lu, 2007). The induction of CYP1A by a certain substrate can result in an enhanced metabolism of another substance. In drug development, the assessment of such drug-drug interactions is important, emphasizing the need of *in vitro* cell culture systems with functional CYP inducibility. The HepG2 organotypic cultures respond better to the CYP1A inducer 3-MC than conventional cultures and are therefore applicable as *in vitro* model for testing CYP1A induction by drug candidates.

The short-term toxicity (24 h exposure) of tamoxifen was tested in the three culture systems. It was reported that tamoxifen causes cytotoxicity in tumor cell lines (Petinari *et al.*, 2004) and human hepatocytes (Li *et al.*, 2004). For HepG2 cells, it was shown that tamoxifen down regulates the expression of *survivin* gene thereby inhibits proliferation (Guo *et al.*, 2009). Concentration-dependent toxic effects were assessed in our study for HepG2 cells in each of the three cultivation systems. The EC<sub>50</sub> value assessed for conventional monolayer culture was similar to a recently reported value (Gerets *et al.*, 2009). For the HepG2 cells cultivated in collagen-sandwich culture, we assessed a higher EC<sub>50</sub> value showing indicating an influence of the extracellular matrix. However, the HepG2 spheroids clearly showed the highest EC<sub>50</sub> value compared with the other two culture systems. This means that the cells in the organotypic cultures are less sensitive to the anti-cancer drug tamoxifen. Tamoxifen and its metabolites are substrates of ATP-binding cassette (ABC) superfamily members such as MDR-1 or MRP-2 (Shin *et al.*, 2006). It has been reported that HepG2 spheroids show higher MDR-1 activity compared to monolayer cultures (Oshikata *et al.*, 2011). In our study, we show that MRP-2 activity is also significantly higher in the organotypic cultures compared to conventional

cultures of HepG2. This could probably lead to an increased efflux of tamoxifen. Moreover, tamoxifen itself induces the expression of MDR-1 and MRP-2 (Kauffmann *et al.*, 1998; Nagaoka *et al.*, 2006) which furthermore contribute to the lower sensitivity of the spheroids to this drug.

The monitoring of morphology and viability showed that mainly the cells on the spheroid surface were affected by exposure to a tamoxifen concentration in the range of the EC<sub>50</sub> value (50 µM). This is probably due to the first contact of the drug to the outer cells. However, by exposure to a higher drug concentration (100 µM), it was clearly shown that also the inner parts of the organotypic cultures were impaired indicating complete diffusion of the drug through the spheroids. The transport of extracellular factors, signal molecules, or drugs through the liver spheroids as well as the formation of gap junctions or bile canaliculi is being further investigated in detail in our lab.

We show that spheroids of different sizes could be produced and maintained viable for more than two weeks in low-serum conditions. The 3D tissue like structure enhanced liver-specific functions such as CYP450 enzyme induction. The assessment of tamoxifen toxicity clearly revealed higher EC<sub>50</sub> values for the 3D cultures indicating that the spheroids are less sensitive to this anti-cancer drug. Moreover, we could show the formation of bile canaliculi in the organotypic cultures as well as the increased expression of MRP-2 membrane transporter compared to conventional cultures.

## 4.5 Conclusion

We report the engineering of HepG2 organotypic cultures with adjustable sizes. The cells reorganize spontaneously and built organotypic cultures (OTC) in the hanging drop without any physical force except gravity. They were characterized including growth, long-term maintenance in low-serum medium, cellular metabolism and CYP450 induction. The toxic potential of tamoxifen was assessed and the results were compared to monolayer and collagen-sandwich cultures. We show that the spheroid cultivation system could be applied to long-term studies. The system has several advantages since both supernatant as well as spheroid sampling is possible, culture conditions can be changed easily, reproducible spheroid sizes are achieved and it is well-suited for high throughput experiments. The micro-tissues achieved represent a more *in vivo* like situation and can be used as *in vitro* model using cell lines to screen anti-cancer drugs and to study tumor-specific mechanisms, e.g. chemotherapy resistance. Primary human cells can also be used for long-term studies especially in preclinical drug development.

## Acknowledgments

We acknowledge the excellent technical assistance of Esther Hoffmann and Michel Fritz.

**CHAPTER 5: GCTOF-MS BASED  
METABOLOMICS REVEALS METABOLIC  
EFFECTS OF THERAPEUTIC DRUG  
CONCENTRATIONS ON HUMAN LIVER CELLS**

This chapter has been submitted as:

**Mueller D**, Tascher G, Müller-Vieira U, Nüssler AK, Heinzle E and Noor F (2012):

**GC-TOFMS based metabolomics reveals metabolic effects of therapeutic drug concentrations on human liver cells**

## **Abstract**

Metabolomics approaches using highly sensitive and precise analytical methods such as LC- or GC-MS are finding important applications in toxicity assessment and safety pharmacology. In this study, we tested therapeutic concentrations of diclofenac (1.64 $\mu$ M) and troglitazone (1 $\mu$ M) on *in vitro* cultures of primary human hepatocytes and HepG2 cells. We compared single dose vs. repeated dose effects on the extracellular metabolome. Supernatant samples were analyzed using gas chromatography time-of-flight mass spectrometry (GC-TOFMS) and further evaluated by principal component analysis (PCA). Distinct separation of untreated control from the treated groups was observed on the basis of the measured metabolite profiles. Changes in levels of metabolites that are involved in metabolic pathways such as glycolysis and TCA cycle gave insights into adaptation of cellular metabolism in response to drug. This method is well-suited for the sensitive assessment of drug induced changes in cellular metabolism even at therapeutic concentrations. It can be applied to any other alternative testing system using human relevant cells such as stem cells or stem cell derived functional cells, in addition to offering the possibility to be adapted to any other cultivation setups e.g. 3D cell cultures.

## **5.1 Introduction**

Hepatocytes as the main site of drug metabolism are commonly used for the prediction of drug-induced effects. *In vitro* assays for drug toxicity assessment often make use of liver cell lines (e.g. HepG2) due to the ease of handling, reproducibility and their proliferation capacities. The main disadvantage of hepatic cell lines is the lack or reduced expression and activity of phase I drug metabolizing enzymes, primarily the cytochrome P450 (CYP450) enzymes. Therefore, primary human hepatocytes are still considered the best cell system in the fields of drug testing and toxicological studies, mainly because of the *in vivo* like CYP450 activity, at least just after isolation (Yuan *et al.*, 2004). Hepatic cell lines are useful for the detection of parent compound toxicity (O'Brien *et al.*, 2006; Noor *et al.*, 2009).

Metabolomics is defined as the systematic study of all metabolites in a cell, fluid, tissue, organ or organism. Many analytical techniques such as nuclear magnetic resonance (NMR), liquid chromatography, gas chromatography, mass spectrometry and combinations of these techniques are used in metabolomics (Villas-Boas *et al.*, 2005). Such approaches were reported recently for the detection of drug-induced metabolic changes (Strigun *et al.*, 2011a; Strigun *et al.*, 2011b; Strigun *et al.*, 2011c).

Gas chromatography (GC) in combination with time-of-flight mass spectrometry (TOFMS) offers new perspectives to diverse research fields e.g. forensic toxicology, doping substance screening and metabolomics/metabonomics. GC-TOFMS has several advantages compared to GC-quadrupole-MS including higher spectral scan rates and therefore unbiased chromatographic deconvolution (Weckwerth *et al.*, 2004). Use of GC-TOFMS technique for the investigation of metabolic profiles in mammalian systems has been recently reported. Lu and colleagues reported a metabonomic approach to differentiate hypertension- and age-related metabolic variations in hypertensive rats (Lu *et al.*, 2008). Other studies using GC-TOFMS show differences in metabolite pattern between different ovarian tumors (Denkert *et al.*, 2006) and colon or colorectal cancer tissues (Denkert *et al.*, 2008). Various statistical methods are used for data processing and analysis of GC-MS data depending on the application. Principal component analysis (PCA) as well as partial least squares-discriminant analysis (PLS-DA) and orthogonal PLS-DA (OPLS-DA) are widely used for GC-MS data analysis in metabolic profiling (Denkert *et al.*, 2006; Wiklund *et al.*, 2008; Schneider *et al.*, 2009; Yan *et al.*, 2009). Moreover, comprehensive computational approaches were used for the improved analysis of large metabonomic datasets (Bunk *et al.*, 2006; Hiller *et al.*, 2009). Such an approach was even extended to a non-targeted elucidation of metabolic pathways, in which all measurable

metabolites deriving from a single, isotope-labeled substrate were quantified (Hiller *et al.*, 2010). These advancements will be highly useful for comprehensive, global metabolic flux analyses in different metabolomics research fields.

In this study, we applied a metabolomics technique for the assessment of drug induced metabolic effects on both primary human hepatocytes as well as HepG2 cells. We investigate the drug metabolizing capacities of the cells using LC-MS/MS. In parallel, we analyzed the exometabolome (extracellular metabolome) of primary human hepatocytes and HepG2 cells upon single or repeated exposure to subtoxic, therapeutic concentrations of two drugs, namely diclofenac and troglitazone. Diclofenac is a non-steroidal, anti-inflammatory drug (NSAID) which can cause severe adverse hepatic reactions. Troglitazone, a thiazolidinedione, anti-diabetic drug, was withdrawn from the UK market in 1997 and in the USA in 2000. The EC<sub>50</sub> values for diclofenac and troglitazone upon 24 h exposure to primary human hepatocytes were in the range of 200 – 300 µM and 80 – 90 µM, respectively (Lauer *et al.*, 2009). Commonly used cytotoxicity assays do not show toxicity of these drugs at these low concentrations. We investigated if the therapeutic concentrations of these drugs produce effects on the cellular metabolism and if these could be identified by exometabolome analysis. Supernatant samples from drug exposed and control cells were analyzed using GC-TOFMS. Principal component analysis (PCA) was applied to identify drug induced changes in the exometabolome of the liver cells. Quantitative differences in metabolite concentrations upon drug exposure at the tested therapeutic concentrations were detected. This shows the sensitivity and potential of the method, which can furthermore be applied to other test systems in pharmacological research.

## 5.2 Materials and Methods

### 5.2.1 Chemicals

Williams Medium E with Glutamax, fetal calf serum (FCS), HEPES, sodium pyruvate and minimal essential medium-nonessential amino acids (MEM-NEAA) were purchased from Gibco (Paisley, Scotland, UK). Fortecortin was from Merck (Darmstadt, Germany) and human Insulin from Sanofi Aventis (Frankfurt am Main, Germany). Percoll was purchased from PAA (Pasching, Austria). Bovine serum albumin (BSA) was obtained from Sigma-Aldrich (St. Louis, USA). Rat tail collagen was prepared as previously described (Rajan *et al.*, 2006). Cold Storage Solution (CSS) was obtained from Hepacult (Regensburg, Germany). Heparmed, a Williams medium E based cell culture medium for the maintenance of primary human hepatocytes was from Biochrom AG (Berlin, Germany). Bufuralol was purchased from BD (Franklin Lakes, USA). Midazolam was from Cerrilant, (Wesel, Germany). Methanol, bupropion, phenacetin, diclofenac and troglitazone were all purchased from Sigma-Aldrich (Steinheim, Germany). N-Methyl-N-(trimethylsilyl)trifluoro-acetamide (MSTFA) was obtained from Macherey-Nagel (Dueren, Germany). Pyridine was purchased from Fisher Scientific (Schwerte, Germany) and methoxyamine-HCl from Sigma-Aldrich (Steinheim, Germany).

### 5.2.2 Isolation of primary human hepatocytes

Primary human hepatocytes (PHH) were isolated from resected liver tissues from patients as explained in a previous study (Mueller *et al.*, 2011). Tissue collection was done according to institutional guidelines and with each patient's written consent. Hepatocytes were isolated using a two-step collagenase P (from *Clostridium histolyticum*) perfusion technique, followed by a Percoll density gradient centrifugation (Nussler *et al.*, 2009). The purity and viability was determined under light microscopy using trypan blue exclusion.

### 5.2.3 Cell culture

Immediately after isolation, PHH were seeded in 6 well plates (BD Falcon) coated with rat tail collagen in Williams medium E, supplemented with penicillin/streptomycin (100 U / 100 µg/ml), HEPES (15 mM), FCS (10%), insulin (1 mM), sodium pyruvate (1mM) and fortecortin (0.8 µg/ml). Cell number was  $10^6$  cells / well as determined by trypan blue exclusion.

The human hepatoblastoma cell line, HepG2, was obtained from the German collection of microorganisms and cell cultures (DMSZ, Braunschweig, Germany). Cells were maintained in

Heparmed supplemented with penicillin/streptomycin (100 U / 100 µg/ml) and insulin (20 IU/l), transferrin (5 mg/l), glucagon (3 µg/l) (ITG, from Biochrom) as well as 10% FCS.  $5 \times 10^5$  cells were seeded per well in a 6-well plate (Greiner Bio-One GmbH, Kremsmuenster, Austria). The cells (PHH and HepG2) were kept at 37°C in a cell incubator (Mettler GmbH, Schwabach, Germany) at 95 % relative humidity with 5 % CO<sub>2</sub> supply.

#### **5.2.4 Drug treatment and sampling**

Stock solutions of diclofenac and troglitazone were prepared in DMSO. The final DMSO concentration in any test solution did not exceed 0.05 %. This concentration was shown to have no influence on the exometabolome of human liver cells in our lab (data not shown). Moreover, it was reported that DMSO concentrations up to 0.5% are tolerable for liver cells without toxicity or altered gene expression (Sumida *et al.*, 2011). PHH from two donors were used in this study. Diclofenac (donor 1) and troglitazone (donor 2) were tested in triplicates. Respective untreated controls from each donor were run in parallel to the tests. 1 µM troglitazone and 1.64 µM diclofenac were chosen as representative therapeutic concentrations based on literature (Emoto *et al.*, 2001; Hinz *et al.*, 2005). Cells were maintained in serum-free conditions during drug exposure and were treated with one dose (single-dose group) of the respective drug for 24 hours (h) or with 4 repeated doses (repeated-dose group) with total exposure time of 96h. For the repeated dose groups, medium containing test drug was refreshed daily. Supernatant samples at 24 h and 96 h time points were analyzed and compared with the respective controls.

#### **5.2.5 Cytochrome P450 activity assay**

The functional enzyme activity test for CYP1A2, CYP2B6, CYP2C9 and CYP3A4 was performed in a cassette approach based on probe reactions as previously described (Mueller *et al.*, 2011). CYP2D6 activity was tested separately prior to the addition of the CYP substrate cassette, since for CYP2D6, interaction was shown with the other substrates (Mueller *et al.*, 2011). The substrates used were bufuralol for CYP2D6, phenacetin for CYP1A2, bupropion for CYP2B6, diclofenac for CYP2C9 and midazolam for CYP3A4. Assay time was 1 hour for CYP2D6 and 2 hours for the CYP cassette.

#### **5.2.6 Quantification of the metabolites in CYP assay by LC-MS/MS**

The HPLC system consisted of an MS Plus pump (Surveyor) and an AS Plus auto sampler (Surveyor). Mass spectrometry was performed on a TSQ Quantum Discovery Max triple

quadrupole mass spectrometer equipped with either a heated electrospray (H-ESI) interface (for analysis of hydroxybupropion, 1-hydroxymidazolam and 4-hydroxydiclofenac) or an APCI probe (for analysis of acetaminophen), respectively, connected to a PC running the standard software Xcalibur 2.0.7 (Thermo Fisher Scientific, USA). The flow rate was set to 300  $\mu\text{l}/\text{min}$  and the compounds were separated on an Uptisphere OBD, 3  $\mu\text{m}$ , 100x2.1 mm (Interchim, France) analytical column with a pre-column (Uptisphere OBD, 3  $\mu\text{m}$ , 10x2.0 mm, Interchim, France). Gradient elution with acetonitrile/0.1% formic acid as organic phase (A) and 10 mM ammonium formate/0.1% formic acid as aqueous phase (B) was performed using the following gradient: % A (t (min)): 5(0-0.2)-97(1.8-4.3)-5(4.5-7.0). The MS-MS identification of characteristic fragment ions was performed using a generic parameter set: ion source temperature 350°C, capillary voltage 3.8 kV, collision gas 0.8 mbar argon, spray and sheath gas, 20 and 8 (arbitrary units), respectively. The stable product ions with the highest S/N ratio were used to quantify the analyte in the selected reaction monitoring mode (SRM).

The transitions used for MS/MS analysis were as follows: 278.2  $\rightarrow$  186.0 for 1-OH-bufuralol, 152.1  $\rightarrow$  65.0 for acetaminophen, 256.2  $\rightarrow$  139.0 for OH-bupropion, 312.1  $\rightarrow$  231.0 for 4-OH-diclofenac and 342.1  $\rightarrow$  203.0 for 1-OH-midazolam.

### **5.2.7 Viability assays**

The activity of liver-specific aspartate aminotransferase (AST) in the culture supernatant was determined using a kinetic UV assay kit (HITADO, Möhnese-Delecke, Germany) according to the manufacturer's instructions.

Sulforhodamin B (SRB) assay was carried out as previously described (Beckers *et al.*, 2010). This colorimetric endpoint assay quantifies the total protein content which is directly correlated to the cell number.

### **5.2.8 Sample preparation for GC-TOFMS**

200  $\mu\text{l}$  methanol was added to 50  $\mu\text{l}$  supernatant or medium samples for protein precipitation. The mixture was vortexed for 3 minutes and incubated for 1h on ice. Afterwards, samples were centrifuged (10 min, 13.000g, 4°C). Supernatant was transferred into glass vials and mixed with 200  $\mu\text{l}$   $\alpha$ -aminobutyric acid (1 mM in  $\text{H}_2\text{O}$ ) used as internal standard. These samples were freeze dried prior to a two-step derivatization. Firstly, 50  $\mu\text{l}$  of methoxyaminin pyridine (20 g/l) was added and the mixture stirred for 30 min at 80°C for methoximation. This was followed by derivatization with 50  $\mu\text{l}$  of the reagent MSTFA (N-Methyl-N-(trimethylsilyl)trifluoro-

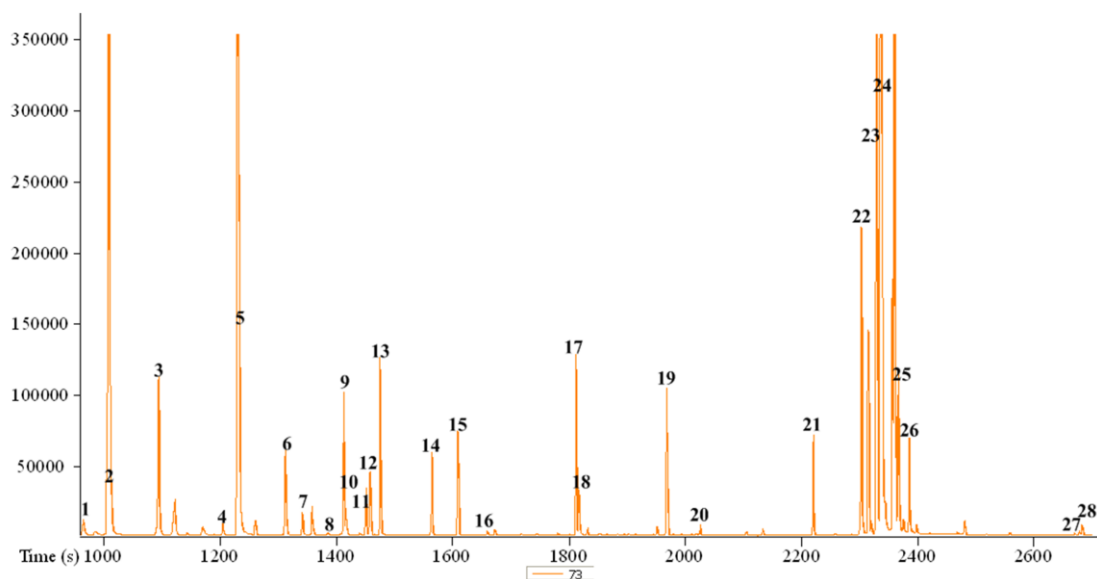
acetamide) for 30 min at 80°C. Derivatization was automatically carried out using a MPS 2XL autosampler equipped with an agitator (both from Gerstel, Karlsruhe, and Germany). Each sample was measured in triplicate, resulting in both three biological and three technical replicates, i.e. 9 samples per test group.

### **5.2.9 GC-TOFMS measurement**

The GC-TOFMS consisted of an Agilent 7890 gas chromatograph (Hewlett-Packard, Atlanta, USA) coupled to a Pegasus HT ToF mass spectrometer (Leco, Mönchengladbach, Germany). A HP5-ms capillary column of 60 m length, 0.25 mm inner diameter and 0.25 µm film thickness was used for separation. Splitless injection (volume 1 µl) was performed. The initial GC-oven temperature was set at 70°C with a ramp of 5°C/min and a final temperature of 320°C. Helium was used as carrier gas and a constant flow rate of 1 ml/min was adjusted. The transfer line temperature was set at 250°C. Mass spectra were acquired within a range of 70 to 700 m/z and scan rate was 20 spectra per second. Ion source voltage was set at 70 eV and temperature at 200°C.

### **5.2.10 Data processing, normalization and multivariate statistical analysis**

Chromatogram acquisition, automated peak deconvolution, identification of suitable fragment mass to charge ratio for peak area determination and reference library search were carried out using ChromaTof 4.22 software (Leco). Similarity threshold, which determines the minimum similarity of the obtained spectrum with the reference library spectrum, was set at 600. Annotation of metabolites were performed using the reference library or by the assessment of retention time and mass spectra from standard substance measurements. Furthermore, the Golm Metabolome Database was used for mass spectra analysis of non-identified metabolites (NIMs) (Hummel *et al.*, 2010). The database supports a decision-tree based prediction of functional groups allowing classification of the compounds. Known artifact peaks such as solvent contamination, column bleeding, plasticizers or reagent peaks were manually excluded. Peak areas of biologically relevant metabolites which were present in both drug-exposed and control samples were normalized to the respective peak area of the internal standard (m/z 130) for each sample. Peak areas of metabolites with more than one derivatization product (e.g. aspartate) were summed as well as peak areas of metabolites with several isomers upon methoximation such as glucose. A range of 25 – 30 metabolites was analyzed by this method. Figure 5-1 shows a representative chromatogram with indicated numbered metabolites.



1 Pyruvate, 2 Lactate, 3 Alanine, 4 3-Hydroxybutyric acid, 5 Aminobutyric acid, 6 Valine, 7 Urea, 8 Serine, 9 Leucine, 10 Glycerol, 11 Isoleucine, 12 Proline, 13 Glycine, 14 Serine, 15 Threonine, 16 Aspartate, 17 Methionine, 18 Pyroglutamic acid, 19 Phenylalanine, 20 Asparagine, 21 Ornithine, 22 Fructose, 23 Galactose, 24 Glucose, 25 Tyrosine, 26 Sorbitol, 27 Tetradecanoic acid, 28 Tryptophan

**Figure 5-1: Representative chromatogram of supernatant samples used in this study (m/z 73, characteristic for MSTFA derivatization). The predominant peaks were chosen and peaks of the indicated metabolites are numbered.**

To assess if a metabolite was released or taken up by the cells, fresh medium controls were prepared, measured and analyzed exactly as described and fresh medium peak areas were compared to peak areas of the cell samples. Normalized peak areas were auto-scaled using standard deviation and then used for PCA to reduce the dimensions of the dataset. The variance in dataset can be described using a set of underlying orthogonal variables (the principal components). Student's *t*-test was used to identify significant quantitative changes in exometabolome of untreated control and drug exposed cells. Fold changes were calculated compared to the control (fold change > 1 indicates increased metabolite concentration in drug exposed group). A threshold of significance was defined as *p*-value <0.05 and fold change  $\geq 1.15$  or  $\leq 0.85$ . The methods were performed using Matlab R2006a (The MathWorks) software.

## **5.3 Results**

### **5.3.1 Precision and reproducibility of the method**

For the assessment of the precision and reproducibility of the method, fresh medium samples were prepared for GCTOF-MS analysis and measured in triplicates. 15 medium components were analyzed and relative standard deviations (RSD) were determined as shown in table 5-1.

**Table 5-1: Precision of sample preparation and GCTOF-MS analysis assessed by %RSD (relative standard deviation) of 15 metabolites and IS from 3 technical replicates of control samples (pure medium).**

<b>Metabolite</b>	<b>%RSD</b>	
	<b>w/o normalization</b>	<b>normalized to IS (m/z 130)</b>
Alanine (2TMS)	10.8	10.1
Valine (2TMS)	7.5	6.9
Threonine (3TMS)	9.3	8.6
Serine (3TMS)	10.7	10.2
Isoleucine (2TMS)	13.3	12.6
Leucine (2TMS)	8.3	7.9
Phenylalanine (2TMS)	8.6	7.9
Ornithine (4TMS)	7.6	8.4
Glycine (3TMS)	6.8	6.1
Galactose (5TMS, 2 MEOX isomers)	8.0	7.2
Glucose (5TMS, 2 MEOX isomers)	8.5	7.7
Fructose (5TMS, 2 MEOX isomers)	9.6	8.9
Sorbitol (6TMS)	6.8	6.0
Tyrosine (2TMS+3TMS)	8.3	7.6
Aspartate (2TMS+3TMS)	10.7	9.9
$\alpha$ -Aminobutyric acid (IS; 2TMS)	0.8	-
<b>mean %RDS (w/o IS)</b>	<b>9.0</b>	<b>8.4</b>

Most of the analytes showed %RSD below 10%. Without peak area normalization, the lowest value was assessed for sorbitol and glycine (6.8%). Isoleucine showed the highest %RSD of 13.3%. By normalization, the RSDs of all metabolites decreased except for ornithine. Peak areas of the internal standard  $\alpha$ -aminobutyric acid were highly reproducible with RSD value of 0.8%.

### 5.3.2 Evaluation of liver-specific drug-metabolizing functions

For the primary human hepatocytes used in this study, the activity of cytochrome P450 enzymes was assessed at day 6 after isolation as depicted in figure 5-2.

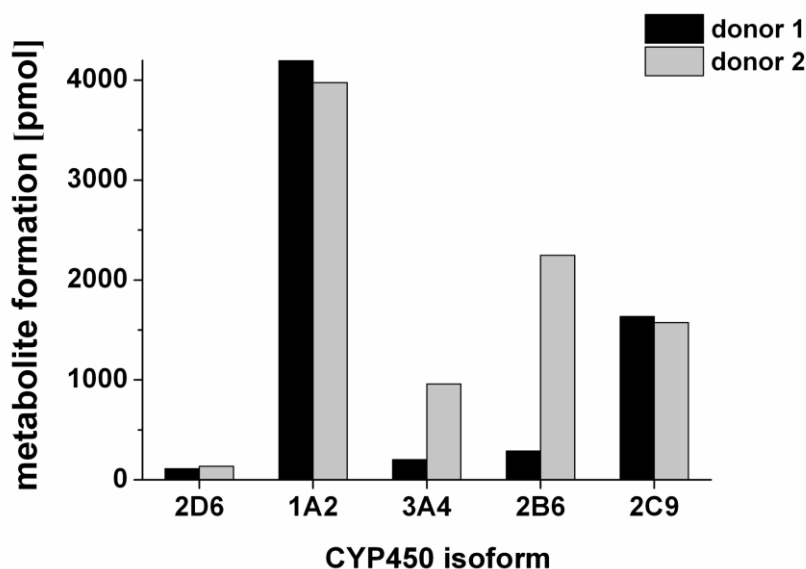


Figure 5-2: CYP450 activities in isolated primary human hepatocytes (day 6 after isolation) from 2 different donors. Activity was determined by quantifying the formation of metabolites which are 1-OH-Midazolam (CYP3A4), 4-OH-Diclofenac (CYP2C9), OH-Bupropion (CYP2B6), Acetaminophen (CYP1A2) and 1-OH-Bufuralol (CYP2D6). Test duration was 1 hour (h) for CYP2D6 and 2 h for CYP cocktail containing substrates for CYP1A2, 3A4, 2B6 and 2C9.

The investigated specific substrates were all transformed to their respective metabolites. Inter-individual differences were observed between the two donors in the activities of CYP3A4 and 2B6 which were higher in liver cells from donor 2. For HepG2 cells, no metabolite formation was detected.

### 5.3.3 Viability assessment

AST activity in supernatant samples was measured as indicator of cell viability. The respective activities for primary human hepatocytes and HepG2 cells after single dose exposure (24h) are shown in table 5-2. For repeated dose experiments, samples were taken every 24h and cumulative values are presented.

**Table 5-2: AST activities in drug-exposed primary human hepatocytes and HepG2 cells and their respective controls as indicator of cell viability. Values after single dose exposure (24h) as well as summed activities after repeated dose exposure (4 doses, 96h) are shown. Activities are given as mean values  $\pm$ SD ( $n=3$ ).**

<b>PHH</b>	<b>AST activity [U/l]</b>		<b>AST activity [U/l]</b>	
	<b>Troglitazone (1 <math>\mu</math>M)</b>		<b>Diclofenac (1.64 <math>\mu</math>M)</b>	
	<i>control</i>	<i>treated</i>	<i>control</i>	<i>treated</i>
<b>24h</b>	50 $\pm$ 3	32 $\pm$ 1**	61 $\pm$ 2	56 $\pm$ 2**
<b>96h</b>	239 $\pm$ 23	221 $\pm$ 20	178 $\pm$ 11	196 $\pm$ 12

<b>HepG2 cells</b>	<b>AST activity [U/l]</b>		<b>AST activity [U/l]</b>	
	<b>Troglitazone (1 <math>\mu</math>M)</b>		<b>Diclofenac (1.64 <math>\mu</math>M)</b>	
	<i>control</i>	<i>treated</i>	<i>control</i>	<i>treated</i>
<b>24h</b>	16 $\pm$ 5	14 $\pm$ 1	14 $\pm$ 1	12 $\pm$ 1
<b>96h</b>	253 $\pm$ 14	95 $\pm$ 13***	254 $\pm$ 9	233 $\pm$ 29

\*\*: $p < 0.01$ , \*\*\*: $p < 0.001$ .

Significant difference in AST activity was found upon single dose exposure to diclofenac and troglitazone, whereby the treated PHH showed lower extracellular enzyme activity compared to the untreated control. During repeated dose testing (96h) for both drugs, the treated primary human hepatocytes showed no significant differences as compared to their respective untreated controls.

For HepG2 cells, single dose exposure to drugs and solvent resulted in low, comparable AST activities in all control and treated samples. However, significant differences upon repeated troglitazone exposure were observed. The respective control shows an enzyme activity of 253 U/l whereas the activity in the troglitazone treated cells was significantly lower (95 U/l). Diclofenac repeated dose exposure did not affect cellular viability.

As further viability test, SRB staining was carried out at the end of the experiment, i.e. after repeated drug exposure (figure 5-3).

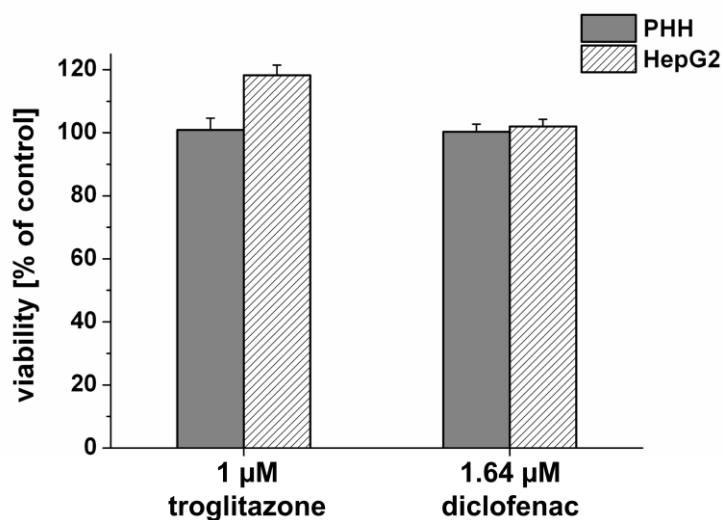


Figure 5-3: Viability (as percentage of untreated control) of drug exposed primary human hepatocytes (PHH) and HepG2 cells after repeated drug exposure. Viability was assessed by SRB endpoint assay. Error bars indicate standard deviations ( $n=3$ ), \*\*:  $p < 0.01$ .

No significant differences in viability were found for the drug exposed cells as compared to the respective untreated controls except for troglitazone treated HepG2 cells, whereby the viability was slightly higher than the control. However, again no cytotoxic effects of the therapeutic drug concentrations were detected by this endpoint assay.

### 5.3.4 Effects of troglitazone on cellular exometabolome

#### *Primary human hepatocytes*

Effects of troglitazone on exometabolome of PHH were visualized with the score plots as depicted in figure 5-4.

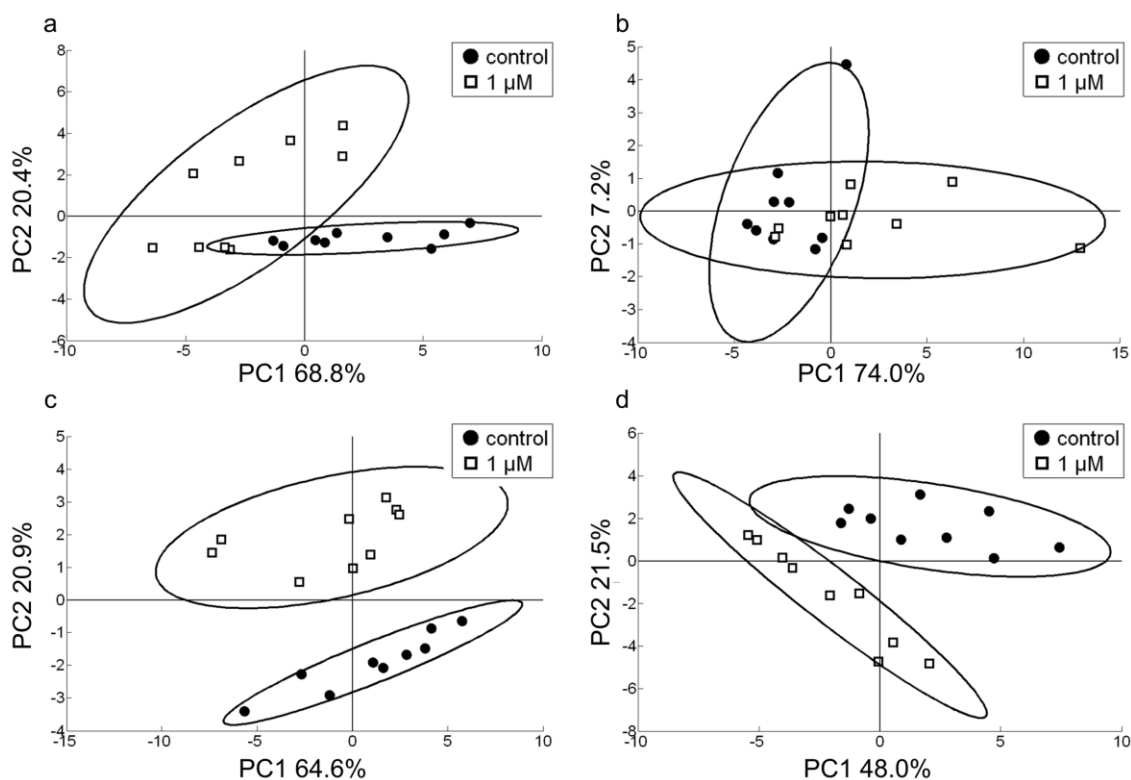


**Figure 5-4: PCA score plots of principal component 1 and 2 for troglitazone-treated (1  $\mu$ M, open squares) and untreated samples (closed circles) with 24 h single dose and repeated doses for 96 h,  $N=3$ ,  $n=3$  a) Primary human hepatocytes at 24 h b) HepG2 cells at 24 h c) Primary human hepatocytes at 96 h d) HepG2 cells at 96 h. The respective classes are shown within 95% confidence ellipses.**

For PHH, a clear separation as seen by 95% confidence ellipses could be observed upon single dose exposure, whereby the first two principal components account for 89% of the total variance (figure 5-4a). Significant quantitative differences were found for 13 metabolites between the control and drug exposed cells (fold change  $\geq 1.15$  or  $\leq 0.85$ ,  $p$ -value  $< 0.05$ ) (table 5-3). Concentrations of the amino acids phenylalanine, valine, serine, threonine and isoleucine were significantly reduced indicating higher uptake upon single troglitazone dose. As observed from loading coefficients, these metabolites contribute most to the separation along the first component. Glucose release and lactate production were reduced. The production of the ketone body 3-hydroxybutyric acid was reduced in addition to decreased urea and ornithine supernatant levels.

Upon repeated troglitazone exposure, PCA score plot again shows clear grouping and PC1 and PC2 describe 85% of the total variance (figure 5-4c). Concentrations of 8 metabolites were significantly changed in exometabolome of PHH (table 5-4). Higher ornithine and urea levels

were measured. Galactose uptake was reduced. Highest fold change (2.04) was observed for a metabolite (NIM1) which could not be reliably identified.

**Table 5-3: Fold changes in normalized metabolite peak areas of troglitazone (1  $\mu$ M) exposed primary human hepatocytes and HepG2 cells (single dose for 24h) compared to untreated control (n = 9/group). Fold change is expressed in comparison to the control and a fold change > 1 indicates increased metabolite concentration in treated group as compared to the untreated control. The indicated m/z ratios were used for peak area determination. Last column shows if the respective metabolite is taken up (-) or released (+) by the cells as compared to medium control (blank).**

24 h Troglitazone (1 $\mu$ M)									
Primary human hepatocytes					HepG2 cells				
Identified metabolite	m/z	fc	p	net	Identified metabolite	m/z	fc	p	net
Valine (2 TMS)	73	0.83	< 0.05	-	Valine (2 TMS)	73	1.24	< 0.05	-
Threonine (3 TMS)	73	0.82	< 0.05	+	Propanoic acid (TMS)	73	1.23	< 0.05	-
Serine (3 TMS)	73	0.81	< 0.05	+	Aspartate (2 TMS+3 TMS)	73;73	1.20	< 0.05	-
Isoleucine (2 TMS)	73	0.80	< 0.05	-	Leucine (2 TMS)	158	1.19	< 0.05	-
Phenylalanine (2 TMS)	73	0.80	< 0.05	+	Phenylalanine (2 TMS)	73	1.19	< 0.05	-
Glucose (5 TMS,2 MEOX)	73, 73	0.78	< 0.01	+	Serine (3 TMS)	73	1.19	< 0.05	+
Pyroglutamic acid (2 TMS)	156	0.77	< 0.05	+	Proline (2 TMS)	142	1.18	< 0.05	+
Glycine (3 TMS)	73	0.68	< 0.001	-	Threonine (3 TMS)	73	1.18	< 0.05	-
Lactate (2 TMS)	117	0.65	< 0.01	+	Galactose (5 TMS, 2 MEOX)	73; 73	1.16	< 0.05	-
3-Hydroxybutyric acid (2 TMS)	73	0.64	< 0.01	+	Lactate (2 TMS)	117	1.05	n.s.	+
Urea (2 TMS)	147	0.46	< 0.001	+	Glucose (5 TMS, 2 MEOX)	73; 73	1.03	n.s.	-
Ornithine (4 TMS)	73	0.36	< 0.001	+					
Galactose (5 TMS,2 MEOX)	73, 73	1.01	n.s.	+					

Fc = fold change, p = p-value, NIM = non-identified metabolite (functional group prediction by Golm Metabolome Database), n.s. = non-significant, TMS=trimethylsilyl, MEOX=methoxyisomer.

***HepG2 cells***

For HepG2 cells, low separation was observed after single, therapeutic troglitazone dose (figure 4-4b), which was mainly determined by alterations in amino acid and galactose levels. After repeated troglitazone exposure, PCA shows a distinct clustering indicated by 95% confidence ellipses as seen in figure 4-4d. PC1 and PC2 describe 69% of the total variance and quantitative differences were found in concentrations of 13 metabolites. The production of urea, ornithine and lactate was significantly elevated (table 5-4). Moreover, the consumption of the sugars namely; fructose, glucose and galactose and of the amino acids; leucine and isoleucine, was significantly increased.

**Table 5-4: Fold changes in normalized metabolite peak areas of troglitazone (1  $\mu$ M) exposed primary human hepatocytes and HepG2 cells (4 doses, total exposure time 96h) compared to untreated control (n = 9/group). Fold change is expressed in comparison to the control and a fold change > 1 indicates increased metabolite concentration in treated group as compared to the untreated control. The indicated m/z ratios were used for peak area determination. Last column shows if the respective metabolite is taken up (-) or released (+) by the cells as compared to medium control (blank). NIM = non-identified metabolite (functional group prediction by Golm Metabolome Database).**

96 h Troglitazone (1 $\mu$ M)									
Primary human hepatocytes					HepG2 cells				
Identified metabolite	m/z	fc	p	net	Identified metabolite	m/z	fc	p	net
<b>NIM1</b> (primary amin)	73	2.04	<0.001	-	<b>Urea</b> (2 TMS)	147	3.34	< 0.05	+
<b>Ornithine</b> (4 TMS)	73	1.76	<0.001	+	<b>Ornithine</b> (4 TMS)	73	2.29	< 0.01	+
<b>Galactose</b> (5 TMS, 2 MEOX)	73;147	1.33	<0.001	-	<b>Glutamine</b> (3 TMS)	73	1.51	< 0.05	-
<b>Urea</b> (2 TMS)	147	1.23	<0.05	+	<b>Lactate</b> (2 TMS)	117	1.28	< 0.01	+
<b>Glycine</b> (3 TMS)	73	1.20	<0.01	-	<b>Alanine</b> (2 TMS)	116	1.24	< 0.05	-
<b>Lactate</b> (2 TMS)	117	1.00	n.s.	+	<b>Threonine</b> (3 TMS)	73	0.78	< 0.05	-
<b>Glucose</b> (5 TMS, 2 MEOX)	73;147	1.03	n.s.	+	<b>Tryptophan</b> (3 TMS)	73	0.71	< 0.05	-
					<b>Serine</b> (3 TMS)	73	0.69	< 0.05	+
					<b>Galactose</b> (5 TMS,2 MEOX)	73;319	0.61	< 0.01	-
					<b>Isoleucine</b> (2 TMS)	73	0.59	< 0.05	-
					<b>Leucine</b> (2 TMS)	158	0.30	< 0.05	-
					<b>Fructose</b> (5 TMS, 2 MEOX)	73	0.24	< 0.01	-
					<b>Glucose</b> (5 TMS, 2 MEOX)	73;160	0.16	< 0.01	-

Fc = fold change,  $p$  = p-value, NIM = non-identified metabolite (functional group prediction by Golm Metabolome Database), n.s. = non-significant, TMS=trimethylsilyl, MEOX=methoxyisomer.

### 5.3.5 Effects of diclofenac on cellular exometabolome

#### *Primary human hepatocytes*

Upon single dose treatment with diclofenac, PCA reveals a complete separation between the two groups for primary human hepatocytes (figure 5-5 a).

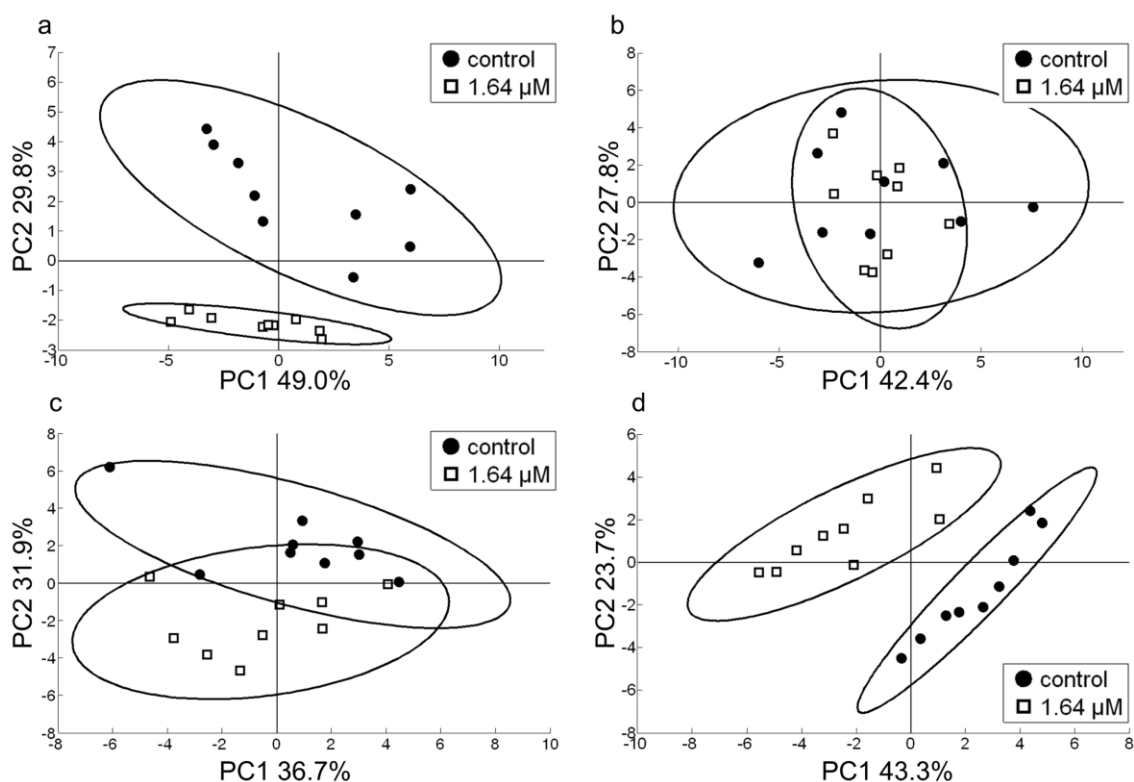


**Figure 5-5:** PCA score plots of principal component 1 and 2 for diclofenac-exposed (1.64  $\mu$ M, open squares) and untreated control samples (closed circles) with 24 h single dose and repeated doses for 96 h,  $N=3$ ,  $n=3$  a) Primary human hepatocytes at 24 h b) HepG2 cells at 24 h c) Primary human hepatocytes at 96 h d) HepG2 cells at 96 h. The respective classes are shown within 95% confidence ellipses.

79% of the total variance is explained by the two first principal components. Significant differences in metabolites between the two groups (fold change  $\geq 1.15$  or  $\leq 0.85$ ,  $p$ -value  $< 0.05$ ) for single dose exposure of primary human hepatocytes to diclofenac are shown in table 5-5. Supernatant levels of 10 metabolites were significantly changed. Lactate production was increased with a fold change of 1.77. The amounts of valine, glycine, isoleucine and leucine in

culture supernatant indicated reduced consumptions. Tyrosine uptake was significantly increased. Although glucose was released by the cells, sorbitol concentration was tremendously decreased (fold change 0.35) in the supernatants of diclofenac exposed cells indicating its highly increased uptake by the cells.

Regarding repeated dose exposure of primary human hepatocytes to diclofenac, PCA score plot shows less separation (figure 5-5c). 69% of the total variance is explained by the first two principal components. Again an increased lactate production (fold change 1.29) was observed as well as higher galactose and sorbitol uptake from culture medium (fold changes 0.82 and 0.68, respectively) compared to untreated control. Overall, ten metabolites were significantly changed upon repeated diclofenac exposure, the highest difference was found for a non-identified metabolite (NIM 3), which was released by the cells (table 5-6).

**Table 5-5: Fold changes in normalized metabolite peak areas of diclofenac (1.64  $\mu$ M) exposed primary human hepatocytes and HepG2 cells (single dose for 24h) compared to untreated control (n = 9/group). Fold change is expressed in comparison to the control and a fold change > 1 indicates increased metabolite concentration in treated group as compared to the untreated control. The indicated m/z ratios were used for peak area determination. Last column shows if the respective metabolite is taken up (-) or released (+) by the cells as compared to medium control (blank).**

24 h Diclofenac (1.64 $\mu$ M)									
Primary human hepatocytes					HepG2 cells				
Identified metabolite	m/z	fc	p	net	Identified metabolite	m/z	fc	p	net
Lactate (2 TMS)	117	1.77	< 0.001	+	Lactate (2 TMS)	117	0.88	n.s.	+
Valine (2 TMS)	73	1.50	< 0.01	-	Glucose (5 TMS, 2 MEOX)	73;147	0.88	n.s.	-
Glucose (5 TMS, 2 MEOX)	73;147	1.47	< 0.001	+	Galactose (5 TMS, 2 MEOX)	73;147	0.99	n.s.	-
Glycine (3 TMS)	73	1.42	< 0.01	-					
Isoleucine (2 TMS)	73	1.31	< 0.05	-					
Leucine (2 TMS)	158	1.24	< 0.01	-					
Galactose (5 TMS, 2 MEOX)	73;73	1.19	< 0.05	-					
Tyrosine (3 TMS, 4 TMS)	179; 73	0.77	< 0.01	-					
NIM 2 (fatty acid)	73	0.72	< 0.05	+					
Sorbitol (6 TMS)	73	0.35	< 0.01	-					
Urea (2 TMS)	147	0.82	n.s.	+					

Fc = fold change, p = p-value, NIM = non-identified metabolite (functional group prediction by Golm Metabolome Database), n.s. = non-significant, TMS=trimethylsilyl, MEOX=methoxyisomer.

***HepG2 cells***

Single dose exposure of HepG2 cells to diclofenac did not affect cellular metabolome (figure 5-5b). No significant, quantitative changes in any metabolite concentrations were found.

In contrast, PCA score plot reveals a clear separation upon repeated diclofenac exposure between treated and untreated cells (figure 5-5d). Increased cellular lactate production (fold change 1.38) and alanine consumption (fold change 1.24) were observed as shown in table 5-6. Branched chain amino acids (BCAAs), sugars and lactate showed the highest loading coefficients responsible for separation along PC1. Moreover, the consumption of glucose was significantly increased (fold change 0.59,  $p < 0.001$ ).

**Table 5-6: Fold changes in normalized metabolite peak areas of diclofenac (1.64  $\mu$ M) exposed primary human hepatocytes and HepG2cells (4 doses, total exposure time 96h) compared to untreated control (n = 9/group). Fold change is expressed in comparison to the control and a fold change > 1 indicates increased metabolite concentration in treated group as compared to the untreated control. The indicated m/z ratios were used for peak area determination. Last column shows if the respective metabolite is taken up (-) or released (+) by the cells as compared to medium control (blank).**

96 h Diclofenac (1.64 $\mu$ M)									
Primary human hepatocytes					HepG2 cells				
Identified metabolite	m/z	fc	p	net	Identified metabolite	m/z	fc	p	net
<b>NIM 3</b> (sec. alcohol)	73	1.58	< 0.001	+	<b>Lactate</b> (2 TMS)	117	1.38	<0.01	+
<b>Chlorogenic acid</b> (6 TMS)	73	1.56	< 0.01	+	<b>Alanine</b> (2 TMS)	116	1.24	< 0.001	-
<b>Lactate</b> (2 TMS)	73	1.29	< 0.01	+	<b>Tryptophan</b> (3 TMS)	73	0.83	< 0.05	-
<b>Pyroglutamic acid</b> (2 TMS)	73	1.28	< 0.01	+	<b>Pyroglutamic acid</b> (2 TMS)	156	0.68	< 0.001	+
<b>Alanine</b> (2 TMS)	116	1.23	< 0.01	-	<b>Glucose</b> (5 TMS, 2 MEOX)	73;147	0.59	< 0.001	-
<b>Galactose</b> (5 TMS, 2 MEOX)	73;147	0.82	< 0.01	-	<b>Galactose</b> (5TMS, 2 MEOX)	73;73	0.93	n.s.	-
<b>Threonine</b> (3 TMS)	73	0.77	< 0.05	-					
<b>Sorbitol</b> (6 TMS)	73	0.68	< 0.01	-					
<b>NIM 1</b> (primary amin)	73	0.66	< 0.05	-					
<b>Urea</b> (2 TMS)	147	1.07	n.s.	+					
<b>Glucose</b> (5 TMS, 2 MEOX)	73;147	0.98	n.s.	+					

Fc = fold change, p = p-value, NIM = non-identified metabolite (functional group prediction by Golm Metabolome Database), n.s. = non-significant, TMS=trimethylsilyl, MEOX=methoxyisomer

## 5.4 Discussion

The aim of this study was to apply a GCTOF-MS based metabolomics approach for the assessment of effects of subtoxic, therapeutic drug concentrations of diclofenac and troglitazone on the exometabolome of human liver cells. In this approach, sampling as well as measurements is rapid and easy to handle since the culture supernatants were analyzed. This avoids labour intensive intracellular metabolite extraction which is more complex for mammalian cells than for microorganism. The precision and reproducibility of the method was tested, showing low %RSD values and further improvement by peak area normalization to the internal standard. As such the method is suitable for the comparison of different sample groups. A threshold for significant metabolite differences was defined, which was  $p$ -value  $< 0.05$  and fold change  $\geq 1.15$  or  $\leq 0.85$ .

Single dose exposure (24h) and repeated doses (96h, 4 doses) was carried out. For all experiments, no toxic effects (AST release; SRB staining) were caused by drug exposure. CYP450 activity assessed by LC-MS/MS showed that the primary human hepatocytes from the two tested donors were metabolically active at day 6 after isolation, albeit donor-to-donor variability. For HepG2 cells, no drug-metabolizing capacities were detected in this assay as no metabolite formation was observed.

Single dose exposure to troglitazone resulted in higher consumption of amino acids by the primary human hepatocytes. Moreover a decreased glucose release was noticed, an observation previously described (Rosa *et al.*, 2004). Regarding AST activity, a higher enzyme release was observed in control cells after 24 hours, correlating with elevated urea and ornithine concentrations in the supernatants. This can be explained by the extracellular conversion of arginine to urea and ornithine by arginase 1 released into supernatant upon cell death (Peters *et al.*, 2008). We also observed a reduced 3-hydroxybutyric acid secretion, a metabolite produced during fatty acid breakdown. This indicates an inhibition of fatty acid oxidation by troglitazone which is also previously reported (Fulgencio *et al.*, 1996). Repeated troglitazone treatment also induced significant metabolic changes. However, fewer effects were observed as compared to single dose experiment. Troglitazone is mainly metabolized by CYP3A4 to a sulfate, a quinone (via CYP3A4) and a glucuronide via phase II enzymes (Loi *et al.*, 1999; Kassahun *et al.*, 2001). Moreover, it was reported that troglitazone induces CYP3A4 (Sahi *et al.*, 2000) and that high CYP3A4 activity induces detoxification pathways.

HepG2 cells showed fewer changes in exometabolome upon single dose troglitazone exposure. However, after repeated troglitazone treatment, higher effects on HepG2 exometabolome were observed. These differences for the cell line could be explained by the limited drug-metabolizing capacity of HepG2 cells leading to an intracellular accumulation of the drug and therefore to increased cellular effects upon repeated dose exposure.

Single therapeutic dose exposure to diclofenac led to changes in supernatant levels of lactate, sugars and amino acids. Sorbitol consumption increased upon single exposure to a therapeutic diclofenac concentration. Previous studies show that diclofenac exerts uncoupling effects on mitochondrial respiratory chain (Petrescu and Tarba, 1997; Chan *et al.*, 2005). Furthermore, it inhibits gluconeogenesis and stimulates glycolysis and glycogenolysis (Petrescu and Tarba, 1997). The observed increased production of lactate is in concordance with these findings as well as the increased net release of glucose, which probably is due to the elevated breakdown of glycogen within the liver cells. After single dose diclofenac exposure, the branched-chained amino acids (valine, leucine and isoleucine) were consumed in lower amounts. BCAA can be converted to acetyl-CoA and fed into the TCA cycle for energy generation. The lower cellular capacity to use BCAAs as energy source may explain increased utilization of sugars to derive ATP *via* glycolysis. After repeated dose testing of diclofenac on PHH, lactate production was still increased, but by lower fold change (1.29) compared to single dose test. Again, sorbitol uptake was increased (fold change 0.68) but to a lesser extent. An increased galactose uptake was observed, indicating higher glycolytic activity after repeated dose exposure. However, these findings are just first indications for alterations in certain metabolic pathways which could be further explored by metabolic flux analysis.

For HepG2 cells, no significant changes in exometabolome were observed at all after single dose diclofenac exposure. On the contrary, repeated dose treatment of HepG2 cells with therapeutic diclofenac concentrations led to significant changes in exometabolome, as shown by principal component analysis. Similar to PHH, diclofenac induced increased lactate production and sugar uptake (glucose), again indicating higher glycolytic rate. The changes in sugar uptake in both PHH and HepG2 cells in our study are probably linked to the uncoupling effect of diclofenac on oxidative phosphorylation.

Diclofenac is mainly metabolized by CYP2C9 and CYP3A4 (Evans *et al.*, 2004; Yan *et al.*, 2005), which were both active in the primary hepatocytes. Similar to troglitazone, the PHH show an adaptation to repeated dose exposure probably due to induced detoxification *via* metabolism. Metabolic flexibility is needed for adaptation of cells to medium components

including drugs. However in case of HepG2 cells, the lack of sufficient metabolism leads to accumulation of the drug upon repeated dose exposure resulting in higher metabolic changes. AST activity and SRB assays as viability parameters showed that diclofenac had no effects on viability of both cell types during the experiments. The observed effects on the exometabolome are therefore not identifiable by commonly used toxicity assays. This also means even therapeutic doses of drugs such as diclofenac result in subtle changes in cellular metabolism which may ultimately be responsible for adverse effects upon chronic use or even idiosyncratic toxicity.

Taken together, this study presents a metabolomics approach for the detection of metabolic alterations in primary human hepatocytes and a hepatic cell line (HepG2) upon single and repeated dose drug exposure. In contrast to many other studies where high drug concentrations are used, we exposed the cells to physiologically relevant drug concentrations at which there is no decrease in the viability of cells. GC-TOFMS analysis and multivariate statistics were successfully applied to detect both overall metabolic changes and indications for specific alterations in certain pathways which could be further analyzed e.g. by using metabolic flux analysis (Niklas and Heinzle, 2011; Niklas *et al.*, 2011c). The observed *in vitro* effects such as increased glycolytic activity upon diclofenac exposure were comparable to *in vivo* studies reported in literature. The analysis of 25-30 metabolites in the culture supernatants was sufficient to detect these metabolic alterations and to gain insights into the altered metabolic pathways. The method could contribute to the prediction of drug induced adverse effects and can also be applied to other pharmacologically relevant cells e.g. cardiomyocytes or stem cells derived differentiated functional cells. It therefore represents an alternative to *in vivo* animal based systems for preliminary drug screening.

## **Acknowledgements**

This study was funded by the German BMBF project “3D-*in vitro* model for hepatic drug toxicity” (01GG0730, 01GG0732, 01GG0733). We thank Michel Fritz for his help in the setup and maintenance of the GC-TOFMS and Alexander Strigun for valuable support.

# CHAPTER 6: BIOTRANSFORMATION OF DICLOFENAC AND EFFECTS ON THE METABOLOME OF PRIMARY HUMAN HEPATOCYTES UPON REPEATED DOSE EXPOSURE

This chapter has been published as:

**Mueller D, Müller-Vieira U, Biemel KM, Tascher G, Nüssler AK and Noor F (2012):  
Biotransformation of diclofenac and effects on the metabolome of primary human  
hepatocytes upon repeated dose exposure**

*European Journal of Pharmaceutical Sciences, 45:716–724*

## **Abstract**

*In vitro* repeated dose testing for the assessment of chronic drug-induced effects is a huge challenge in preclinical pharmaceutical drug development. Long term toxicity results in discontinuation of therapy or post-marketing withdrawal of drugs despite *in vivo* preclinical screening. In case of hepatotoxicity, due to limited long term viability and functionality of primary hepatocytes, chronic hepatic effects are difficult to detect. In this study, we maintained primary human hepatocytes in a serum-free cultivation medium for more than three weeks and analyzed physiology, viability and drug metabolizing capacities of the hepatocytes. Moreover, we assessed acute (24h) diclofenac toxicity in a range of concentrations. The chronic (9 repeated doses) toxicity at one clinically relevant and another relatively higher concentration (6.4  $\mu$ M and 100  $\mu$ M) was also tested. We investigated phase I and II metabolism of diclofenac upon repeated dose exposure and analyzed changes in the cellular exometabolome. Acute 24h assessment revealed toxicity only for the highest tested concentration (1 mM). Upon repeated dose exposure toxicity was observed even at a low concentration (6.4  $\mu$ M). Biotransformation pathways were active for three weeks and diclofenac-acylglucuronide was detected as the predominant metabolite. Dose dependent diclofenac-induced effects on exometabolome, such as on the production of lactate and 3-hydroxybutyric acid as well as glucose and galactose metabolism, were observed upon 9 repeated doses. Summarizing, we show that repeated dose testing on long-term functional cultures of primary human hepatocytes should be included for chronic drug induced effects for preclinical toxicity assessment and can potentially help replace/reduce *in vivo* animal testing.

## **6.1 Introduction**

Alternative *in vitro* methods based on the principle of the three R's (reduction, refinement and replacement of animal tests) are highly needed for safety and risk assessment (Pauwels and Rogiers, 2010). Drug regulatory authorities are emphasizing for improved *in vitro* test methods (Collins *et al.*, 2008). However, *in vitro* chronic toxicity prediction is a huge challenge to the pharmaceutical industry in preclinical drug development. Even the consumer industry such as the cosmetics industry is facing this challenge with the upcoming total ban in 2013 on animal testing for cosmetics in Europe. The replacement of repeated dose *in vivo* testing to assess chronic long-term drug-induced effects by *in vitro* systems is urgently needed and is therefore a major focus of research.

Since one of the main reasons for drug attrition and post marketing withdrawal is hepatotoxicity, liver cell culture systems are extensively used for the assessment of adverse effects. Standard *in vitro* test systems with primary human hepatocytes (PHH) are extensively used to predict acute toxicity but it is difficult to assess long-term chronic drug effects (Guillouzo, 1998). For repeated dose chronic toxicity, primary hepatocytes should show long-term viability and maintain functionality, particularly drug-metabolizing activities.

Several diverse and often complex approaches for long term maintenance of liver cells already exist including 3D cultivation systems. Such 3D cell culture (e.g. bioreactors, spheroids and sandwich cultures) is considered to improve cellular functionality (Abu-Absi *et al.*, 2002; Bokhari *et al.*, 2007; Mizumoto *et al.*, 2008b; Miranda *et al.*, 2009). Gel-based systems were applied to liver cell cultivation, e.g. matrigel (Sellaro *et al.*, 2010), poly(lactic-co-glycolic) acid (PLGA) scaffolds (Zhu *et al.*, 2009) or peptide-nanofibers (Mehta *et al.*, 2010). Alginate microencapsulated hepatocytes show enhanced long-term viability as well as liver-specific functions compared to monolayers (Miranda *et al.*, 2010; Tostoes *et al.*, 2011b). Hollow-fiber bioreactors for 3D cultivation of primary liver cells allow *in vivo* tissue simulation and liver-specific functions could be maintained for three weeks in these bioreactors (Mueller *et al.*, 2011). However, these improved cell cultivation methods require higher technical expertise, high amount of cells and costs. Conventional 2D culture is still the handiest method, requires less cell material and is extensively used. In addition such simple cultivation allows multiplexing of assays including application of state-of-the-art "omics" technologies which seem promising for pharmaceutical drug testing and toxicity studies (Amacher *et al.*, 2005; Wishart, 2008). Besides membrane integrity, mitochondrial activity or ATP content, toxic effects are also reflected in modified cellular metabolic activities resulting in increased or

decreased metabolite levels (Kim *et al.*, 2010). Therefore, metabolomics investigations as well as metabolic flux analysis are sensitive tools to detect drug-induced effects in cellular systems (Niklas *et al.*, 2009; Strigun *et al.*, 2011a; Strigun *et al.*, 2011b; Strigun *et al.*, 2011d). These techniques of systems biology are expected to play a significant role in the study and eventually prediction of repeated dose toxicity.

We studied diclofenac which is a commonly used nonsteroidal antiinflammatory drug (NSAID) drug. Diclofenac causes rare but significant cases of serious hepatotoxicity including liver necrosis, jaundice, fulminant hepatitis with and without jaundice, and liver failure leading to liver transplant or death. Assessment of diclofenac toxicity and adverse effects is difficult because there is no simple dose relationship and hepatotoxic effects are not reproducible in current animal models, indicating idiosyncrasy of diclofenac (Boelsterli, 2003). In clinical practice the liver function should be monitored on long term therapy with diclofenac since increased AST/ALT levels are observed. Moreover, metabolism of diclofenac by CYP2C9 and CYP3A4 and UGT2B7 (Evans *et al.*, 2004; Yan *et al.*, 2005; Daly *et al.*, 2007) is most critical in diclofenac toxicity assessment due to the formation of reactive metabolites (Bort *et al.*, 1999). *In vivo*, delayed diclofenac induced hepatotoxicity usually occurs (Boelsterli, 2003). Previous studies showed that *in vitro*, only high concentrations of diclofenac (200 – 500  $\mu$ M) induced acute toxicity (Bort *et al.*, 1999; Lauer *et al.*, 2009) in primary cultures of human hepatocytes. Therefore, assessment of long-term toxicity of diclofenac using functional *in vitro* models would be of high interest to study diclofenac related chronic toxicity.

In this study, we tested diclofenac in a repeated dose study (9 doses, 3 weeks) on primary human hepatocytes cultivated in a serum free medium (Ullrich *et al.*, 2009). Basal cellular metabolism and liver specific functions (CYP450 activity, urea production) were analyzed to prove stable cellular physiology, functionality and viability during repeated dose experiment.

The acute and chronic toxicity as well as the effects on cellular exometabolome upon repeated dose exposure were analyzed. The elimination of diclofenac was also investigated in detail over time giving an in-depth overview on the drug metabolism during repeated dose testing. This integrated study of physiology, drug metabolism, toxicity and drug-induced effects on the extracellular metabolites shows that *in vitro* repeated dose testing using adequate cell system can improve preclinical toxicity assessment and can help minimize animal testing.

## **6.2 Materials and Methods**

### **6.2.1 Materials**

Williams medium E with Glutamax, HEPES, sodium pyruvate and minimum essential medium-non essential amino acids (MEM-NEAA) were purchased from Gibco (Paisley, Scotland, UK). Fortecortin was purchased from Merck (Darmstadt, Germany) and human insulin from Sanofi Aventis (Frankfurt am Main, Germany). Percoll and fetal calf serum (FCS) was purchased from PAA (Pasching, Austria). Bovine serum Albumin (BSA) was from Sigma-Aldrich (St. Louis, USA). Rat tail collagen was prepared according to a published protocol (Rajan *et al.*, 2006).

Human Hepatocyte Maintenance Medium (HHMM) was kindly provided by Primacyt Cell Culture Technology GmbH (Schwerin, Germany).

For Cytochrome P450 activity assays, midazolam was purchased from Cerrilant (Wesel, Germany). Bupropion, phenacetin, diclofenac sodium and all other chemicals and solvents of reagent grade were purchased from Sigma-Aldrich (Steinheim, Germany) unless otherwise specified.

### **6.2.2 Isolation of primary human hepatocytes**

The primary human hepatocytes (PHH) were isolated from resected liver tissues from patients with primary and secondary tumors at the Charité hospital, Berlin. Tissue collection was done according to institutional guidelines and with patient's written consent. The liver tissues used for cell isolation were carefully selected and regularly checked for satellite tumors. Only tumor free tissue was used on the basis of visual and physical checkup. Isolation was carried out as previously described (Nussler *et al.*, 2006) using a two-step collagenase perfusion followed by a Percoll density gradient centrifugation.

### **6.2.3 Cell culture**

After isolation, PHH were seeded on rat tail collagen coated 6 or 24 well plates (Falcon) in Williams medium E, supplemented with penicillin/streptomycin (100 U / 100 µg/ml), HEPES (15 mM), fetal calf serum (10%), insulin (1 mM), sodium pyruvate (1 mM) and fortectortin (0.8 µg/ml). The cells were incubated in a humidified incubator with 95 % air and 5 % CO<sub>2</sub> at 37°C. One day after seeding, the cells were shipped to our lab under standardized operating procedures. After arrival in our lab, cells were allowed to recover for 24 h before medium was

changed to Human Hepatocyte Maintenance Medium (HHMM; n=12). Medium was refreshed every 48 hours and supernatants were collected for analyses of extracellular metabolites.

One plate (24 well plate) was used for the quantification of general cellular parameter as well as liver-specific urea production; one 24-well plate was used for repeated dose exposure to diclofenac and one 6-well plate was used for CYP450 activity assay.

#### **6.2.4 Quantification of substrates and products in culture supernatants**

To assess cellular viability and metabolism, D-glucose, D-galactose and L-lactate concentrations were determined in supernatant samples of primary human hepatocytes using routinely used enzymatic kits (R-Biopharm, Darmstadt, Germany). The assays were performed according to manufacturer's instructions.

Urea concentration in culture supernatants was quantified using a recently described HPLC method (Clark *et al.*, 2007). Briefly, urea was automatically derivatized using xanthydrol and the soluble product N-9H-xanthen-9-ylurea was analyzed after chromatographic separation from interferences using an Eclipse XBD RP-18 column (150 x 4.6 mm I.D., 5  $\mu$ m, Agilent Technologies). 20 mM Sodium acetate (pH 7.2) was used as eluent A and acetonitrile as eluent B in a gradient elution. The flow rate was adjusted to 1 ml / min. Peaks were detected using a fluorescence detector (ex/em 213/308 nm).

#### **6.2.5 Cytochrome P450 activity assay**

The functional enzyme activity of CYP1A2, CYP2B6, CYP2C9 and CYP3A4 was performed in a cassette approach based on probe reactions. The probe substrates, their test concentrations and the products used for quantification of the enzyme reaction are recently reported (Mueller *et al.*, 2011). Assay duration was 2 hours. The assay was performed in 6 well plates ( $10^6$  cells / well). The quantification of the probe metabolites by LC-MS was performed as recently described (Mueller *et al.*, 2011).

#### **6.2.6 Sulforhodamin B viability assay**

Sulforhodamin B (SRB) viability assay was carried out as previously described (Beckers *et al.*, 2010). This colorimetric endpoint assay allows quantification of the protein content which is directly correlated to the cell number.

### **6.2.7 LDH assay**

The activity of lactate dehydrogenase (LDH) in the culture supernatant was determined using a colorimetric enzymatic assay kit (Cytotoxicity Detection Kit; Roche, Grenzach, Germany). A dilution series of standard serum (NobiCal-MULTI, Hitado, Möhnesee-Delecke, Germany) was measured in parallel for quantification.

### **6.2.8 Acute toxicity**

The PHH were tested for acute toxicity. Two days after isolation, the cells seeded in 24 well plates were exposed to 4 diclofenac concentrations (10-1000  $\mu\text{M}$ ) in triplicates for 24 h. Diclofenac stock solution (100 mM) was prepared in DMSO. Vehicle control (medium supplemented with 1% DMSO) was included and corresponds to the highest DMSO concentration i.e. used for 1 mM diclofenac. Cells were maintained in serum-free HHMM. Viability was assessed using Sulforhodamin B assay.

### **6.2.9 Repeated doses toxicity**

For the assessment of long-term, repeated dose toxicity of diclofenac, the hepatocytes were exposed to two concentrations of diclofenac in triplicates. One of these concentrations represents the therapeutic serum concentration ( $C_{max}$ ) in patients (6.4  $\mu\text{M}$ ) (Hinz *et al.*, 2005) and the other one a significantly higher concentration (100  $\mu\text{M}$ ). Diclofenac stock solution (100 mM) was prepared in DMSO. Vehicle control (0.1% DMSO) was included. Serum free HHMM was used as cultivation medium during drug treatment. Repeated doses were given every 48 h upon medium change. Supernatant samples were collected and used for LC-MS and GC-TOFMS analysis. Moreover, viability was assessed by LDH activity measurements in supernatants (upon 1, 4 and 9 doses) and by Sulforhodamine B endpoint assay upon 9 doses representing day 23 after isolation of the hepatocytes.

### **6.2.10 Statistical analysis**

The control was compared with tests in SRB (figure 3) and LDH (figure 4) assays using students *t*- test (Matlab R2006a). Significance is reported at  $p < 0.05$ . Normalized peak areas for sugars and lactate (figure 7) from control and tests was similarly compared.

### **6.2.11 Quantification of phase I and II metabolites of diclofenac by LC-MS**

Proteins in the supernatants were precipitated by the addition of acetonitrile. After centrifugation, the supernatants (containing 10% acetonitrile) were subjected to LC/MS analysis. An HPLC system consisting of an Accela U-HPLC pump and an Accela auto sampler (Thermo Fisher Scientific, USA) was used. The LC was performed in the gradient mode using acetonitrile/0.1% formic acid as organic phase (eluent A), and 10 mM ammonium formate/0.1% formic acid (eluent B); the pump flow rate was set to 300  $\mu$ l/min (% A (t (min), 5(0-0.1)-97(3.0-4.6)-5(4.8-6.5)). A Gemini C6-Phenyl, 3  $\mu$ m, 50x2.0 mm (Phenomenex, Germany) analytical column with a pre-column (Gemini C6-Phenyl, 3  $\mu$ m, 4x2.0 mm) was used. Mass spectrometry was performed on an Exactive mass spectrometer (Orbitrap technology with accurate mass) equipped with a heated electrospray interface (Thermo Fisher Scientific, USA) connected to a PC running the standard software Xcalibur 2.1.

As MS tune file, a generic tune file was used, applying the positive ion mode. As lock mass for internal mass calibration the  $[M+H]^+$  ion of the Diisooctyl phthalate ( $m/z$  391.28429), which is ubiquitously present in the solvent system, was used. The analytes were acquired by scanning  $\pm 1$  Thomson around the expected mass of the monoisotopic  $[M+H]^+$  peak. High-resolution mass measurement was performed in Orbitrap mode with a resolution of 50,000. The accurate mass of each metabolite was used for peak integration. Further instruments settings were as follows: HCD 20 eV, AGC high dynamic range, max. trap injection time 100 ms, sheath gas 30, aux gas 8, sweep gas 2, spray voltage 4 kV, capillary temperature 250°C, ESI 2 heater temperature 250°C. The data acquisition was performed on a Thermo Fisher Scientific mass spectrometer, consisting of a standalone Orbitrap mass analyser (Exactive).

For the analysis of metabolites, the accurate masses of diclofenac and the metabolites are presented in table 6-1.

**Table 6-1: Analysis of diclofenac metabolites by LC-MS/MS: theoretical and experimentally determined accurate masses of diclofenac and indicated metabolites.**

<b>Metabolite</b>	<b>M-H<sup>-</sup>, theoretical exact mass / experimentally determined exact mass</b>
<b>M0</b> (Diclofenac)	294.0084 / 294.0099
<b>M1</b> (Diclofenac +O)	310.0033 / 310.0052
<b>M2</b> (Diclofenac +O <sub>2</sub> )	328.0138 / 325.9998
<b>M3</b> (Diclofenac +C <sub>2</sub> H <sub>3</sub> NO)	351.0298 / 351.0318
<b>M4</b> (Diclofenac +C <sub>3</sub> H <sub>5</sub> NOS)	397.0175 / 397.0186
<b>M5</b> (Diclofenac +C <sub>3</sub> H <sub>5</sub> NO <sub>2</sub> S)	413.0125 / 413.0148
<b>M6</b> (Diclofenac +SO <sub>4</sub> )	389.9601 / 389.9623
<b>M7</b> (Diclofenac +C <sub>6</sub> H <sub>8</sub> O <sub>6</sub> )	470.0405 / 470.0426
<b>M8</b> (Diclofenac +C <sub>6</sub> H <sub>8</sub> O <sub>7</sub> )	486.0354 / 486.0374

### **6.2.12 Metabolic profiling using GC-TOFMS**

#### *Sample preparation*

To assess effects of diclofenac on the exometabolome (extracellular metabolites) of PHH after repeated dose exposure (day 23), each supernatant sample was analyzed in triplicate, resulting in three biological and three technical replicates. 200 µl methanol was added to 50 µl supernatant for protein precipitation. The mixture was vortexed for 3 minutes and placed on ice for 1 h. Afterwards, samples were centrifuged (10 min, 13.000 g, 4°C). Supernatant was transferred into glass vials and mixed with 200 µl α-aminobutyric acid (1 mM) used as internal standard. These samples were freeze dried prior to derivatization. A two-step derivatization was carried out. Firstly, 50 µl of methoxyamin in pyridine (20 g/l) was added and the mixture stirred for 30 min at 80 °C for methoximation. This was followed by derivatization with 50 µl of the reagent MSTFA (N-Methyl-N-(trimethylsilyl)trifluoroacetamide) for 30 min at 80 °C. This two-step derivatization procedure was automatized using a MPS 2XL auto sampler equipped with an agitator (both from Gerstel, Karlsruhe, Germany).

### ***GC-TOFMS measurements***

An Agilent 7890 gas chromatograph (Hewlett-Packard, Atlanta, USA) coupled to a Pegasus HT ToF mass spectrometer (Leco, Mönchengladbach, Germany) was used. An HP5-ms capillary column of 60 m length, 0.25 mm inner diameter and 0.25  $\mu\text{m}$  film thickness was used for separation. Splitless injection was performed. Injection volume was 1  $\mu\text{l}$ . The initial GC-oven temperature was set at 70°C with a ramp of 5°C/min and a final temperature of 320°C. Helium was used as carrier gas and a constant flow rate of 1 ml/min was adjusted. The transfer line temperature was set at 250°C. Mass spectra were acquired within a range of 70 to 700  $m/z$  and scan rate was 20 spectra per second. Ion source voltage was set at 70 eV and temperature at 200°C.

### ***Data analysis and multivariate statistics***

For data processing, the obtained raw GC-TOFMS data were first analyzed by ChromaTof 4.22 software (Leco). Chromatogram acquisition, automated peak deconvolution, identification of suitable fragment mass to charge ratio for peak area determination and reference library search were automatically carried out. Similarity threshold, which determines the minimum similarity of the obtained spectrum with the reference library spectrum, was set at 600. Known artifact peaks such as solvent contamination, column bleeding, plasticizers or reagent peaks were manually excluded. Peak areas of trimethylsilyl (TMS)-derivates were normalized to the respective peak area of the internal standard  $\alpha$ -aminobutyric acid-TMS ( $m/z$  130). Averages of the respective three technical replicates were calculated. 17 metabolites were analyzed (galactose, glucose, lactate, urea, 3-hydroxybutyric acid and 12 amino acids). Peak areas of metabolites which form two or more isomers upon methoximation e.g. glucose were summed as well as of compounds with several TMS-derivates e.g. aspartate. Normalized peak areas were pareto-scaled. Principal component analysis (PCA), a multivariate data analysis method, was applied to reduce dimensions of the dataset. The variance in dataset can be described using a set of underlying orthogonal variables (the principal components). PCA was performed using Matlab R2006a (The MathWorks) software.

## 6.3 Results

### 6.3.1 Physiological characterization

For the investigation of cellular physiology and metabolism, glucose and galactose consumption as well as lactate and urea production were measured (figure 6-1).

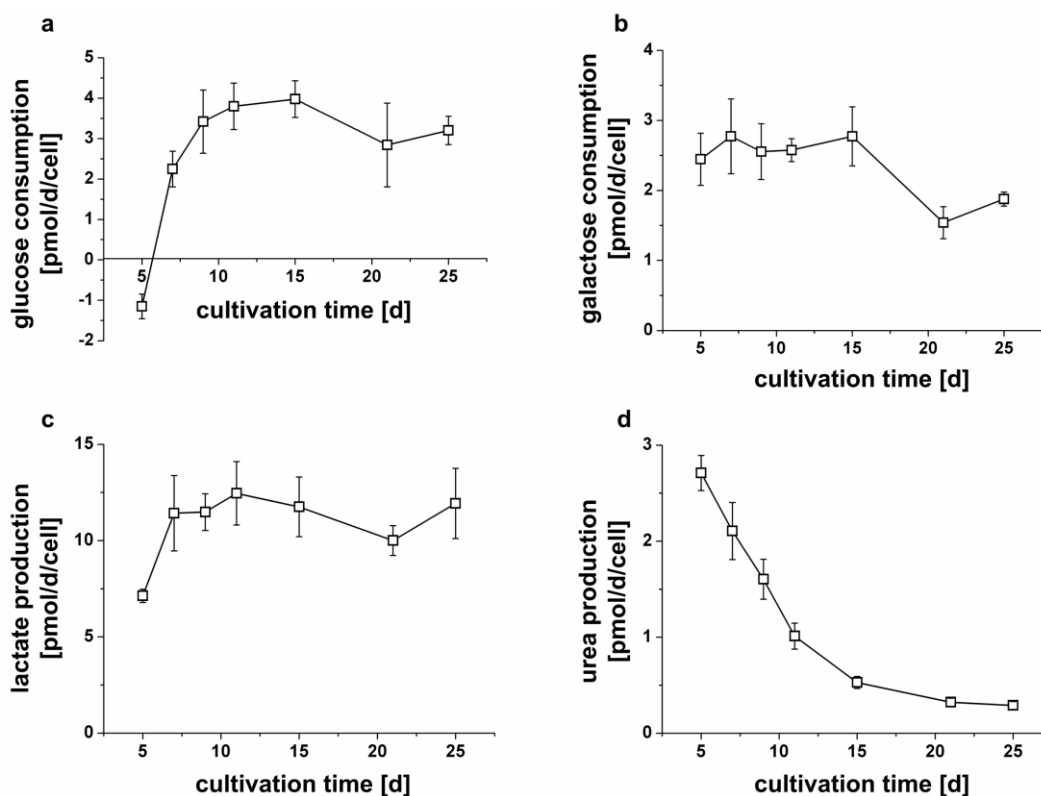


**Figure 6-1: Metabolic activity of primary human hepatocytes for 25 days a) glucose consumption b) galactose consumption c) lactate production d) urea production. Rates are given as pmol/d/cell. Error bars indicate  $\pm$ SD ( $n=3$ , total 12 wells and 4 wells were pooled).**

The primary hepatocytes released glucose at the first measurement day (day 5 after isolation). Secretion rate was 1.2 pmol/d/cell. Thereafter glucose was constantly consumed over a time period of more than three weeks (figure 6-1a). Galactose consumption rate (figure 6-1 b) was 2.4-2.8 pmol/d/cell between day 5 and day 15 after isolation and decreased to 1.9 pmol/d/cell at day 25.

The primary hepatocytes produced lactate (7.1 pmol/d/cell) at day 5 after isolation (figure 6-1c), which then increased and stayed constant around 10-12.5 pmol/d/cell over the whole cultivation period.

Urea production (figure 6-1d) was 2.7 pmol/d/cell at day 5 and decreased between day 5 and day 15. However, the cells still produced urea at a rate of 0.3 pmol/d/cell at day 25.

### 6.3.2 CYP450 activity

The basal activities (without induction) of four different CYP450 isoforms were assessed at days 7, 15 and 23 and are shown in figure 6-2.

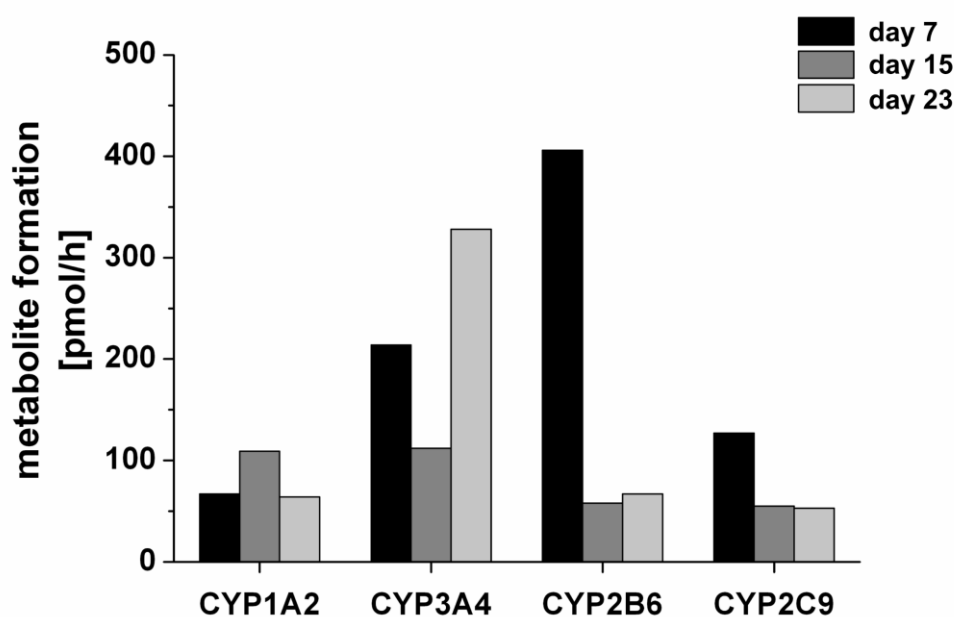


**Figure 6-2: Activity of CYP450 enzymes at days 7, 15 and 23, expressed as pmol metabolite formation per hour.**

The activity of CYP1A2 was 62 pmol/h at day 7 and stayed constant until day 23. CYP3A4 activity was 214 pmol/h at day 7 and increased to 328 pmol/h at day 23. CYP2B6 activity significantly decreased over time from 406 pmol/h to 67 pmol/h. CYP2C9 enzyme activity was highest at day 7 (127 pmol/h) and constant between day 15 and 23 (53-55 pmol/h).

### 6.3.3 Acute and chronic repeated dose toxicity

Acute toxicity (24 h) of diclofenac on the PHH is presented in figure 6-3 a. In this experiment, we observed a significant toxic effect only for the highest tested concentration (1 mM), whereby the cell viability significantly decreased to 77%. During repeated dose experiments, PHH were exposed to 9 diclofenac doses in two concentrations (6.4 and 100  $\mu$ M). A dose-dependent toxic

effect was clearly observed (figure 6-3 b). At day 23, the cell viability decreased after repeated exposure to the therapeutic concentration (6.4  $\mu\text{M}$ ) to 78% of untreated vehicle control. The exposure to 100  $\mu\text{M}$  diclofenac led to significantly higher decrease in viability (58% of control).

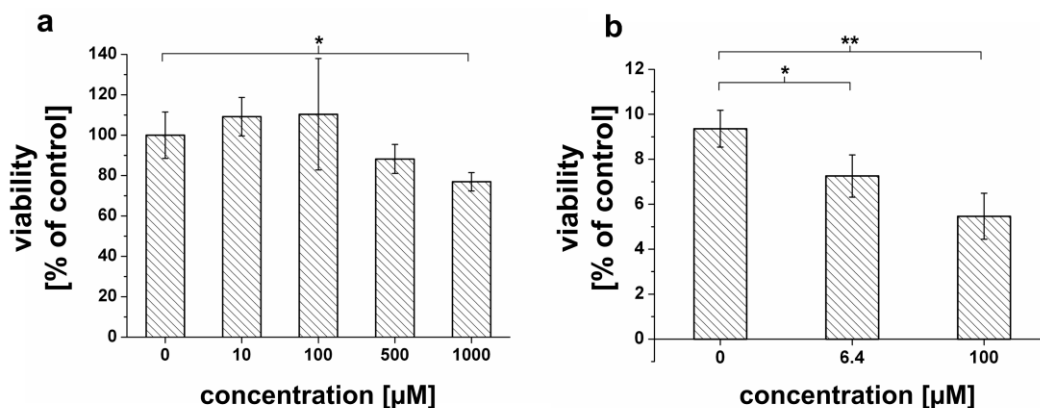


Figure 6-3: a) Acute toxicity of diclofenac (24 h exposure) screened on PHH. Cell viability was assessed using SRB assay and is given as % of untreated control (1% DMSO). Error bars indicate  $\pm\text{SD}$  ( $n=3$ ) b) Chronic toxicity of diclofenac (9 repeated doses): Viability of control (0.1 % DMSO) and repeated dose diclofenac treated cells (6.4 and 100  $\mu\text{M}$ ) in HHMM at day 23. Viability assessed by SRB assay is given as % of untreated controls. Error bars indicate  $\pm\text{SD}$  ( $n=3$ ). \*  $p < 0.05$ , \*\*  $p < 0.01$ , \*\*\*  $p < 0.001$ .

LDH release was measured upon single, 4 or 9 repeated doses (figure 6-4).

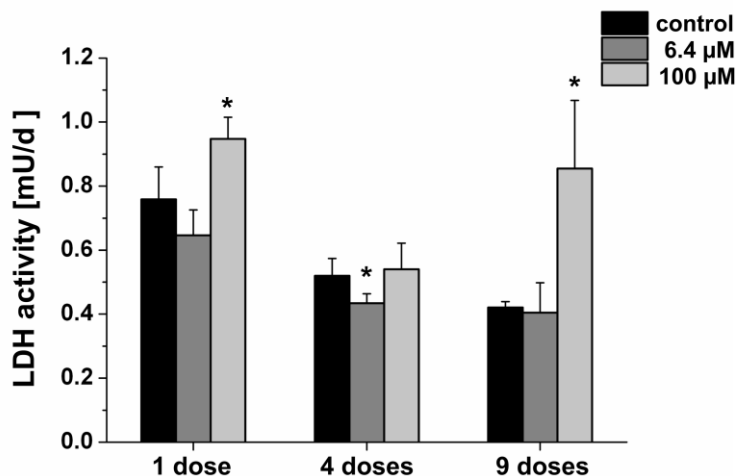


Figure 6-4: LDH activities in supernatants of primary human hepatocytes exposed to the indicated diclofenac concentrations upon 1, 4 or 9 repeated doses. Error bars represent standard deviations ( $n=3$ ).

Upon single dose exposure, the highest activity was found for 100  $\mu\text{M}$  diclofenac. No differences were found between control and 4 repeated 100  $\mu\text{M}$  doses, whereas LDH release was lower in 6.4  $\mu\text{M}$  exposed cells. 9 repeated diclofenac doses also resulted in higher LDH activity in culture supernatants for 100  $\mu\text{M}$  treated cells compared to the untreated control.

#### 6.3.4 Formation of phase I / phase II metabolites during repeated dose testing

Phase I and II metabolism was investigated during repeated diclofenac exposure. The remaining parent compound and 8 diclofenac metabolites were measured. The relative percentages of metabolites after a single dose, four and 9 repeated diclofenac doses are shown in table 6-2.

**Table 6-2: Relative concentration of diclofenac and its metabolites (phase I and II) after 1, 4 and 9 diclofenac dose(s) (6.4  $\mu$ M or 100  $\mu$ M). Concentrations are given as percentages of total peak areas of all compounds.**

			6.4 $\mu$ M			100 $\mu$ M		
			1x	4x	9x	1x	4x	9x
<b>M0</b>	<b>Diclofenac</b>		44.8	69.1	72.4	25.7	66.8	63.6
<b>M1</b>	<b>Diclofenac</b>	<b>+O</b>	25.3	1.3	1.9	46.7	10.2	15.4
<b>M2</b>	<b>Diclofenac</b>	<b>+O<sub>2</sub></b>	n.d.	n.d.	n.d.	<1	n.d.	<1
<b>M3</b>	<b>Diclofenac</b>	<b>+C<sub>2</sub>H<sub>3</sub>NO</b>	n.d.	n.d.	n.d.	n.d.	<1	<1
<b>M4</b>	<b>Diclofenac</b>	<b>+C<sub>3</sub>H<sub>5</sub>NOS</b>	n.d.	n.d.	n.d.	n.d.	n.d.	n.d.
<b>M5</b>	<b>Diclofenac</b>	<b>+C<sub>3</sub>H<sub>5</sub>NO<sub>2</sub>S</b>	n.d.	n.d.	n.d.	<1	<1	<1
<b>M6</b>	<b>Diclofenac</b>	<b>+SO<sub>4</sub></b>	2.6	<1	<1	4.2	<1	2.4
<b>M7</b>	<b>Diclofenac</b>	<b>+C<sub>6</sub>H<sub>8</sub>O<sub>6</sub></b>	24.6	29.4	25.3	12.1	20.7	16.2
<b>M8</b>	<b>Diclofenac</b>	<b>+C<sub>6</sub>H<sub>8</sub>O<sub>7</sub></b>	2.8	<1	<1	11.0	1.9	1.9

*n.d.: not detected*

After single diclofenac dose, the hepatocytes metabolized diclofenac, whereas monohydroxylated diclofenac (M1) was the main phase I metabolite. For phase II, diclofenac-acylglucuronide (M7) and diclofenac glucuronide (M8) were the predominant metabolites.

After 4 repeated doses of diclofenac, the predominant metabolite was again diclofenac-acylglucuronide (29% and 21% for 6.4  $\mu$ M and 100  $\mu$ M respectively).

The liver cells were still able to metabolize diclofenac even after 9 repeated doses. Both phase I and II metabolites were identified. Diclofenac-acylglucuronide was again detected at highest amounts (25% and 16% for 6.4  $\mu$ M and 100  $\mu$ M respectively). Moreover, monohydroxylated diclofenac derivatives (M1) as well as diclofenac glucuronide (M8) and sulfate (M6) conjugates were also detected after repeated exposure.

### 6.3.5 Diclofenac effects on exometabolome upon repeated dose testing

The effects of repeated, long-term diclofenac exposure on the extracellular metabolome were analyzed by principal component analysis (PCA). Score plot is depicted in figure 6-5.

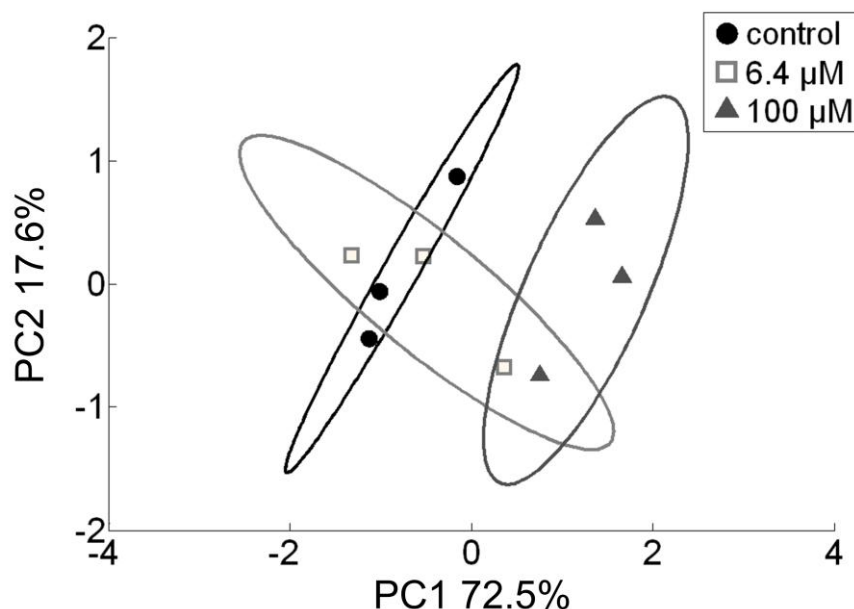


**Figure 6-5:** PCA score plots of principal component 1 and 2 for diclofenac-treated (6.4 μM, open squares, 100 μM grey triangles) and control (0.1% DMSO, black circles). Metabolic profiling was performed on supernatant samples from primary human hepatocytes ( $n=3$ ). The respective 3 classes are shown within 95% confidence ellipses.

A separation between untreated control and drug treated cells was observed. The therapeutic concentration was less separated from the control compared to the higher concentration, indicating a dose dependent effect on cellular metabolome. Untreated control samples and the samples exposed to the high diclofenac concentrations were completely separated as shown by 95% confidence ellipses. The first two principal components described 90% of the total variance. As shown by loading coefficients (figure 6-6), the dose-dependent separation between control and the two drug concentrations along PC1 was mainly caused by changes in the production of lactate and 3-hydroxybutyric acid as well as due to differences in glucose and galactose uptake.

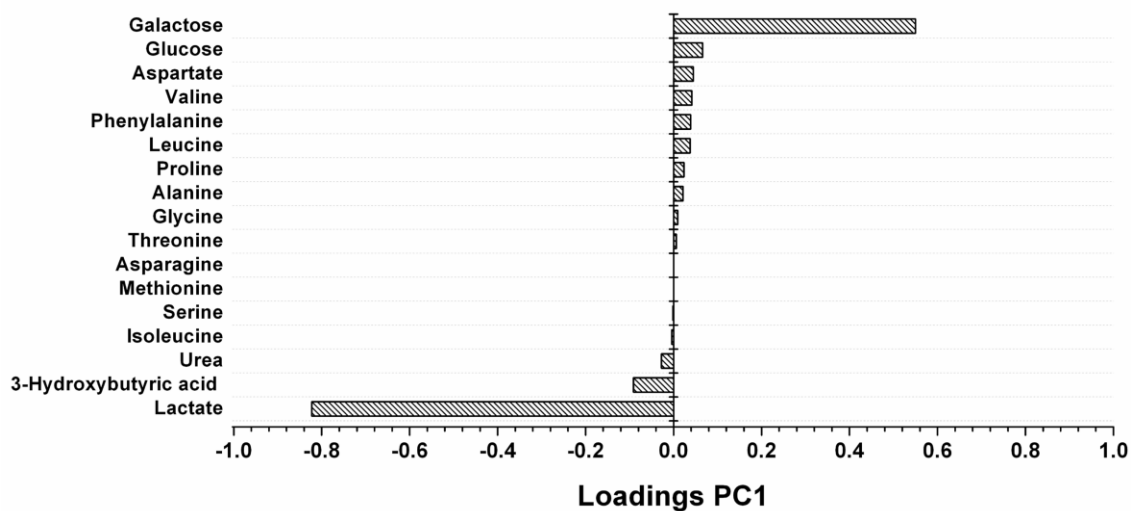


**Figure 6-6:** Loading coefficients of 17 metabolites for the first principal component, obtained from PCA shown in Fig. 6-5.

To assess diclofenac-induced effects independent of decrease in viability, the peak areas of lactate, glucose and galactose were normalized to the peak areas of the control, which was set as 100% (figure 6-7).

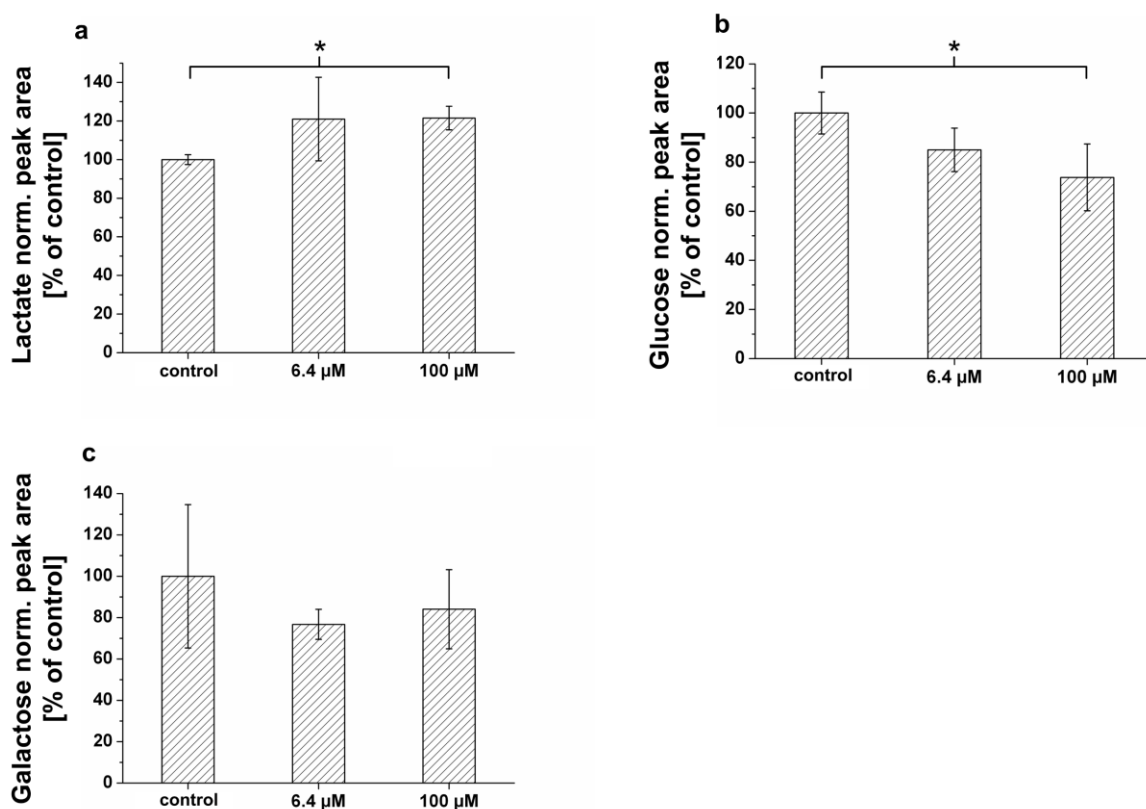


Figure 6-7: Peak areas of a) lactate, b) glucose and c) galactose, normalized to the respective peak areas of the control which was set as 100% after repeated dose diclofenac exposure at day 23. Error bars indicate  $\pm$ SD ( $n=3$ ), \*  $p < 0.05$ .

As indicated, the production of lactate was increased upon diclofenac treatment (figure 6-7a) as well as glucose consumption (figure 6-7b). No significant differences were found for galactose consumption although lower galactose amounts were detected upon diclofenac exposure also indicating an increased consumption rate.

## **6.4 Discussion**

Chronic effects upon repeated dose exposures which correspond to pharmacologically relevant concentrations are difficult to detect using standardized *in vitro* test systems and common endpoint assays. In this study, we performed repeated dose testing of diclofenac on primary human hepatocytes. Thereby, the cells were maintained in serum-free medium for three weeks. To prove stable physiology and viability, general and liver specific parameter of untreated cells maintained in long-term hepatocyte medium were analyzed.

The primary hepatocytes released glucose up to day 5 after isolation. Liver cells are the main site of gluconeogenesis, which results in glucose synthesis from lactate, glycerol or amino acids. Moreover, glycogenolysis, the catabolic pathway from glycogen to glucose monomers, also contributes to the net glucose synthesis by the hepatocytes. Beginning from day 7, the liver cells consumed glucose up to day 23 at high rates, probably because of exhausted intracellular glycogen pools during the first 5 days. Galactose, which is converted to glucose-6-phosphate via the Leloir-pathway and then used in glycolysis, was also constantly consumed by the cells at high rates up to day 23 (71% of day 5). Galactose contributes to replenishing of glycogen stores and also for the synthesis of membrane glycoproteins and extracellular matrix. In addition, under stress conditions, galactose may be incorporated into glycogen to slow down its degradation (Nordin and Hansen, 1963). Lactate, produced from pyruvate by lactate dehydrogenase as end product of glycolysis, was released by the PHH maintained at a stable rate during the whole cultivation. Release of urea, as liver-specific metabolite which is produced during amino acid catabolism, was also investigated in both cultivation media. A decrease of production rates was observed for both cultures. Nevertheless, the hepatocytes constantly produced urea. Though the average production rate of  $0.33 \pm 0.15$  pmol/d/seeded cell between day 15 and day 30 is lower than the *in vivo* urea production rate of 2.6 pmol/d/cell (Bhatia *et al.*, 1999), the urea production up to day 25 reflects long-term cell viability as well as liver-specific functionality. Taken together, the specific rates of glucose, galactose and lactate were quite stable during more than three weeks, showing stable cellular metabolism of the cells and maintained viability which is a prerequisite for long-term toxicity studies.

As further liver-specific parameter, the activities of four CYP450 isoforms were investigated. CYP1A2 was shown to be active over the whole cultivation time. CYP2B6 activity rapidly decreased and a remaining metabolite formation of 17% was found at day 23 compared to day 7. Basal activities for CYP3A4 and CYP2C9, the two CYP isoforms mainly responsible for diclofenac phase I metabolism, were detected during cultivation. CYP3A4 activity even slightly

increased and remaining activity for CYP2C9 was 42%. This shows that drug-metabolizing activities could partly be maintained during cultivation and that the cells were capable for diclofenac phase I metabolism during the whole repeated dose experiment.

Acute toxicity assessment (24 h) of diclofenac was carried out on PHH from the same donor, showing that only the highest tested concentration of 1 mM was significantly toxic to the cells (survival rate 77%). Repeated dose testing was also carried out with diclofenac on PHH of the same donor. Concentration dependent cytotoxic effects were observed upon exposure to 9 repeated diclofenac doses even at the therapeutic concentration (survival rate 78%). This chronic toxic effect of diclofenac was assessed on day 23 after cell isolation. LDH activity as further viability parameter was not increased at the investigated time points for the physiological relevant concentration of 6.4  $\mu$ M, but even slightly decreased upon 4 doses. In case of 100  $\mu$ M diclofenac exposure, increased LDH activity was found upon single exposure as well as upon 9 repeated doses. This shows that commonly used viability assays based on different parameter (here: cellular protein content and membrane integrity) could give different results and that methods and results from *in vitro* assessment of cell viability have to be carefully evaluated. Obviously, the determination of such chronic effects is only possible if the PHH can be kept viable for several weeks. The long-term maintenance medium used in this study is enriched with growth factors and contains albumin, which affects free drug concentration. However, to compare our results of acute and chronic toxicity as well as cell functionality, all experiments were done with cells from the same donor maintained in the same medium batch. Regarding diclofenac metabolism, either the parent compound or the hydroxylated metabolites are conjugated by UGT2B7 and excreted (Tang, 2003; Daly *et al.*, 2007). The metabolites include 4'-hydroxy-, 5-hydroxy-, 3'-hydroxy-, 4',5-dihydroxy- and 3'-hydroxy-4'-methoxy-diclofenac. Both diclofenac and its oxidative metabolites undergo glucuronidation or sulfation followed by biliary excretion. Acylglucuronidation mediated by UGT2B7 and oxidation mediated by CYP2C9 may also play a role in diclofenac metabolism. CYP3A4 is responsible for the formation of minor metabolites, 5-hydroxy- and 3'-hydroxy-diclofenac. Moreover, a reactive benzochinone imine could be generated by CYP450 enzyme system, which is then detoxified *via* GSH conjugation and subsequent elimination (Lauer *et al.*, 2009). In our study, we show that phase I and II enzymes were active during the whole repeated dose experiment. The predominant phase II metabolite found in this study was diclofenac-acylglucuronide which was reported to play an important role in diclofenac-mediated toxicity due to covalent protein binding (Kretz-Rommel and Boelsterli, 1993). This metabolite probably contributes to the toxicity upon repeated dose exposure observed in our study. About 20% of the

total administered doses of diclofenac were excreted as diclofenac-acylglucuronide which is in the range of *in vivo* values (Riess *et al.*, 1978; Stierlin and Faigle, 1979). Diclofenac glucuronide and sulfate conjugates were also detected upon single and repeated dose exposure, both at lower but particularly for 100  $\mu$ M diclofenac at constant relative concentrations. Hydroxydiclofenac was found at highest amounts upon single dose exposure as the predominant phase I metabolite. Upon repeated drug exposure, the relative concentration of this metabolite decreased, indicating reduced CYP2C9 activity over time but also induced conjugation of this metabolite since CYP2C9 was proved to be active during the whole experiment.

In addition, diclofenac induced effects on cellular exometabolome of the PHH were also investigated after 9 repeated treatments (6.4  $\mu$ M, 100  $\mu$ M) and compared to the untreated control. Clear differences in profiles of 17 analyzed metabolites could be detected for the cells in a dose-dependent manner. The control was clearly separated from the 100  $\mu$ M diclofenac exposed samples whereas the therapeutic concentration clustered in between. Lactate mainly contributed to the separation between control and drug exposed samples. Enhanced lactate production has recently been shown as a biomarker for cellular stress and toxicity (Limonciel *et al.*, 2011). In our study, lactate showed a trend towards increased production which was significant in case of 100 $\mu$ M diclofenac when the decrease in viability is taken into account. This increased lactate production upon diclofenac exposure indicates higher glycolytic activity which was previously found in rat liver as well as inhibition of gluconeogenesis (Petrescu and Tarba, 1997). Accordingly, higher uptakes of glucose and galactose were found upon 9 repeated diclofenac doses. These alterations in metabolic pathways indicate diclofenac-induced uncoupling effect of oxidative phosphorylation and mitochondrial dysfunction resulting in an increased glycolysis which then serves as the main cellular energy source. Moreover, the ketone body 3-hydroxybutyric acid was also contributing to the separation along PC1 between control and drug-exposed samples, indicating effects of diclofenac on fatty acid metabolism as already reported (Baldwin *et al.*, 1998). Therefore, we conclude that the analysis of the exometabolome gives an insight into changes in cellular metabolism upon exposure to test drug and can help to assess adverse drug reactions.

Taken together, *in vitro* repeated dose testing using metabolically active cells combined with analysis of physiology, drug metabolism, toxicity and drug-induced effects on the extracellular metabolome shows correlations to *in vivo* studies and can improve preclinical toxicity assessment using human relevant systems and are an important step towards alternative *in vitro* methods for the replacement of animal testing.

## **Acknowledgements**

This work was funded by the German BMBF project “3D *in vitro* model for hepatic drug toxicity” (01GG0730, 01GG0732, 01GG0733). We thank Primacyt Cell Culture Technology GmbH for kindly providing the Human Hepatocyte Maintenance Medium (HHMM) used in this study. We would also like to thank Angela Sudhoff and Esther Hoffmann for excellent technical assistance as well as Alexander Strigun for valuable help.

# CHAPTER 7: SUMMARY, CONCLUSION AND OUTLOOK

## **7.1 Summary**

The work in this thesis focused on long-term cultivation human liver cells while maintaining functionality and viability (Chapter 2, 3, 4 and 6) as well as on the sensitive assessment of drug-induced effects on the liver cell metabolome using a newly developed, GCTOF-MS based method (Chapter 5 and 6).

In **Chapter 2**, primary human hepatocytes of three different donors were cultivated in 3D bioreactors and investigated in terms of liver specific functions (urea and albumin production). It could be shown that the cells could be maintained functional for two weeks in the 3D bioreactor. Moreover, the 3D bioreactor system was modified for the measurement of oxygen uptake rates. It was proved that the 3D bioreactor system can be used for long-term cultivation of liver cells allowing physiological, pharmacological and toxicological applications.

In **Chapter 3**, a viability assay was established in the 3D bioreactor system to improve pharmacological long-term studies. It was shown that this assay can be performed within 6 hours similar to 2D cultures. Moreover, the developed assay is non-invasive and can be routinely applied during 3D cultivation. Upon assay establishment by using HepG2 cells, primary human hepatocytes cultivated in the 3D bioreactor were exposed to a physiologically relevant amiodarone concentration for several days. Cell viability was assessed before and upon drug exposure. It was observed that the exposure to clinically relevant concentrations of amiodarone over 4 days did not affect cell viability in this experiment. This also proves the non-invasiveness of the assay. The method can routinely be applied to long-term pharmacological studies in the future for the investigation of drug-induced effects on cells maintained in 3D culture. However, free drug concentrations should be measured in the future since drug binding to the hollow-fibers could occur and influence the experimental setup.

In **Chapter 4**, the human liver cell line HepG2 was used for the production and investigation of three dimensional organotypic cultures. By using the hanging drop method, micro-organotypic cultures of adjustable sizes could be produced which were further analyzed including viability, cellular metabolism and long-term cultivation. Liver specific albumin production of the organotypic cultures was higher than in monolayer- or collagen-sandwich cultures. Due to the high reproducibility and the low amount of required cells, the system could be applied to pharmacological studies. Induction capacity of CYP1A was also increased compared to monolayer- and collagen-sandwich cultures. The toxicity of the reference compound tamoxifen, an anti-cancer drug, was lower in the organotypic cultures. Concurrently, the activity of the membrane transporter MRP-2 was increased in the organotypic cultures, indicating increased

drug efflux across the cell membrane. We therefore concluded that the engineered HepG2 organotypic cultures could be used for the investigation of CYP450 induction, anti-cancer drug effects and moreover for the study of chemotherapy resistance mechanisms.

A metabolomics-based approach to detect drug-induced effects on primary human hepatocytes and HepG2 cell was developed and applied in **Chapter 5**. The reference drugs diclofenac and troglitazone were tested in single and repeated dose exposure experiments. Using physiological subtoxic concentrations, it was shown that exometabolome changes could significantly be detected for primary human hepatocytes, whereas the effect was decreased upon repeated exposure. In contrast, HepG2 cells showed higher metabolic alterations upon repeated drug exposure due to the different drug metabolizing capacities of the two cell types. Taken together, this method is well-suited for the sensitive assessment of drug induced metabolic changes at physiologically relevant concentrations and can also be applied to any other alternative testing system.

The assessment of long-term, chronic drug toxicity is still a major hurdle in preclinical drug development using *in vitro* test systems since primary hepatocytes have limited viability and functionality of about one week at conventional culture conditions. However, chronic toxicity mostly occurs upon long-term repeated dose applications of a drug at low concentrations. In **Chapter 6**, primary human hepatocytes were maintained in a long-term serum free cultivation medium and physiology, viability and drug metabolizing capacities of the cells were analyzed. Moreover, we assessed acute (24 h) and chronic (3 weeks) toxicity of diclofenac. Acute toxicity (24 h) assessment revealed toxicity only for the highest tested diclofenac concentration (1 mM). In sharp contrast, we observed toxic effects even at a low concentration (6.4  $\mu$ M) upon repeated dose exposure. *In vitro* biotransformation of diclofenac was comparable to *in vivo* data. Metabolomics showed dose dependent drug-induced effects on exometabolome, indicating increased glycolytic activity as again already reported *in vivo*. Therefore, we conclude that *in vitro* testing of repeated dose effects is of high importance in drug safety evaluation and the combination of metabolically functional systems and sensitive detection methods will improve the assessment of long-term chronic drug effects.

## 7.2 Conclusion and Outlook

The 3D bioreactor presented and characterized in this thesis provides a liver like environment for the cultivation of primary human hepatocytes for about 3 weeks with maintained functionality. The system was improved in terms of respiration measurements. Cellular metabolism and liver-like parameters were analyzed (**Chapter 2**). The modified gas supply, i.e. oxygenation of the medium instead of direct gassing into the bioreactor cell compartment is thereby more physiological and allows the measurement of oxygen consumption rates, which is attractive for future studies using this bioreactor system.

However, the high amount of required cells limits experimental setups such as parallel cultivation or testing different drug concentrations using cells from the same donor. Moreover, the required technical expertise and the high costs of the bioreactor and of the perfusion system (including pumps, heating units, gas supply etc.) restrict the throughput of the system.

Therefore, a miniaturization and simplification of the 3D bioreactor system is highly needed to apply this technique for pharmaceutical studies. Smaller prototypes of an inner volume of 0.5 ml (compared to 2 ml) and a required cell number of  $2.5 \cdot 10^7$  (compared to  $1 \cdot 10^8$ ) are already available. Nevertheless, a more simple construction, further miniaturization and therefore higher cost effectiveness should be achieved. For this, we constructed ourselves some simple prototypes as shown in figure7-1, where the bioreactor consists of a glass T-fitting packed with about 15 hollow-fibers (diameter: 500  $\mu\text{m}$ ). Connections to tubing are made via Luer-lock adapter as well as the cell inoculation port. The cell compartment is sealed so that the cells are kept within the bioreactor chamber. This miniaturized architecture will be tested and improved in future projects in our laboratory. It will allow parallel studies as well as easier access to the cell compartment.

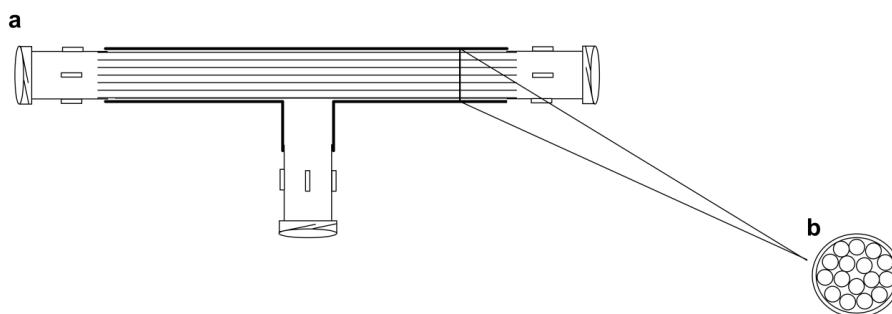


**Figure 7-1: Design of a self-developed 3D minibioreactor. a) Schematic overview of glass tubing, Luer-lock adapter and hollow-fibers inside the glass tubing, b) cross section through glass tube and hollow-fibers.**

Nevertheless, the closed character of these 3D bioreactors restricts important methods such as staining of liver-specific proteins e.g. phase III membrane transporters or structures such as bile-canaliculi. Access to the cells is only possible by breaking up the device at the end of the cultivation. Therefore, the analysis of intracellular factors (proteins, metabolites) is also unfeasible.

The 3D cultivation method developed by the Kajiwara group, where the cells are maintained within hollow-fibers instead of between them, is promising in terms of long-term functionality and also for hepatic differentiation of embryonic stem cells (Mizumoto *et al.*, 2008a; Mizumoto *et al.*, 2008b; Amimoto *et al.*, 2011). For this, liver cell suspension is filled into hollow-fibers, centrifuged for dense packing and then cultivated in a rotating petri dish (figure 7-2).

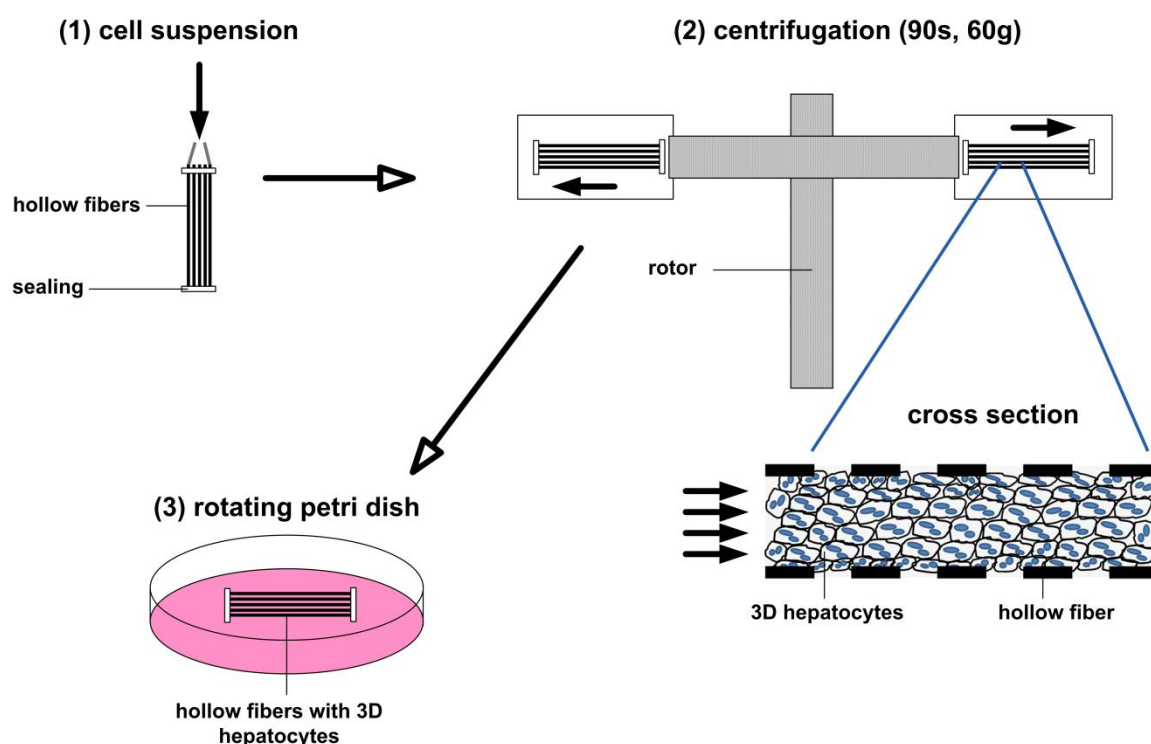


**Figure 7-2: Inoculating hepatocytes into hollow-fibers by centrifugation, modified from (Mizumoto *et al.*, 2008b).**

By this approach, parallel studies are possible since number and length of the hollow-fibers and therefore the required cell number is freely adjustable. Staining methods are easily performable by cutting the hollow-fibers in small slices and subsequent incubation with specific antibodies or dyes. Cell harvesting is also possible including the extraction of intracellular metabolites and proteins.

**Chapter 3** describes the development of a viability assay in the 3D bioreactor system. We show that this method is applicable to pharmacological long-term studies in the 3D bioreactor system.

However, we suggest that it is necessary to quantify the free drug concentration in the system because of the large hollow-fiber surface within the bioreactor on which drugs can bind. Furthermore, specific coating of the fibers with hydrophilic substances such as poly-lysine could prevent this binding, improve studies in this field and should be tested in future.

**Chapter 4** describes the production and characterization of organotypic cultures made of HepG2 cells. Therefore, the scaffold-free Gravity<sup>Plus</sup> technology from InSphero (Zurich, Switzerland) was used. Drug testing indicated that the organotypic cultures are well-suited for high-throughput investigation of drug toxicity and of chemotherapy resistance related to increased drug efflux. Future studies using this system should include the production of organotypic cultures of primary hepatocytes or functional hepatic cell lines such as HepaRG. Preliminary experiments have already been done in our laboratory showing that these both cell types are also capable to form three-dimensional organotypic cultures in the hanging drop. Further studies will be performed in terms of metabolic characterization, functional analysis and investigation of drug toxicity and drug-induced effects. Moreover, microstructures of the spheroids could be investigated by electron microscopy and the formation of liver-specific function such as bile-canaliculi could be analyzed by fluorescence microscopy to get deeper insights into the 3D architecture of the organotypic cultures.

The GCTOF-MS based metabolomics approach was successfully developed and applied as presented in **Chapter 5**. The method was shown to detect drug-induced effects more sensitive than other assays such as AST or SRB assay. The sampling is easy since the supernatants were measured and quantitative and qualitative information of 20-30 extracellular metabolites was sufficient to evaluate drug-induced metabolic effects. In future, this method can be applied to other cells such as stem cells, stem cell derived cells or cardiomyocytes due to their respective high potential in pharmacological research. Moreover, 3D systems can be investigated using this method and the assessed effects can be compared to 2D cultures. Quantification of intracellular metabolites would further give a more detailed view on the drug's effects, however methods for metabolite extraction have to be chosen carefully and to be developed for the respective cell types and cultivation systems. Metabolic flux analysis can furthermore provide valuable information about drug-induced effects on certain metabolic pathways. Finally, an integrated approach including transcriptomics, proteomics and metabolomics would lead to a global assessment of adverse drug effects, indicating the potential of systems biology in terms of pharmacological and toxicological research.

The repeated dose testing described in **Chapter 6** indicates the importance of chronic toxicity assessment in the process of drug development. Metabolically active long-term cell cultures are

thereby essential, particularly during studies of drug metabolism and for the assessment of drug metabolite toxicity. In this study, we used a commercially available serum free medium (enriched with growth factors) for long-term cultivation of primary liver cells. Future studies could include repeated dose exposure on long-term cultures HepaRG cells, which were shown to maintain their biotransformation capacities for more than 3 weeks. Moreover, serum-free cultivation offers the possibility to include quantitative proteomics analyses upon drug exposure to get a more detailed view on drug induced effects.

## REFERENCES

- Abu-Absi, S. F., Friend, J. R., Hansen, L. K., and Hu, W. S. (2002). Structural polarity and functional bile canaliculi in rat hepatocyte spheroids. *Exp Cell Res* **274**, 56-67.
- Aden, D. P., Fogel, A., Plotkin, S., Damjanov, I., and Knowles, B. B. (1979). Controlled synthesis of HBsAg in a differentiated human liver carcinoma-derived cell line. *Nature* **282**, 615-616.
- Aithal, G. P. (2004). Diclofenac-induced liver injury: a paradigm of idiosyncratic drug toxicity. *Expert Opin Drug Saf* **3**, 519-523.
- Altmann, B., Giselbrecht, S., Weibezahn, K. F., Welle, A., and Gottwald, E. (2008). The three-dimensional cultivation of the carcinoma cell line HepG2 in a perfused chip system leads to a more differentiated phenotype of the cells compared to monolayer culture. *Biomed Mater* **3**, 034120.
- Amacher, D. E., Adler, R., Herath, A., and Townsend, R. R. (2005). Use of proteomic methods to identify serum biomarkers associated with rat liver toxicity or hypertrophy. *Clin Chem* **51**, 1796-1803.
- Amimoto, N., Mizumoto, H., Nakazawa, K., Ijima, H., Funatsu, K., and Kajiwara, T. (2011). Hepatic differentiation of mouse embryonic stem cells and induced pluripotent stem cells during organoid formation in hollow fibers. *Tissue Eng Part A* **17**, 2071-2078.
- Anton, F., Suck, K., Diederichs, S., Behr, L., Hitzmann, B., van Griensven, M., Scheper, T., and Kasper, C. (2008). Design and characterization of a rotating bed system bioreactor for tissue engineering applications. *Biotechnol Prog* **24**, 140-147.
- Baldwin, G. S., Murphy, V. J., Yang, Z., and Hashimoto, T. (1998). Binding of nonsteroidal antiinflammatory drugs to the alpha-subunit of the trifunctional protein of long chain fatty acid oxidation. *J Pharmacol Exp Ther* **286**, 1110-1114.
- Bartles, J. R., Braiterman, L. T., and Hubbard, A. L. (1985). Endogenous and exogenous domain markers of the rat hepatocyte plasma membrane. *J Cell Biol* **100**, 1126-1138.
- Batey, A. J., and Coker, S. J. (2002). Proarrhythmic potential of halofantrine, terfenadine and clofilium in a modified in vivo model of torsade de pointes. *Br J Pharmacol* **135**, 1003-1012.
- Bazou, D., Coakley, W. T., Hayes, A. J., and Jackson, S. K. (2008). Long-term viability and proliferation of alginate-encapsulated 3-D HepG2 aggregates formed in an ultrasound trap. *Toxicol In Vitro* **22**, 1321-1331.
- Beckers, S., Noor, F., Muller-Vieira, U., Mayer, M., Strigun, A., and Heinzle, E. (2010). High throughput, non-invasive and dynamic toxicity screening on adherent cells using respiratory measurements. *Toxicol In Vitro* **24**, 686-694.

- Beger, R. D., Sun, J., and Schnackenberg, L. K. (2010). Metabolomics approaches for discovering biomarkers of drug-induced hepatotoxicity and nephrotoxicity. *Toxicol Appl Pharmacol* **243**, 154-166.
- Bhadriraju, K., and Chen, C. S. (2002). Engineering cellular microenvironments to improve cell-based drug testing. *Drug Discov Today* **7**, 612-620.
- Bhatia, S. N., Balis, U. J., Yarmush, M. L., and Toner, M. (1999). Effect of cell-cell interactions in preservation of cellular phenotype: cocultivation of hepatocytes and nonparenchymal cells. *Faseb J* **13**, 1883-1900.
- Blomme, E. A., Yang, Y., and Waring, J. F. (2009). Use of toxicogenomics to understand mechanisms of drug-induced hepatotoxicity during drug discovery and development. *Toxicol Lett* **186**, 22-31.
- Boelsterli, U. A. (2003). Diclofenac-induced liver injury: a paradigm of idiosyncratic drug toxicity. *Toxicol Appl Pharmacol* **192**, 307-322.
- Bokhari, M., Carnachan, R. J., Cameron, N. R., and Przyborski, S. A. (2007). Novel cell culture device enabling three-dimensional cell growth and improved cell function. *Biochem Biophys Res Commun* **354**, 1095-1100.
- Bonarius, H. P., Ozemre, A., Timmerarends, B., Skrabal, P., Tramper, J., Schmid, G., and Heinzle, E. (2001). Metabolic-flux analysis of continuously cultured hybridoma cells using (13)CO(2) mass spectrometry in combination with (13)C-lactate nuclear magnetic resonance spectroscopy and metabolite balancing. *Biotechnol Bioeng* **74**, 528-538.
- Bort, R., Ponsoda, X., Jover, R., Gomez-Lechon, M. J., and Castell, J. V. (1999). Diclofenac toxicity to hepatocytes: a role for drug metabolism in cell toxicity. *J Pharmacol Exp Ther* **288**, 65-72.
- Brien, G. L., and Bracken, A. P. (2009). Transcriptomics: unravelling the biology of transcription factors and chromatin remodelers during development and differentiation. *Semin Cell Dev Biol* **20**, 835-841.
- Bunk, B., Kucklick, M., Jonas, R., Munch, R., Schobert, M., Jahn, D., and Hiller, K. (2006). MetaQuant: a tool for the automatic quantification of GC/MS-based metabolome data. *Bioinformatics* **22**, 2962-2965.
- Celebi, B., Mantovani, D., and Pineault, N. (2011). Effects of extracellular matrix proteins on the growth of haematopoietic progenitor cells. *Biomed Mater* **6**, 055011.
- Chan, K., Truong, D., Shangari, N., and O'Brien, P. J. (2005). Drug-induced mitochondrial toxicity. *Expert Opin Drug Metab Toxicol* **1**, 655-669.
- Clark, S., Francis, P. S., Conlan, X. A., and Barnett, N. W. (2007). Determination of urea using high-performance liquid chromatography with fluorescence detection after automated derivatisation with xanthidrol. *J Chromatogr A* **1161**, 207-213.

- Collins, F. S., Gray, G. M., and Bucher, J. R. (2008). Toxicology. Transforming environmental health protection. *Science* **319**, 906-907.
- Corstorphine, L., and Sefton, M. V. (2011). Effectiveness factor and diffusion limitations in collagen gel modules containing HepG2 cells. *J Tissue Eng Regen Med* **5**, 119-129.
- Cukierman, E., Pankov, R., Stevens, D. R., and Yamada, K. M. (2001). Taking cell-matrix adhesions to the third dimension. *Science* **294**, 1708-1712.
- Cukierman, E., Pankov, R., and Yamada, K. M. (2002). Cell interactions with three-dimensional matrices. *Curr Opin Cell Biol* **14**, 633-639.
- Daly, A. K., Aithal, G. P., Leathart, J. B., Swainsbury, R. A., Dang, T. S., and Day, C. P. (2007). Genetic susceptibility to diclofenac-induced hepatotoxicity: contribution of UGT2B7, CYP2C8, and ABC2 genotypes. *Gastroenterology* **132**, 272-281.
- De Bartolo, L., Salerno, S., Curcio, E., Piscioneri, A., Rende, M., Morelli, S., Tasselli, F., Bader, A., and Drioli, E. (2009). Human hepatocyte functions in a crossed hollow fiber membrane bioreactor. *Biomaterials* **30**, 2531-2543.
- Demetriou, A. A., Rozga, J., Podesta, L., Lepage, E., Morsiani, E., Moscioni, A. D., Hoffman, A., McGrath, M., Kong, L., Rosen, H., and et al. (1995). Early clinical experience with a hybrid bioartificial liver. *Scand J Gastroenterol Suppl* **208**, 111-117.
- Denkert, C., Budczies, J., Kind, T., Weichert, W., Tablack, P., Sehouli, J., Niesporek, S., Konsgen, D., Dietel, M., and Fiehn, O. (2006). Mass spectrometry-based metabolic profiling reveals different metabolite patterns in invasive ovarian carcinomas and ovarian borderline tumors. *Cancer Res* **66**, 10795-10804.
- Denkert, C., Budczies, J., Weichert, W., Wohlgemuth, G., Scholz, M., Kind, T., Niesporek, S., Noske, A., Buckendahl, A., Dietel, M., and Fiehn, O. (2008). Metabolite profiling of human colon carcinoma--deregulation of TCA cycle and amino acid turnover. *Mol Cancer* **7**, 72.
- Depreter, M., Walker, T., De Smet, K., Beken, S., Kerckaert, I., Rogiers, V., and Roels, F. (2002). Hepatocyte polarity and the peroxisomal compartment: a comparative study. *Histochem J* **34**, 139-151.
- Deshpande, R. R., Wittmann, C., and Heinzle, E. (2004). Microplates with integrated oxygen sensing for medium optimization in animal cell culture. *Cytotechnology* **46**, 1-8.
- Diesen, D. L., and Kuo, P. C. (2009). Nitric oxide and redox regulation in the liver: Part I. General considerations and redox biology in hepatitis. *J Surg Res* **162**, 95-109.
- Domansky, K., Inman, W., Serdy, J., Dash, A., Lim, M. H., and Griffith, L. G. (2010). Perfused multiwell plate for 3D liver tissue engineering. *Lab Chip* **10**, 51-58.
- Ellis, A. J., Hughes, R. D., Wendon, J. A., Dunne, J., Langley, P. G., Kelly, J. H., Gislason, G. T., Sussman, N. L., and Williams, R. (1996). Pilot-controlled trial of the extracorporeal liver assist device in acute liver failure. *Hepatology* **24**, 1446-1451.

## REFERENCES

---

- Emoto, M., Anno, T., Sato, Y., Tanabe, K., Okuya, S., Tanizawa, Y., Matsutani, A., and Oka, Y. (2001). Troglitazone treatment increases plasma vascular endothelial growth factor in diabetic patients and its mRNA in 3T3-L1 adipocytes. *Diabetes* **50**, 1166-1170.
- Esch, M. B., King, T. L., and Shuler, M. L. (2011). The role of body-on-a-chip devices in drug and toxicity studies. *Annu Rev Biomed Eng* **13**, 55-72.
- Evans, D. C., Watt, A. P., Nicoll-Griffith, D. A., and Baillie, T. A. (2004). Drug-protein adducts: an industry perspective on minimizing the potential for drug bioactivation in drug discovery and development. *Chem Res Toxicol* **17**, 3-16.
- Eyer, K., Oeggerli, A., and Heinzle, E. (1995). On-line gas analysis in animal cell cultivation: II. Methods for oxygen uptake rate estimation and its application to controlled feeding of glutamine. *Biotechnol Bioeng* **45**, 54-62.
- Fisher, J. P., Jo, S., Mikos, A. G., and Reddi, A. H. (2004). Thermoreversible hydrogel scaffolds for articular cartilage engineering. *J Biomed Mater Res A* **71**, 268-274.
- Flendrig, L. M., Chamuleau, R. A., Maas, M. A., Daalhuisen, J., Hasset, B., Kilty, C. G., Doyle, S., Ladiges, N. C., Jorning, G. G., la Soe, J. W., Sommeijer, D., and te Velde, A. A. (1999). Evaluation of a novel bioartificial liver in rats with complete liver ischemia: treatment efficacy and species-specific alpha-GST detection to monitor hepatocyte viability. *J Hepatol* **30**, 311-320.
- Frisk, T., Rydholm, S., Liebmann, T., Svahn, H. A., Stemme, G., and Brismar, H. (2007). A microfluidic device for parallel 3-D cell cultures in asymmetric environments. *Electrophoresis* **28**, 4705-4712.
- Fulgencio, J. P., Kohl, C., Girard, J., and Pegorier, J. P. (1996). Troglitazone inhibits fatty acid oxidation and esterification, and gluconeogenesis in isolated hepatocytes from starved rats. *Diabetes* **45**, 1556-1562.
- Gerets, H. H., Hanon, E., Cornet, M., Dhalluin, S., Depelchin, O., Canning, M., and Atienzar, F. A. (2009). Selection of cytotoxicity markers for the screening of new chemical entities in a pharmaceutical context: a preliminary study using a multiplexing approach. *Toxicol In Vitro* **23**, 319-332.
- Gerlach, J. C., Brayfield, C., Puhl, G., Borneman, R., Muller, C., Schmelzer, E., and Zeilinger, K. (2010a). Lidocaine/monoethylglycinexylidide test, galactose elimination test, and sorbitol elimination test for metabolic assessment of liver cell bioreactors. *Artif Organs* **34**, 462-472.
- Gerlach, J. C., Hout, M., Edsbage, J., Bjorquist, P., Lubberstedt, M., Miki, T., Stachelscheid, H., Schmelzer, E., Schatten, G., and Zeilinger, K. (2010b). Dynamic 3D culture promotes spontaneous embryonic stem cell differentiation in vitro. *Tissue Eng Part C Methods* **16**, 115-121.
- Gerlach, J. C., Mutig, K., Sauer, I. M., Schrade, P., Efimova, E., Mieder, T., Naumann, G., Grunwald, A., Pless, G., Mas, A., Bachmann, S., Neuhaus, P., and Zeilinger, K. (2003a). Use of primary human liver cells originating from discarded grafts in a

- bioreactor for liver support therapy and the prospects of culturing adult liver stem cells in bioreactors: a morphologic study. *Transplantation* **76**, 781-786.
- Gerlach, J. C., Zeilinger, K., Grebe, A., Puhl, G., Pless, G., Sauer, I., Grunwald, A., Schnoy, N., Muller, C., and Neuhaus, P. (2003b). Recovery of preservation-injured primary human hepatocytes and nonparenchymal cells to tissuelike structures in large-scale bioreactors for liver support: an initial transmission electron microscopy study. *J Invest Surg* **16**, 83-92.
- Gerlach, J. C., Zeilinger, K., and Patzer Ii, J. F. (2008). Bioartificial liver systems: why, what, whither? *Regen Med* **3**, 575-595.
- Glicklis, R., Shapiro, L., Agbaria, R., Merchuk, J. C., and Cohen, S. (2000). Hepatocyte behavior within three-dimensional porous alginate scaffolds. *Biotechnol Bioeng* **67**, 344-353.
- Gloeckner, H., Jonuleit, T., and Lemke, H. D. (2001). Monitoring of cell viability and cell growth in a hollow-fiber bioreactor by use of the dye Alamar Blue. *J Immunol Methods* **252**, 131-138.
- Godoy, P., Hengstler, J. G., Ilkavets, I., Meyer, C., Bachmann, A., Muller, A., Tuschl, G., Mueller, S. O., and Dooley, S. (2009). Extracellular matrix modulates sensitivity of hepatocytes to fibroblastoid dedifferentiation and transforming growth factor beta-induced apoptosis. *Hepatology* **49**, 2031-2043.
- Gomase, V. S., and Tagore, S. (2008). Epigenomics. *Curr Drug Metab* **9**, 232-237.
- Gripon, P., Rumin, S., Urban, S., Le Seyec, J., Glaise, D., Cannie, I., Guyomard, C., Lucas, J., Trepo, C., and Guguen-Guillouzo, C. (2002). Infection of a human hepatoma cell line by hepatitis B virus. *Proc Natl Acad Sci U S A* **99**, 15655-15660.
- Guengerich, F. P. (2011). Mechanisms of drug toxicity and relevance to pharmaceutical development. *Drug Metab Pharmacokinet* **26**, 3-14.
- Guillouzo, A. (1998). Liver cell models in in vitro toxicology. *Environ Health Perspect* **106 Suppl 2**, 511-532.
- Guillouzo, A., Corlu, A., Aninat, C., Glaise, D., Morel, F., and Guguen-Guillouzo, C. (2007). The human hepatoma HepaRG cells: a highly differentiated model for studies of liver metabolism and toxicity of xenobiotics. *Chem Biol Interact* **168**, 66-73.
- Guo, R., Huang, Z., Shu, Y., Jin, S., and Ge, H. (2009). Tamoxifen inhibits proliferation and induces apoptosis in human hepatocellular carcinoma cell line HepG2 via down-regulation of survivin expression. *Biomed Pharmacother* **63**, 375-379.
- Haouzi, D., Baghdiguan, S., Granier, G., Travo, P., Mangeat, P., and Hibner, U. (2005). Three-dimensional polarization sensitizes hepatocytes to Fas/CD95 apoptotic signalling. *J Cell Sci* **118**, 2763-2773.

- Harrill, A. H., Ross, P. K., Gatti, D. M., Threadgill, D. W., and Rusyn, I. (2009). Population-based discovery of toxicogenomics biomarkers for hepatotoxicity using a laboratory strain diversity panel. *Toxicol Sci* **110**, 235-243.
- Herder, C., Karakas, M., and Koenig, W. (2011). Biomarkers for the prediction of type 2 diabetes and cardiovascular disease. *Clin Pharmacol Ther* **90**, 52-66.
- Hiller, K., Hangebrauk, J., Jager, C., Spura, J., Schreiber, K., and Schomburg, D. (2009). MetaboliteDetector: comprehensive analysis tool for targeted and nontargeted GC/MS based metabolome analysis. *Anal Chem* **81**, 3429-3439.
- Hiller, K., Metallo, C. M., Kelleher, J. K., and Stephanopoulos, G. (2010). Nontargeted elucidation of metabolic pathways using stable-isotope tracers and mass spectrometry. *Anal Chem* **82**, 6621-6628.
- Hinz, B., Chevts, J., Renner, B., Wuttke, H., Rau, T., Schmidt, A., Szelenyi, I., Brune, K., and Werner, U. (2005). Bioavailability of diclofenac potassium at low doses. *Br J Clin Pharmacol* **59**, 80-84.
- Hoekstra, D., Zegers, M. M., and van Ijzendoorn, S. C. (1999). Membrane flow, lipid sorting and cell polarity in HepG2 cells: role of a subapical compartment. *Biochem Soc Trans* **27**, 422-428.
- Holmes, F. A., and Liticker, J. D. (2005). Pharmacogenomics of tamoxifen in a nutshell-and who broke the nutcracker? *J Oncol Pract* **1**, 155-159.
- Homolya, L., Varadi, A., and Sarkadi, B. (2003). Multidrug resistance-associated proteins: Export pumps for conjugates with glutathione, glucuronate or sulfate. *Biofactors* **17**, 103-114.
- Hosseinkhani, H., Hosseinkhani, M., Hattori, S., Matsuoka, R., and Kawaguchi, N. (2009). Micro and nano-scale in vitro 3D culture system for cardiac stem cells. *J Biomed Mater Res A*.
- Hummel, J., Strehmel, N., Selbig, J., Walther, D., and Kopka, J. (2010). Decision tree supported substructure prediction of metabolites from GC-MS profiles. *Metabolomics* **6**, 322-333.
- Ijichi, C., Matsumura, T., Tsuji, T., and Eto, Y. (2003). Branched-chain amino acids promote albumin synthesis in rat primary hepatocytes through the mTOR signal transduction system. *Biochem Biophys Res Commun* **303**, 59-64.
- Iwahori, T., Matsuno, N., Johjima, Y., Konno, O., Akashi, I., Nakamura, Y., Hama, K., Iwamoto, H., Uchiyama, M., Ashizawa, T., and Nagao, T. (2005). Radial flow bioreactor for the creation of bioartificial liver and kidney. *Transplant Proc* **37**, 212-214.
- Jaeschke, H. (2005). Role of inflammation in the mechanism of acetaminophen-induced hepatotoxicity. *Expert Opin Drug Metab Toxicol* **1**, 389-397.

- Jerina, D. M. (1983). The 1982 Bernard B. Brodie Award Lecture. Metabolism of Aromatic hydrocarbons by the cytochrome P-450 system and epoxide hydrolase. *Drug Metab Dispos* **11**, 1-4.
- Johnson, T. E., Zhang, X., Bleicher, K. B., Dysart, G., Loughlin, A. F., Schaefer, W. H., and Umbenhauer, D. R. (2004). Statins induce apoptosis in rat and human myotube cultures by inhibiting protein geranylgeranylation but not ubiquinone. *Toxicol Appl Pharmacol* **200**, 237-250.
- Josse, R., Aninat, C., Glaise, D., Dumont, J., Fessard, V., Morel, F., Poul, J. M., Guguen-Guillouzo, C., and Guillouzo, A. (2008). Long-term functional stability of human HepaRG hepatocytes and use for chronic toxicity and genotoxicity studies. *Drug Metab Dispos* **36**, 1111-1118.
- Kassahun, K., Pearson, P. G., Tang, W., McIntosh, I., Leung, K., Elmore, C., Dean, D., Wang, R., Doss, G., and Baillie, T. A. (2001). Studies on the metabolism of troglitazone to reactive intermediates in vitro and in vivo. Evidence for novel biotransformation pathways involving quinone methide formation and thiazolidinedione ring scission. *Chem Res Toxicol* **14**, 62-70.
- Kauffmann, H. M., Keppler, D., Gant, T. W., and Schrenk, D. (1998). Induction of hepatic mrp2 (cmrp/cmoat) gene expression in nonhuman primates treated with rifampicin or tamoxifen. *Arch Toxicol* **72**, 763-768.
- Kelm, J. M., Ehler, E., Nielsen, L. K., Schlatter, S., Perriard, J. C., and Fussenegger, M. (2004). Design of artificial myocardial microtissues. *Tissue Eng* **10**, 201-214.
- Kelm, J. M., and Fussenegger, M. (2004). Microscale tissue engineering using gravity-enforced cell assembly. *Trends Biotechnol* **22**, 195-202.
- Kelm, J. M., Ittner, L. M., Born, W., Djonov, V., and Fussenegger, M. (2006). Self-assembly of sensory neurons into ganglia-like microtissues. *J Biotechnol* **121**, 86-101.
- Kelm, J. M., Timmins, N. E., Brown, C. J., Fussenegger, M., and Nielsen, L. K. (2003). Method for generation of homogeneous multicellular tumor spheroids applicable to a wide variety of cell types. *Biotechnol Bioeng* **83**, 173-180.
- Kidambi, S., Yarmush, R. S., Novik, E., Chao, P., Yarmush, M. L., and Nahmias, Y. (2009). Oxygen-mediated enhancement of primary hepatocyte metabolism, functional polarization, gene expression, and drug clearance. *Proc Natl Acad Sci U S A* **106**, 15714-15719.
- Kim, K. B., Um, S. Y., Chung, M. W., Jung, S. C., Oh, J. S., Kim, S. H., Na, H. S., Lee, B. M., and Choi, K. H. (2010). Toxicometabolomics approach to urinary biomarkers for mercuric chloride (HgCl<sub>2</sub>)-induced nephrotoxicity using proton nuclear magnetic resonance ((<sup>1</sup>H)NMR) in rats. *Toxicol Appl Pharmacol* **249**, 114-126.
- Kim, S. S., Utsunomiya, H., Koski, J. A., Wu, B. M., Cima, M. J., Sohn, J., Mukai, K., Griffith, L. G., and Vacanti, J. P. (1998). Survival and function of hepatocytes on a novel three-

- dimensional synthetic biodegradable polymer scaffold with an intrinsic network of channels. *Ann Surg* **228**, 8-13.
- Kipp, H., and Arias, I. M. (2000). Newly synthesized canalicular ABC transporters are directly targeted from the Golgi to the hepatocyte apical domain in rat liver. *J Biol Chem* **275**, 15917-15925.
- Kleinstreuer, N. C., Smith, A. M., West, P. R., Conard, K., Fontaine, B., Weir-Hauptman, A., Palmer, J., Knudsen, T. B., Dix, D. J., Donley, E. L., and Cezar, G. G. (2011). Identifying developmental toxicity pathways for a subset of ToxCast chemicals using human embryonic stem cells and metabolomics. *Toxicol Appl Pharmacol*.
- Kono, Y., Yang, S., and Roberts, E. A. (1997). Extended primary culture of human hepatocytes in a collagen gel sandwich system. *In Vitro Cell Dev Biol Anim* **33**, 467-472.
- Kretz-Rommel, A., and Boelsterli, U. A. (1993). Diclofenac covalent protein binding is dependent on acyl glucuronide formation and is inversely related to P450-mediated acute cell injury in cultured rat hepatocytes. *Toxicol Appl Pharmacol* **120**, 155-161.
- Kromer, J. O., Fritz, M., Heinzle, E., and Wittmann, C. (2005). In vivo quantification of intracellular amino acids and intermediates of the methionine pathway in *Corynebacterium glutamicum*. *Anal Biochem* **340**, 171-173.
- Labbe, G., Pessayre, D., and Fromenty, B. (2008). Drug-induced liver injury through mitochondrial dysfunction: mechanisms and detection during preclinical safety studies. *Fundam Clin Pharmacol* **22**, 335-353.
- Laine, J. E., Auriola, S., Pasanen, M., and Juvonen, R. O. (2009). Acetaminophen bioactivation by human cytochrome P450 enzymes and animal microsomes. *Xenobiotica* **39**, 11-21.
- Lan, S. F., and Starly, B. (2011). Alginate based 3D hydrogels as an in vitro co-culture model platform for the toxicity screening of new chemical entities. *Toxicol Appl Pharmacol* **256**, 62-72.
- Lang, R., Stern, M. M., Smith, L., Liu, Y., Bharadwaj, S., Liu, G., Baptista, P. M., Bergman, C. R., Soker, S., Yoo, J. J., Atala, A., and Zhang, Y. (2011). Three-dimensional culture of hepatocytes on porcine liver tissue-derived extracellular matrix. *Biomaterials*.
- Lauer, B., Tuschl, G., Kling, M., and Mueller, S. O. (2009). Species-specific toxicity of diclofenac and troglitazone in primary human and rat hepatocytes. *Chem Biol Interact* **179**, 17-24.
- LeCluyse, E. L. (2001). Human hepatocyte culture systems for the in vitro evaluation of cytochrome P450 expression and regulation. *Eur J Pharm Sci* **13**, 343-368.
- Li, A. P., Bode, C., and Sakai, Y. (2004). A novel in vitro system, the integrated discrete multiple organ cell culture (IdMOC) system, for the evaluation of human drug toxicity: comparative cytotoxicity of tamoxifen towards normal human cells from five major organs and MCF-7 adenocarcinoma breast cancer cells. *Chem Biol Interact* **150**, 129-136.

## REFERENCES

---

- Li, C. L., Tian, T., Nan, K. J., Zhao, N., Guo, Y. H., Cui, J., Wang, J., and Zhang, W. G. (2008). Survival advantages of multicellular spheroids vs. monolayers of HepG2 cells in vitro. *Oncol Rep* **20**, 1465-1471.
- Liebler, D. C., and Guengerich, F. P. (2005). Elucidating mechanisms of drug-induced toxicity. *Nat Rev Drug Discov* **4**, 410-420.
- Liebmann, T., Rydholm, S., Akpe, V., and Brismar, H. (2007). Self-assembling Fmoc dipeptide hydrogel for in situ 3D cell culturing. *BMC Biotechnol* **7**, 88.
- Limonciel, A., Aschauer, L., Wilmes, A., Prajczek, S., Leonard, M. O., Pfaller, W., and Jennings, P. (2011). Lactate is an ideal non-invasive marker for evaluating temporal alterations in cell stress and toxicity in repeat dose testing regimes. *Toxicol In Vitro* **25**, 1855-1862.
- Loi, C. M., Alvey, C. W., Vassos, A. B., Randinitis, E. J., Sedman, A. J., and Koup, J. R. (1999). Steady-state pharmacokinetics and dose proportionality of troglitazone and its metabolites. *J Clin Pharmacol* **39**, 920-926.
- Lu, Y., A. J., Wang, G., Hao, H., Huang, Q., Yan, B., Zha, W., Gu, S., Ren, H., Zhang, Y., Fan, X., Zhang, M., and Hao, K. (2008). Gas chromatography/time-of-flight mass spectrometry based metabonomic approach to differentiating hypertension- and age-related metabolic variation in spontaneously hypertensive rats. *Rapid Commun Mass Spectrom* **22**, 2882-2888.
- Lubberstedt, M., Muller-Vieira, U., Mayer, M., Biemel, K. M., Knospel, F., Knobloch, D., Nussler, A. K., Gerlach, J. C., and Zeilinger, K. (2010). HepaRG human hepatic cell line utility as a surrogate for primary human hepatocytes in drug metabolism assessment in vitro. *J Pharmacol Toxicol Methods*.
- Lubberstedt, M., Muller-Vieira, U., Mayer, M., Biemel, K. M., Knospel, F., Knobloch, D., Nussler, A. K., Gerlach, J. C., and Zeilinger, K. (2011). HepaRG human hepatic cell line utility as a surrogate for primary human hepatocytes in drug metabolism assessment in vitro. *J Pharmacol Toxicol Methods* **63**, 59-68.
- Ma, Q., and Lu, A. Y. (2007). CYP1A induction and human risk assessment: an evolving tale of in vitro and in vivo studies. *Drug Metab Dispos* **35**, 1009-1016.
- Mandenius, C. F., Andersson, T. B., Alves, P. M., Batzl-Hartmann, C., Bjorquist, P., Carrondo, M. J., Chesne, C., Coecke, S., Edsbacke, J., Fredriksson, J. M., Gerlach, J. C., Heinzle, E., Ingelman-Sundberg, M., Johansson, I., Koppers-Munther, B., Muller-Vieira, U., Noor, F., and Zeilinger, K. (2011a). Toward preclinical predictive drug testing for metabolism and hepatotoxicity by using in vitro models derived from human embryonic stem cells and human cell lines - a report on the Vitrocellomics EU-project. *Altern Lab Anim* **39**, 147-171.
- Mandenius, C. F., Steel, D., Noor, F., Meyer, T., Heinzle, E., Asp, J., Arain, S., Kraushaar, U., Bremer, S., Class, R., and Sartipy, P. (2011b). Cardiotoxicity testing using pluripotent stem cell-derived human cardiomyocytes and state-of-the-art bioanalytics: a review. *J Appl Toxicol* **31**, 191-205.

- Manna, S. K., Patterson, A. D., Yang, Q., Krausz, K. W., Idle, J. R., Fornace, A. J., and Gonzalez, F. J. (2011). UPLC-MS-based Urine Metabolomics Reveals Indole-3-lactic Acid and Phenyllactic Acid as Conserved Biomarkers for Alcohol-induced Liver Disease in the Ppara-null Mouse Model. *J Proteome Res* **10**, 4120-4133.
- Manna, S. K., Patterson, A. D., Yang, Q., Krausz, K. W., Li, H., Idle, J. R., Fornace, A. J., Jr., and Gonzalez, F. J. (2010). Identification of noninvasive biomarkers for alcohol-induced liver disease using urinary metabolomics and the Ppara-null mouse. *J Proteome Res* **9**, 4176-4188.
- Marion, M. J., Hantz, O., and Durantel, D. (2010). The HepaRG cell line: biological properties and relevance as a tool for cell biology, drug metabolism, and virology studies. *Methods Mol Biol* **640**, 261-272.
- Maruyama, M., Matsunaga, T., Harada, E., and Ohmori, S. (2007). Comparison of basal gene expression and induction of CYP3As in HepG2 and human fetal liver cells. *Biol Pharm Bull* **30**, 2091-2097.
- Maurice, M., Schell, M. J., Lardeux, B., and Hubbard, A. L. (1994). Biosynthesis and intracellular transport of a bile canalicular plasma membrane protein: studies in vivo and in the perfused rat liver. *Hepatology* **19**, 648-655.
- Mehta, G., Williams, C. M., Alvarez, L., Lesniewski, M., Kamm, R. D., and Griffith, L. G. (2010). Synergistic effects of tethered growth factors and adhesion ligands on DNA synthesis and function of primary hepatocytes cultured on soft synthetic hydrogels. *Biomaterials* **31**, 4657-4671.
- Meier, P. J., and Stieger, B. (2002). Bile salt transporters. *Annu Rev Physiol* **64**, 635-661.
- Mikos, A. G., Bao, Y., Cima, L. G., Ingber, D. E., Vacanti, J. P., and Langer, R. (1993). Preparation of poly(glycolic acid) bonded fiber structures for cell attachment and transplantation. *J Biomed Mater Res* **27**, 183-189.
- Miranda, J. P., Leite, S. B., Muller-Vieira, U., Rodrigues, A., Carrondo, M. J., and Alves, P. M. (2009). Towards an extended functional hepatocyte in vitro culture. *Tissue Eng Part C Methods* **15**, 157-167.
- Miranda, J. P., Rodrigues, A., Tostoes, R. M., Leite, S., Zimmerman, H., Carrondo, M. J., and Alves, P. M. (2010). Extending hepatocyte functionality for drug-testing applications using high-viscosity alginate-encapsulated three-dimensional cultures in bioreactors. *Tissue Eng Part C Methods* **16**, 1223-1232.
- Miyazawa, M., Torii, T., Toshimitsu, Y., Okada, K., and Koyama, I. (2007). Hepatocyte dynamics in a three-dimensional rotating bioreactor. *J Gastroenterol Hepatol* **22**, 1959-1964.
- Mizumoto, H., Aoki, K., Nakazawa, K., Ijima, H., Funatsu, K., and Kajiwara, T. (2008a). Hepatic differentiation of embryonic stem cells in HF/organoid culture. *Transplant Proc* **40**, 611-613.

- Mizumoto, H., Ishihara, K., Nakazawa, K., Ijima, H., Funatsu, K., and Kajiwara, T. (2008b). A new culture technique for hepatocyte organoid formation and long-term maintenance of liver-specific functions. *Tissue Eng Part C Methods* **14**, 167-175.
- Mueller, D., Tascher, G., Muller-Vieira, U., Knobloch, D., Nuessler, A. K., Zeilinger, K., Heinzle, E., and Noor, F. (2011). In-depth physiological characterization of primary human hepatocytes in a 3D hollow-fiber bioreactor. *J Tissue Eng Regen Med* **5**, e207-218.
- Nagaoka, R., Iwasaki, T., Rokutanda, N., Takeshita, A., Koibuchi, Y., Horiguchi, J., Shimokawa, N., Iino, Y., Morishita, Y., and Koibuchi, N. (2006). Tamoxifen activates CYP3A4 and MDR1 genes through steroid and xenobiotic receptor in breast cancer cells. *Endocrine* **30**, 261-268.
- Nakamura, K., Mizutani, R., Sanbe, A., Enosawa, S., Kasahara, M., Nakagawa, A., Ejiri, Y., Murayama, N., Miyamoto, Y., Torii, T., Kusakawa, S., Yamauchi, J., Fukuda, M., Yamazaki, H., and Tanoue, A. (2011). Evaluation of drug toxicity with hepatocytes cultured in a micro-space cell culture system. *J Biosci Bioeng* **111**, 78-84.
- Nicholson, J. K., Lindon, J. C., and Holmes, E. (1999). 'Metabonomics': understanding the metabolic responses of living systems to pathophysiological stimuli via multivariate statistical analysis of biological NMR spectroscopic data. *Xenobiotica* **29**, 1181-1189.
- Nie, L., Wu, G., Culley, D. E., Scholten, J. C., and Zhang, W. (2007). Integrative analysis of transcriptomic and proteomic data: challenges, solutions and applications. *Crit Rev Biotechnol* **27**, 63-75.
- Nie, L., Wu, G., and Zhang, W. (2006). Correlation of mRNA expression and protein abundance affected by multiple sequence features related to translational efficiency in *Desulfovibrio vulgaris*: a quantitative analysis. *Genetics* **174**, 2229-2243.
- Niklas, J., and Heinzle, E. (2011). Metabolic Flux Analysis in Systems Biology of Mammalian Cells. *Adv Biochem Eng Biotechnol*.
- Niklas, J., Noor, F., and Heinzle, E. (2009). Effects of drugs in subtoxic concentrations on the metabolic fluxes in human hepatoma cell line Hep G2. *Toxicol Appl Pharmacol* **240**, 327-336.
- Niklas, J., Priesnitz, C., Rose, T., Sandig, V., and Heinzle, E. (2011a). Primary metabolism in the new human cell line AGE1.HN at various substrate levels: increased metabolic efficiency and alpha(1)-antitrypsin production at reduced pyruvate load. *Appl Microbiol Biotechnol*.
- Niklas, J., Sandig, V., and Heinzle, E. (2011b). Metabolite channeling and compartmentation in the human cell line AGE1.HN determined by (13)C labeling experiments and (13)C metabolic flux analysis. *J Biosci Bioeng*.
- Niklas, J., Schneider, K., and Heinzle, E. (2011c). Metabolic flux analysis in eukaryotes. *Curr Opin Biotechnol* **21**, 63-69.

- Niklas, J., Schrader, E., Sandig, V., Noll, T., and Heinzle, E. (2011d). Quantitative characterization of metabolism and metabolic shifts during growth of the new human cell line AGE1.HN using time resolved metabolic flux analysis. *Bioprocess Biosyst Eng* **34**, 533-545.
- Noor, F., Niklas, J., Muller-Vieira, U., and Heinzle, E. (2009). An integrated approach to improved toxicity prediction for the safety assessment during preclinical drug development using Hep G2 cells. *Toxicol Appl Pharmacol* **237**, 221-231.
- Nordin, J. H., and Hansen, R. G. (1963). Isolation and characterization of galactose from hydrolysates of glycogen. *J Biol Chem* **238**, 489-494.
- Nussler, A., Konig, S., Ott, M., Sokal, E., Christ, B., Thasler, W., Brulport, M., Gabelein, G., Schormann, W., Schulze, M., Ellis, E., Kraemer, M., Nocken, F., Fleig, W., Manns, M., Strom, S. C., and Hengstler, J. G. (2006). Present status and perspectives of cell-based therapies for liver diseases. *J Hepatol* **45**, 144-159.
- Nussler, A. K., Nussler, N. C., Merk, V., Brulport, M., Schormann, W., and Hengstler, J. G. (2009). The Holy Grail of Hepatocyte Culturing and Therapeutic Use. In *Strategies in Regenerative Medicine* (M. Santin, Ed.), pp. 1-38. Springer, New York, NY, USA.
- O'Brien, J., Wilson, I., Orton, T., and Pognan, F. (2000). Investigation of the Alamar Blue (resazurin) fluorescent dye for the assessment of mammalian cell cytotoxicity. *Eur J Biochem* **267**, 5421-5426.
- O'Brien, P. J., Irwin, W., Diaz, D., Howard-Cofield, E., Krejsa, C. M., Slaughter, M. R., Gao, B., Kaludercic, N., Angeline, A., Bernardi, P., Brain, P., and Hougham, C. (2006). High concordance of drug-induced human hepatotoxicity with in vitro cytotoxicity measured in a novel cell-based model using high content screening. *Arch Toxicol* **80**, 580-604.
- Oeggerli, A., Eyer, K., and Heinzle, E. (1995). On-line gas analysis in animal cell cultivation: I. Control of dissolved oxygen and pH. *Biotechnol Bioeng* **45**, 42-53.
- Oshikata, A., Matsushita, T., and Ueoka, R. (2011). Enhancement of drug efflux activity via MDR1 protein by spheroid culture of human hepatic cancer cells. *J Biosci Bioeng* **111**, 590-593.
- Pampaloni, F., Reynaud, E. G., and Stelzer, E. H. (2007). The third dimension bridges the gap between cell culture and live tissue. *Nat Rev Mol Cell Biol* **8**, 839-845.
- Park, S. H., Park, S. R., Chung, S. I., Pai, K. S., and Min, B. H. (2005). Tissue-engineered cartilage using fibrin/hyaluronan composite gel and its in vivo implantation. *Artif Organs* **29**, 838-845.
- Pauwels, M., and Rogiers, V. (2010). Human health safety evaluation of cosmetics in the EU: a legally imposed challenge to science. *Toxicol Appl Pharmacol* **243**, 260-274.
- Peters, S. J., Haagsman, H. P., and van Norren, K. (2008). Arginase release by primary hepatocytes and liver slices results in rapid conversion of arginine to urea in cell culture media. *Toxicol In Vitro* **22**, 1094-1098.

- Petinari, L., Kohn, L. K., de Carvalho, J. E., and Genari, S. C. (2004). Cytotoxicity of tamoxifen in normal and tumoral cell lines and its ability to induce cellular transformation in vitro. *Cell Biol Int* **28**, 531-539.
- Petrescu, I., and Tarba, C. (1997). Uncoupling effects of diclofenac and aspirin in the perfused liver and isolated hepatic mitochondria of rat. *Biochim Biophys Acta* **1318**, 385-394.
- Pless, G., Steffen, I., Zeilinger, K., Sauer, I. M., Katenz, E., Kehr, D. C., Roth, S., Mieder, T., Schwartlander, R., Muller, C., Wegner, B., Hout, M. S., and Gerlach, J. C. (2006). Evaluation of primary human liver cells in bioreactor cultures for extracorporeal liver support on the basis of urea production. *Artif Organs* **30**, 686-694.
- Rajan, N., Habermehl, J., Cote, M. F., Doillon, C. J., and Mantovani, D. (2006). Preparation of ready-to-use, storable and reconstituted type I collagen from rat tail tendon for tissue engineering applications. *Nat Protoc* **1**, 2753-2758.
- Riess, W., Stierlin, H., Degen, P., Faigle, J. W., Gerardin, A., Moppert, J., Sallmann, A., Schmid, K., Schweizer, A., Sulc, M., Theobald, W., and Wagner, J. (1978). Pharmacokinetics and metabolism of the anti-inflammatory agent Voltaren. *Scand J Rheumatol Suppl*, 17-29.
- Robertson, D. G., Watkins, P. B., and Reily, M. D. (2011). Metabolomics in toxicology: preclinical and clinical applications. *Toxicol Sci* **120 Suppl 1**, S146-170.
- Rodriguez, B., Burrage, K., Gavaghan, D., Grau, V., Kohl, P., and Noble, D. (2010). The systems biology approach to drug development: application to toxicity assessment of cardiac drugs. *Clin Pharmacol Ther* **88**, 130-134.
- Rodriguez, J. V., Pizarro, M. D., Scandizzi, A. L., Guibert, E. E., Almada, L. L., and Mamprin, M. E. (2008). Construction and performance of a minibioreactor suitable as experimental bioartificial liver. *Artif Organs* **32**, 323-328.
- Rosa, J., Pancirov, H., Skala, H., and Gadzic, A. (2004). Effects of troglitazone and insulin on glucose production in cultured hepatocytes isolated from rats on high fat diet. *Coll Antropol* **28**, 631-637.
- Rotem, A., Toner, M., Bhatia, S., Foy, B. D., Tompkins, R. G., and Yarmush, M. L. (1994). Oxygen is a factor determining in vitro tissue assembly: Effects on attachment and spreading of hepatocytes. *Biotechnol Bioeng* **43**, 654-660.
- Sahi, J., Hamilton, G., Sinz, M., Barros, S., Huang, S. M., Lesko, L. J., and LeCluyse, E. L. (2000). Effect of troglitazone on cytochrome P450 enzymes in primary cultures of human and rat hepatocytes. *Xenobiotica* **30**, 273-284.
- Sauer, I. M., Kardassis, D., Zeillinger, K., Pascher, A., Gruenwald, A., Pless, G., Irgang, M., Kraemer, M., Puhl, G., Frank, J., Muller, A. R., Steinmuller, T., Denner, J., Neuhaus, P., and Gerlach, J. C. (2003a). Clinical extracorporeal hybrid liver support--phase I study with primary porcine liver cells. *Xenotransplantation* **10**, 460-469.
- Sauer, I. M., Neuhaus, P., and Gerlach, J. C. (2002). Concept for modular extracorporeal liver support for the treatment of acute hepatic failure. *Metab Brain Dis* **17**, 477-484.

- Sauer, I. M., Zeilinger, K., Pless, G., Kardassis, D., Theruvath, T., Pascher, A., Goetz, M., Neuhaus, P., and Gerlach, J. C. (2003b). Extracorporeal liver support based on primary human liver cells and albumin dialysis--treatment of a patient with primary graft non-function. *J Hepatol* **39**, 649-653.
- Schmelzer, E., Mutig, K., Schrade, P., Bachmann, S., Gerlach, J. C., and Zeilinger, K. (2009). Effect of human patient plasma ex vivo treatment on gene expression and progenitor cell activation of primary human liver cells in multi-compartment 3D perfusion bioreactors for extra-corporeal liver support. *Biotechnol Bioeng* **103**, 817-827.
- Schmelzer, E., Triolo, F., Turner, M. E., Thompson, R. L., Zeilinger, K., Reid, L. M., Gridelli, B., and Gerlach, J. C. (2010). Three-Dimensional Perfusion Bioreactor Culture Supports Differentiation of Human Fetal Liver Cells. *Tissue Eng Part A*.
- Schmitmeier, S., Langsch, A., Jasmund, I., and Bader, A. (2006). Development and characterization of a small-scale bioreactor based on a bioartificial hepatic culture model for predictive pharmacological in vitro screenings. *Biotechnol Bioeng* **95**, 1198-1206.
- Schneider, K., Kromer, J. O., Wittmann, C., Alves-Rodrigues, I., Meyerhans, A., Diez, J., and Heinzle, E. (2009). Metabolite profiling studies in *Saccharomyces cerevisiae*: an assisting tool to prioritize host targets for antiviral drug screening. *Microb Cell Fact* **8**, 12.
- Sellaro, T. L., Ranade, A., Faulk, D. M., McCabe, G. P., Dorko, K., Badylak, S. F., and Strom, S. C. (2010). Maintenance of human hepatocyte function in vitro by liver-derived extracellular matrix gels. *Tissue Eng Part A* **16**, 1075-1082.
- Shim, J. H., Kim, J. Y., Park, M., Park, J., and Cho, D. W. (2011). Development of a hybrid scaffold with synthetic biomaterials and hydrogel using solid freeform fabrication technology. *Biofabrication* **3**, 034102.
- Shin, S. C., Choi, J. S., and Li, X. (2006). Enhanced bioavailability of tamoxifen after oral administration of tamoxifen with quercetin in rats. *Int J Pharm* **313**, 144-149.
- Shiraki, N., Umeda, K., Sakashita, N., Takeya, M., Kume, K., and Kume, S. (2008). Differentiation of mouse and human embryonic stem cells into hepatic lineages. *Genes Cells* **13**, 731-746.
- Sin, A., Chin, K. C., Jamil, M. F., Kostov, Y., Rao, G., and Shuler, M. L. (2004). The design and fabrication of three-chamber microscale cell culture analog devices with integrated dissolved oxygen sensors. *Biotechnol Prog* **20**, 338-345.
- Snykers, S., Vanhaecke, T., Papeleu, P., Lutun, A., Jiang, Y., Vander Heyden, Y., Verfaillie, C., and Rogiers, V. (2006). Sequential exposure to cytokines reflecting embryogenesis: the key for in vitro differentiation of adult bone marrow stem cells into functional hepatocyte-like cells. *Toxicol Sci* **94**, 330-341; discussion 235-339.
- Sodunke, T. R., Turner, K. K., Caldwell, S. A., McBride, K. W., Reginato, M. J., and Noh, H. M. (2007). Micropatterns of Matrigel for three-dimensional epithelial cultures. *Biomaterials* **28**, 4006-4016.

## REFERENCES

---

- Stachelscheid, H., Urbaniak, T., Ring, A., Spengler, B., Gerlach, J. C., and Zeilinger, K. (2009). Isolation and characterization of adult human liver progenitors from ischemic liver tissue derived from therapeutic hepatectomies. *Tissue Eng Part A* **15**, 1633-1643.
- Stewart, J. D., and Bolt, H. M. (2011). Metabolomics: biomarkers of disease and drug toxicity. *Arch Toxicol* **85**, 3-4.
- Stierlin, H., and Faigle, J. W. (1979). Biotransformation of diclofenac sodium (Voltaren) in animals and in man. II. Quantitative determination of the unchanged drug and principal phenolic metabolites, in urine and bile. *Xenobiotica* **9**, 611-621.
- Strigun, A., Noor, F., Pironti, A., Niklas, J., Yang, T. H., and Heinzle, E. (2011a). Metabolic flux analysis gives an insight on verapamil induced changes in central metabolism of HL-1 cells. *J Biotechnol* **155**, 299-307.
- Strigun, A., Wahrheit, J., Beckers, S., Heinzle, E., and Noor, F. (2011b). Metabolic profiling using HPLC allows classification of drugs according to their mechanisms of action in HL-1 cardiomyocytes. *Toxicol Appl Pharmacol* **252**, 183-191.
- Strigun, A., Wahrheit, J., Niklas, J., Heinzle, E., and Noor, F. (2011c). Doxorubicin increases oxidative metabolism in HL-1 cardiomyocytes as shown by <sup>13</sup>C-metabolic flux analysis. *Toxicol Sci*.
- Strigun, A., Wahrheit, J., Niklas, J., Heinzle, E., and Noor, F. (2011d). Doxorubicin increases oxidative metabolism in HL-1 cardiomyocytes as shown by <sup>13</sup>C-metabolic flux analysis. *Toxicol. Sci.* **in press**.
- Sumida, K., Igarashi, Y., Toritsuka, N., Matsushita, T., Abe-Tomizawa, K., Aoki, M., Urushidani, T., Yamada, H., and Ohno, Y. (2011). Effects of DMSO on gene expression in human and rat hepatocytes. *Hum Exp Toxicol* **30**, 1701-1709.
- Sung, J. H., Choi, J. R., Kim, D., and Shuler, M. L. (2009). Fluorescence optical detection in situ for real-time monitoring of cytochrome P450 enzymatic activity of liver cells in multiple microfluidic devices. *Biotechnol Bioeng* **104**, 516-525.
- Sung, J. H., Kam, C., and Shuler, M. L. (2010). A microfluidic device for a pharmacokinetic-pharmacodynamic (PK-PD) model on a chip. *Lab Chip* **10**, 446-455.
- Sung, J. H., and Shuler, M. L. (2009). A micro cell culture analog (microCCA) with 3-D hydrogel culture of multiple cell lines to assess metabolism-dependent cytotoxicity of anti-cancer drugs. *Lab Chip* **9**, 1385-1394.
- Sung, J. H., and Shuler, M. L. (2010). In vitro microscale systems for systematic drug toxicity study. *Bioprocess Biosyst Eng* **33**, 5-19.
- Tang, W. (2003). The metabolism of diclofenac--enzymology and toxicology perspectives. *Curr Drug Metab* **4**, 319-329.
- Temenoff, J. S., and Mikos, A. G. (2000). Review: tissue engineering for regeneration of articular cartilage. *Biomaterials* **21**, 431-440.

## REFERENCES

---

- Theunissen, P. T., Pennings, J. L., Robinson, J. F., Claessen, S. M., Kleinjans, J. C., and Piersma, A. H. (2011). Time-response evaluation by transcriptomics of methylmercury effects on neural differentiation of murine embryonic stem cells. *Toxicol Sci* **122**, 437-447.
- Tibbitt, M. W., and Anseth, K. S. (2009). Hydrogels as extracellular matrix mimics for 3D cell culture. *Biotechnol Bioeng* **103**, 655-663.
- Torres, M. J., and Blanca, M. (2010). The complex clinical picture of beta-lactam hypersensitivity: penicillins, cephalosporins, monobactams, carbapenems, and clavams. *Med Clin North Am* **94**, 805-820, xii.
- Tostoes, R., Leite, S. B., Serra, M., Jensen, J., Bjorquist, P., Carrondo, M., Brito, C., and Alves, P. (2011a). Human liver cell spheroids in extended perfusion bioreactor culture for repeated dose drug testing. *Hepatology*.
- Tostoes, R. M., Leite, S. B., Miranda, J. P., Sousa, M., Wang, D. I., Carrondo, M. J., and Alves, P. M. (2011b). Perfusion of 3D encapsulated hepatocytes--a synergistic effect enhancing long-term functionality in bioreactors. *Biotechnol Bioeng* **108**, 41-49.
- Tuschl, G., Hrach, J., Walter, Y., Hewitt, P. G., and Mueller, S. O. (2009). Serum-free collagen sandwich cultures of adult rat hepatocytes maintain liver-like properties long term: a valuable model for in vitro toxicity and drug-drug interaction studies. *Chem Biol Interact* **181**, 124-137.
- Uehara, T., Kiyosawa, N., Shimizu, T., Omura, K., Hirode, M., Imazawa, T., Mizukawa, Y., Ono, A., Miyagishima, T., Nagao, T., and Urushidani, T. (2008). Species-specific differences in coumarin-induced hepatotoxicity as an example toxicogenomics-based approach to assessing risk of toxicity to humans. *Hum Exp Toxicol* **27**, 23-35.
- Ulker, P., Meiselman, H. J., and Baskurt, O. K. (2010). Nitric oxide generation in red blood cells induced by mechanical stress. *Clin Hemorheol Microcirc* **45**, 169-175.
- Ullrich, A., Stolz, D. B., Ellis, E. C., Strom, S. C., Michalopoulos, G. K., Hengstler, J. G., and Runge, D. (2009). Long term cultures of primary human hepatocytes as an alternative to drug testing in animals. *Altex* **26**, 295-302.
- van de Kerkhove, M. P., Di Florio, E., Scuderi, V., Mancini, A., Belli, A., Bracco, A., Dauri, M., Tisone, G., Di Nicuolo, G., Amoroso, P., Spadari, A., Lombardi, G., Hoekstra, R., Calise, F., and Chamuleau, R. A. (2002). Phase I clinical trial with the AMC-bioartificial liver. *Int J Artif Organs* **25**, 950-959.
- van de Kerkhove, M. P., Di Florio, E., Scuderi, V., Mancini, A., Belli, A., Bracco, A., Scala, D., Scala, S., Zeuli, L., Di Nicuolo, G., Amoroso, P., Calise, F., and Chamuleau, R. A. (2003). Bridging a patient with acute liver failure to liver transplantation by the AMC-bioartificial liver. *Cell Transplant* **12**, 563-568.
- van den Berg, R. A., Hoefsloot, H. C., Westerhuis, J. A., Smilde, A. K., and van der Werf, M. J. (2006). Centering, scaling, and transformations: improving the biological information content of metabolomics data. *BMC Genomics* **7**, 142.

## REFERENCES

---

- van der Smissen, A., Hintze, V., Scharnweber, D., Moeller, S., Schnabelrauch, M., Majok, A., Simon, J. C., and Anderegg, U. (2011). Growth promoting substrates for human dermal fibroblasts provided by artificial extracellular matrices composed of collagen I and sulfated glycosaminoglycans. *Biomaterials* **32**, 8938-8946.
- Van Summeren, A., Renes, J., Bouwman, F. G., Noben, J. P., van Delft, J. H., Kleinjans, J. C., and Mariman, E. C. (2011). Proteomics investigations of drug-induced hepatotoxicity in HepG2 cells. *Toxicol Sci* **120**, 109-122.
- Venter, J. C., Adams, M. D., Myers, E. W., Li, P. W., Mural, R. J., Sutton, G. G., Smith, H. O., Yandell, M., Evans, C. A., Holt, R. A., Gocayne, J. D., Amanatides, P., Ballew, R. M., Huson, D. H., Wortman, J. R., Zhang, Q., Kodira, C. D., Zheng, X. H., Chen, L., Skupski, M., Subramanian, G., Thomas, P. D., Zhang, J., Gabor Miklos, G. L., Nelson, C., Broder, S., Clark, A. G., Nadeau, J., McKusick, V. A., Zinder, N., Levine, A. J., Roberts, R. J., Simon, M., Slayman, C., Hunkapiller, M., Bolanos, R., Delcher, A., Dew, I., Fasulo, D., Flanigan, M., Florea, L., Halpern, A., Hannenhalli, S., Kravitz, S., Levy, S., Mobarry, C., Reinert, K., Remington, K., Abu-Threideh, J., Beasley, E., Biddick, K., Bonazzi, V., Brandon, R., Cargill, M., Chandramouliswaran, I., Charlab, R., Chaturvedi, K., Deng, Z., Di Francesco, V., Dunn, P., Eilbeck, K., Evangelista, C., Gabrielian, A. E., Gan, W., Ge, W., Gong, F., Gu, Z., Guan, P., Heiman, T. J., Higgins, M. E., Ji, R. R., Ke, Z., Ketchum, K. A., Lai, Z., Lei, Y., Li, Z., Li, J., Liang, Y., Lin, X., Lu, F., Merkulov, G. V., Milshina, N., Moore, H. M., Naik, A. K., Narayan, V. A., Neelam, B., Nusskern, D., Rusch, D. B., Salzberg, S., Shao, W., Shue, B., Sun, J., Wang, Z., Wang, A., Wang, X., Wang, J., Wei, M., Wides, R., Xiao, C., Yan, C., et al. (2001). The sequence of the human genome. *Science* **291**, 1304-1351.
- Villas-Boas, S. G., Mas, S., Akesson, M., Smedsgaard, J., and Nielsen, J. (2005). Mass spectrometry in metabolome analysis. *Mass Spectrom Rev* **24**, 613-646.
- Weckwerth, W., Loureiro, M. E., Wenzel, K., and Fiehn, O. (2004). Differential metabolic networks unravel the effects of silent plant phenotypes. *Proc Natl Acad Sci U S A* **101**, 7809-7814.
- West, P. R., Weir, A. M., Smith, A. M., Donley, E. L., and Cezar, G. G. (2010). Predicting human developmental toxicity of pharmaceuticals using human embryonic stem cells and metabolomics. *Toxicol Appl Pharmacol* **247**, 18-27.
- Wiklund, S., Johansson, E., Sjostrom, L., Mellerowicz, E. J., Edlund, U., Shockcor, J. P., Gottfries, J., Moritz, T., and Trygg, J. (2008). Visualization of GC/TOF-MS-based metabolomics data for identification of biochemically interesting compounds using OPLS class models. *Anal Chem* **80**, 115-122.
- Wilkening, S., Stahl, F., and Bader, A. (2003). Comparison of primary human hepatocytes and hepatoma cell line Hepg2 with regard to their biotransformation properties. *Drug Metab Dispos* **31**, 1035-1042.
- Wishart, D. S. (2008). Applications of metabolomics in drug discovery and development. *Drugs R D* **9**, 307-322.

## REFERENCES

---

- Xu, J. J., Diaz, D., and O'Brien, P. J. (2004). Applications of cytotoxicity assays and pre-lethal mechanistic assays for assessment of human hepatotoxicity potential. *Chem Biol Interact* **150**, 115-128.
- Yan, B., A, J., Hao, H., Wang, G., Zhu, X., Zha, W., Liu, L., Guan, E., Zhang, Y., Gu, S., Huang, Q., and Zheng, Y. (2009). Metabonomic phenotype and identification of "heart blood stasis obstruction pattern" and "qi and yin deficiency pattern" of myocardial ischemia rat models. *Sci China C Life Sci* **52**, 1081-1090.
- Yan, Z., Li, J., Huebert, N., Caldwell, G. W., Du, Y., and Zhong, H. (2005). Detection of a novel reactive metabolite of diclofenac: evidence for CYP2C9-mediated bioactivation via arene oxides. *Drug Metab Dispos* **33**, 706-713.
- Yang, H. J., Choi, M. J., Wen, H., Kwon, H. N., Jung, K. H., Hong, S. W., Kim, J. M., Hong, S. S., and Park, S. (2011). An effective assessment of simvastatin-induced toxicity with NMR-based metabonomics approach. *PLoS One* **6**, e16641.
- Yuan, J., Liu, L., Shimada, M., Wang, A., Ruhnke, M., Heeckt, P., Muller, A. R., Nussler, N. C., Neuhaus, P., and Nussler, A. (2004). Induction, expression and maintenance of cytochrome P450 isoforms in long-term cultures of primary human hepatocytes. *Altex* **21 Suppl 3**, 3-11.
- Zeilinger, K., Holland, G., Sauer, I. M., Efimova, E., Kardassis, D., Obermayer, N., Liu, M., Neuhaus, P., and Gerlach, J. C. (2004). Time course of primary liver cell reorganization in three-dimensional high-density bioreactors for extracorporeal liver support: an immunohistochemical and ultrastructural study. *Tissue Eng* **10**, 1113-1124.
- Zhu, X. H., Wang, C. H., and Tong, Y. W. (2009). In vitro characterization of hepatocyte growth factor release from PHBV/PLGA microsphere scaffold. *J Biomed Mater Res A* **89**, 411-423.

## CURRICULUM VITAE

### PERSÖNLICHE DATEN

**Name:** Daniel Müller  
**Anschrift:** Großwies 2, 66802 Überherrn-Felsberg  
**Geburtsdatum:** 25.04.1982  
**Geburtsort:** Saarlouis  
**Staatsangehörigkeit:** deutsch  
**Familienstand:** ledig

### AKADEMISCHE AUSBILDUNG

**03/2008 – 12/2011:** Promotion am Institut für Technische Biochemie von Prof. Elmar Heinzle an der Universität des Saarlandes:  
**Organotypic functional cultures of human liver cells for long-term maintenance and assessment of drug-induced metabolome effects**

**10/2002 – 10/2007:** Studium der Human-und Molekularbiologie an der Universität des Saarlandes, Abschluss als Diplom-Biologe mit Schwerpunkt Human- und Molekularbiologie,  
Note: sehr gut 1.3

**12/2006 – 10/2007:** Diplomarbeit am José-Carreras-Zentrum für Immun- und Gentherapie in der Arbeitsgruppe von Prof. Klaus Römer

### SCHULBILDUNG

**1992 – 2001:** Max-Planck-Gymnasium Saarlouis, Abitur (Note 1.5)  
Leistungskurse: Englisch, Politik, Chemie

**1988 – 1992:** Grundschule Steinrausch

## PUBLIKATIONEN

- **Mueller D**, Tascher G, Müller-Vieira U, Knobloch D, Nuessler AK, Zeilinger K, Heinzle E and Noor F (2011):

---

In-depth physiological characterization of primary human hepatocytes in a 3D-hollow fiber bioreactor

*Journal of Tissue Engineering and Regenerative Medicine*, 5: e207-e218, DOI: 10.1002/term.418

- **Mueller D**, Koetemann A and Noor F (2011):

---

Organotypic cultures of HepG2 generated by hanging drop method as *in vitro* model for toxicity studies

*Journal of Bioengineering and Biomedical Sciences*, DOI: 10.4172/2155-9538.S2-002

- **Mueller D**, Müller-Vieira U, Biemel KM, Tascher G, Nüssler AK and Noor F (2012):

---

Biotransformation of diclofenac and effects on the metabolome of primary human hepatocytes upon repeated dose exposure

*European Journal of Pharmaceutical Sciences*, 45:716–724

- **Mueller D**, Tascher G, Damm G, Nüssler AK, Heinzle E and Noor F (2012):

---

Real-time *in situ* viability assessment in 3D bioreactor with liver cells using resazurin assay during drug exposure

*Cytotechnology*, **in press**

- **Mueller D**, Tascher G, Müller-Vieira U, Knobloch D, Nüssler AK, Heinzle E and Noor F (2012):

---

GC-TOFMS based metabolomics for the assessment of therapeutic drug concentration effects on human liver cells

**submitted**

## VORTRÄGE

“GC-TOF-MS for the assessment of drug-induced changes in primary human hepatocyte metabolome”

LECO Pegasus Users Meeting, University Hospital Aachen, 30.11 – 01.12.2010

## KONFERENZBEITRÄGE

- **Mueller D**, Tascher G, Zeilinger K, Lübberstedt M, Noor F and Heinzle E:
- 

3D *in vitro* bioreactor system for the assessment of drug toxicity using human hepatic cells  
(Best Poster Award from eposters.net)

*ADMET EUROPE 24. - 25.02.2009, Berlin, Germany*

- **Mueller D**, Müller S, Tascher G, Noor F, Knobloch D, Nüssler AK and Heinzle E:
- 

A metabolomic approach for the investigation of drug induced hepatic toxicity using GC-ToF-MS

*Metabolomics and More, 10. – 12.03.2010, Freising, Germany*

- Tascher G, Noor F, **Mueller D**, Knobloch D, Nüssler AK, Zeilinger K and Heinzle E:
- 

Toxicoproteomic analysis on primary human hepatocytes in 3D-jellyfish bioreactor

*ADMET Europe 2010 08. - 09.04.10, München, Germany*

- **Mueller D**, Mueller S, Tascher G, Knobloch D, Nüssler AK, Heinzle E and Noor F:
- 

Sensitive assessment of drug-induced changes in primary human hepatocyte metabolome using a combination of GC-MS and multivariate statistics (Altex Best Poster Award).

*Congress on Alternatives to Animal Testing, 02. - 04.09.2010, Linz, Austria*

- **Mueller D**, Tascher G, Müller-Vieira U, Knobeloch D, Nüssler AK, Lübberstedt M, Zeilinger K, Heinzle E and Noor F:
- 

Cultivation of primary human hepatocytes in a 3D membrane bioreactor as an alternative to 2D culture systems for improved hepatotoxicity testing

*Congress on Alternatives to Animal Testing, 02. - 04.09.2010, Linz, Austria*

- Tascher G, **Mueller D**, Knobeloch D, Nüssler AK, Zeilinger K, Heinzle E and Noor F:
- 

Secretome analysis of primary human hepatocytes in 2D- and 3D-culture for *in-vitro* toxicology

*Congress on Alternatives to Animal Testing, 02. - 04.09.2010, Linz, Austria*

- Noor F, Mueller S, **Mueller D** and Heinzle E:
- 

3D organoid like culture of Hep G2 using alginate matrix for hepatotoxicity assessment

*Congress on Alternatives to Animal Testing, 02. - 04.09.2010, Linz, Austria*

- Tascher G, **Mueller D**, Knobeloch D, Nüssler AK, Zeilinger K, Heinzle E and Noor F:
- 

Secretome analysis of human hepatocytes in 2D- and 3D-culture for *in-vitro* toxicology

*4<sup>th</sup> EuPA Meeting, 23. - 27.10.2010, Estoril, Portugal*

- **Mueller D**, Koetemann A, Heinzle E and Noor F:
- 

HepaRG spheroids using the hanging drop method and their application to toxicity studies

*HepaRG Workshop, 21. – 23.09.2011, Rennes, France*